Copy 16 of 20

CR

ECO.-75: C-2-1

THE APPLICATION OF REMOTE SENSING TO THE DEVELOPMENT AND FORMULATION OF HYDROLOGIC PLANNING MODELS

Peter A. Castruccio, Harry L. Loats, Jr.

Thomas R. Fowler, Susan L. Frech

PROPERTY OF MARSHALL LIBRARY A&TS-MSFC

FINAL REPORT - NAS8-30539

ECOSYSTEMS INTERNATIONAL, INC.

Post Office Box 225

Gambrills, Maryland 21054

JANUARY 7, 1975

(NASA-CR-144079) THE APPLICATION OF REMOTE SENSING TO THE DEVELOPMENT AND FORMULATION OF HYDROLOGIC PLANNING MODELS Final Report (Ecosystems International, Inc.) 196 p HC $7.50 CSCL 08H G3/43

N76-14577

Unclas 06315

ECO.-75: C-2-1

THE APPLICATION OF REMOTE SENSING TO THE DEVELOPMENT AND FORMULATION OF HYDROLOGIC PLANNING MODELS

Peter A. Castruccio, Harry L. Loats, Jr.

Thomas R. Fowler, Susan L. Frech

FINAL REPORT - NAS8-30539

ECOSYSTEMS INTERNATIONAL, INC.

Post Office Box 225

Gambrills, Maryland 21054

JANUARY 7, 1975

This report was prepared by Ecosystems International, Inc., under NAS8-30539, "Research Study on the Application of Remote Sensing to the Development and Formulation of Hydrologic Planning Models" for the George C. Marshall Space Flight Center of the National Aeronautics and Space Administration.

1.0 INTRODUCTION AND BACKGROUND

Hydrologists and water resource planners are continually faced with developing two types of information concerning watersheds: 1) Management information which deals with the response of the watershed to specific individual event(s), and 2) Planning information necessary to define the expected response of the watershed to statistically recurring peak events. Management information is required for the real-time optimization of supply versus demand; planning information is needed for the optimal sizing of waterworks.

Typical planning events treated by water resources agencies include: probability of recurrence of peak flow rates (flood flows), in order to size spillways and determine floodways; recurrence-duration of the high flow event (volume of water), in order to determine storage required to prevent flooding; recurrence-duration of the low flow event to maintain dependable basin yield; and other water-related characteristics such as sediment yield and water quality.

Due to the pressures of urbanization, one of the most important of the planning events above as regards both manpower employed and value resulting from optimal operations, is the prediction of the peak flow event - flood frequency.

Not all of the watershed physical characteristics are equally important in determining the recurrence and magnitude of peak flow events. It is thus fruitful to investigate in detail the following elements:

1. Which of the watershed physical parameters are the most significant contributors to flood events;
2. What are the errors in prediction committed by neglecting the less important parameters;
3. What are the errors induced by imperfect knowledge of the principal parameters (sensitivity); and
4. How do the important "driver" parameters vary as a function of regional conditions. Understanding and reduction to engineering practice of this last item would yield the important result of being able to specify the functional form, and hopefully the coefficients, of a planning model for each region, following a procedure valid for all regions (regionalization).

The principal, conventional flood frequency planning models employ either 1) statistical extrapolation, particularly for small-medium watersheds, or 2) digital parametric simulation modeling for large watersheds having high economic value. Both of these methods require extensive historical rainfall and runoff records. Many watersheds do not have the required

length of records, particularly if the watershed is undergoing rapid changes due to urbanization; in this case, in fact, length of record is of very limited value.

Another important question pertaining to planning models is being asked more and more frequently by local users: specifically, what is the effect upon the hydrologic regime of planned modifications to the watershed, such as construction, deforestation, and reforestation, and how will these changes affect the size, type and location of waterworks?

Rapid, repetitive survey techniques are required which relate the physical characteristics of the watershed, particularly the surface characteristics, to information necessary for optimal planning of watershed development. If this information can be practically incorporated into planning models sensitive to the spatially distributed characteristics of the watershed (e.g. vegetative cover, impermeable/permeable areas, surface water, drainage pattern, and evapotranspiration potential), it will prove of major interest to:

- Federal Agencies operating in the Water Resources field, such as the Corps of Engineers, the U.S. Geological Survey, the USDA-Soil Conservation Service, the Agricultural Research Service, and the National Oceanographic and Atmospheric Administration.
- Federal Agencies whose mission is to guide and foster Water Resources Research, such as DOI - Office of

Water Research and Technology and the National Science Foundation - International Hydrologic Program.

- The developing nations wherein water resources development is a major influence in well-being and where in general the paucity of records and the lack of a hydrologic infra-structure place critical importance on this effort.
- Foreign governmental and extra-governmental agencies with water resources development orientation, such as the United Nations, the FAO, and the International Water Resources Association.

1.1 State of the Art of Planning Models

The historical evolution of planning models has progressed along three lines, leading to the formulation of three broad categories of methods.

1.1.1 Method 1: The Empirical Approach

The earliest to be devised, and perhaps still the most widely employed, particularly in ungaged areas, are empirical formulations of the general type:

$$q = A^{-n} f(A) h(W) g(T)$$

Where:

q = peak flow rate from unit watershed area

A = total watershed area

$f(A)$ = functional adjustment for area

h(W) = functional relationship of watershed physical characteristics, e.g., slope, vegetative cover

g(T) = recurrence period, years

n = empirically derived coefficient

There exist perhaps a hundred models of this type in use in the U.S. and the world, particularly in ungaged areas. The significant models in general use in the world are presented in Table 1.* Their performances are compared graphically in Figures 1 and 2. As can be seen, there is a variation in the predicted peak discharge between models of at least one order of magnitude for the small and medium watersheds, increasing to two orders of magnitude for the large watersheds.

This variation, per se, would not constitute a major problem if a unique model could be attributed to each region. In reality, even within the same geographic area, the model formulations vary significantly, as shown by Figure 3. An example of the variability of the results of typical empirical regression models is given in Figure 4 for a large watershed in Maryland. There is a significant uncertainty in predictions for long recurrence periods which are usually related to design of civil structures. Improvement in model accuracies in this region - and in many similarly developed regions - are of significant economic value.

*Source: Gray, Introduction to Hydrology

Table I. Principal Planning Models in Current Use

DESIGNATION	REGION	EQUATIONS	UNITS	RANGE OF APPLICATION	AUTHOR
	World	$Q = \frac{131,000A}{(107+A)^{0.78}}$	E	Max. recorded flood throughout the world.	Baird and McIlraith
	Australia	$Q = \frac{222,000A}{(185+A)^{0.9}}$	E		"
I_1	India	$Q = \frac{7,000A}{\sqrt{A+4}}$	E	For fan-shape area	Inglis
I_2		$Q = 1,795\,A^{0.75}$	E	Rain approximately 100 in.	Dickens
I_3		$Q = 149A^{0.75}$	E	Rainfall 30 to 40 in.	"
I_4		$Q = 675A^{0.67}$	E	Maximum flood	Ryves
I_5		$Q = 560A^{0.67}$	E	Average flood	"
I_6		$Q = 450A^{0.67}$	E	Minimum flood	"
I_7		Curve only	E	Bombay area	Whiting
I_8		$Q = 2,000A \exp(0.92 - \frac{1}{3} \log A)$	E	Tungabhadra River	Madras formula
I_9		$Q = 1,750A \exp(0.92 - \frac{1}{14} \log A)$	E	"	Hyderabad formula
UK_1	United Kingdom	$Qm = 2,700A^{0.75}$	E	A smaller than 10 sq. mi	Bransby Williams
UK_2		$Qm = 4,600A^{0.52}$	E	A greater than 10 sq. mi.	"
UK_3		Curve	E		Institute of Civil Eng. 1933
U_1	U.S.A.	$Q = 200\,A^{5/6}$	E		Fanning
U_2		$Q = (\frac{48,790}{A+320} + 15)A$	E	A between 5.5 and 2,000 sq. mi.	Murphy
U_3		$Q = (1,400A^{0.476}$	E	A between 1,000 and 24,000 sq. mi	U.S. Geological Survey for Columbia
U_4		$Q = (\frac{44,000}{A+170} + 20)A$	E	For frequent floods	Kuichling
U_5		$Q = (\frac{127,000}{A+370} + 7.4)A$	E	For rare floods	"
U_6		$Q = 4,600A^{-0.048A^{-0.048}}$	E	Upper limit	Creager
U_7		$Q = 1,380A^{0.894}$	E	Lower limit	"
U_8		$Q = 10,000A^{0.5}$	E		Myer
N	New Zealand	$Qm = 20,000A^{0.5}$	E	A smaller than 10 sq. mi	

Note: Qm = maximum flood.
M = Metric System
E = English System
Q = Peak flow (m^3/sec or cfs)
A = Area (Km^2 or sq. mi)

FIGURE 1. COMPARISON OF PRINCIPAL U.S. PLANNING MODEL PREDICTIONS

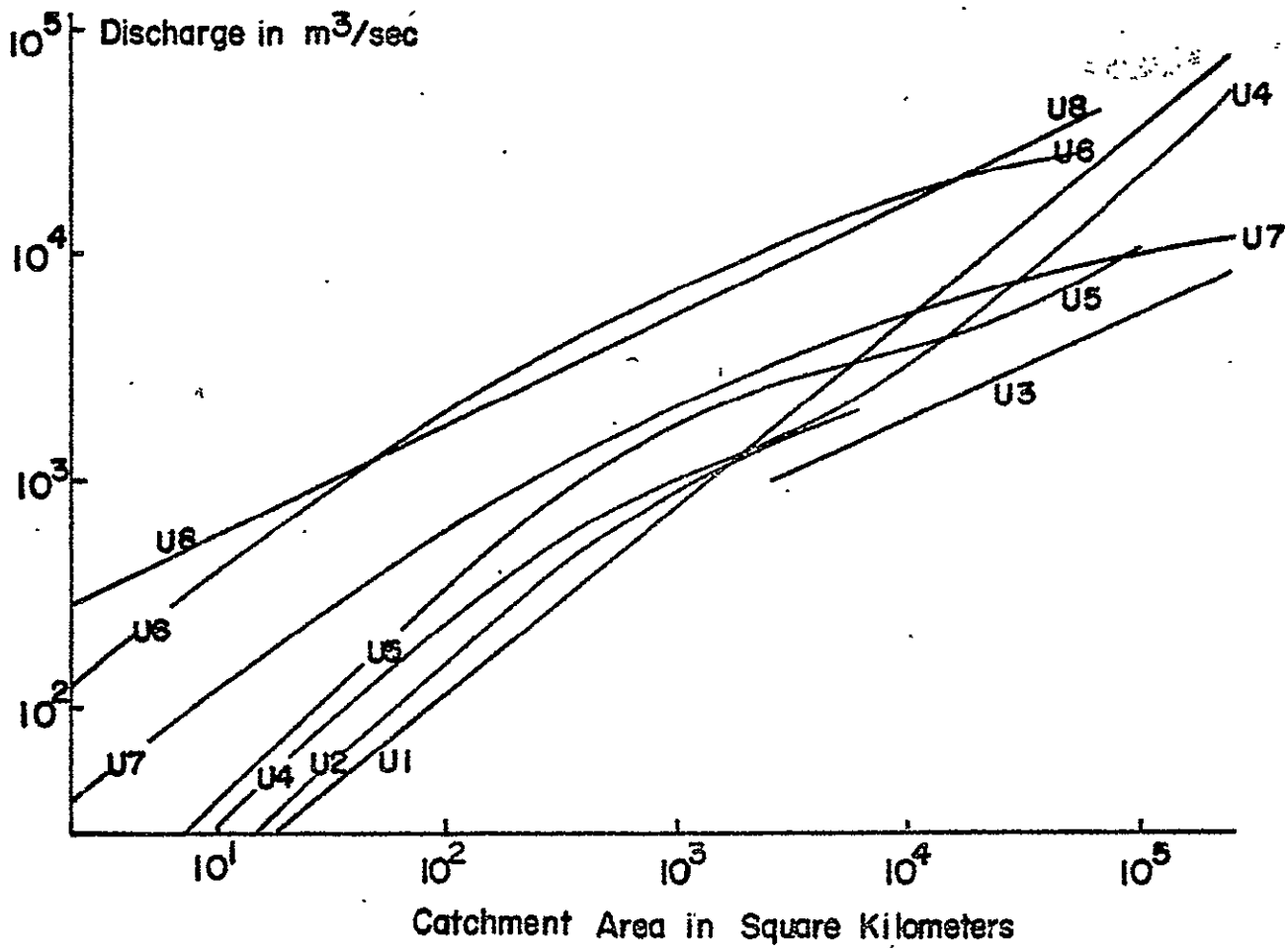

FIGURE 2. COMPARISON OF SELECTED FOREIGN PLANNING MODEL PREDICTIONS

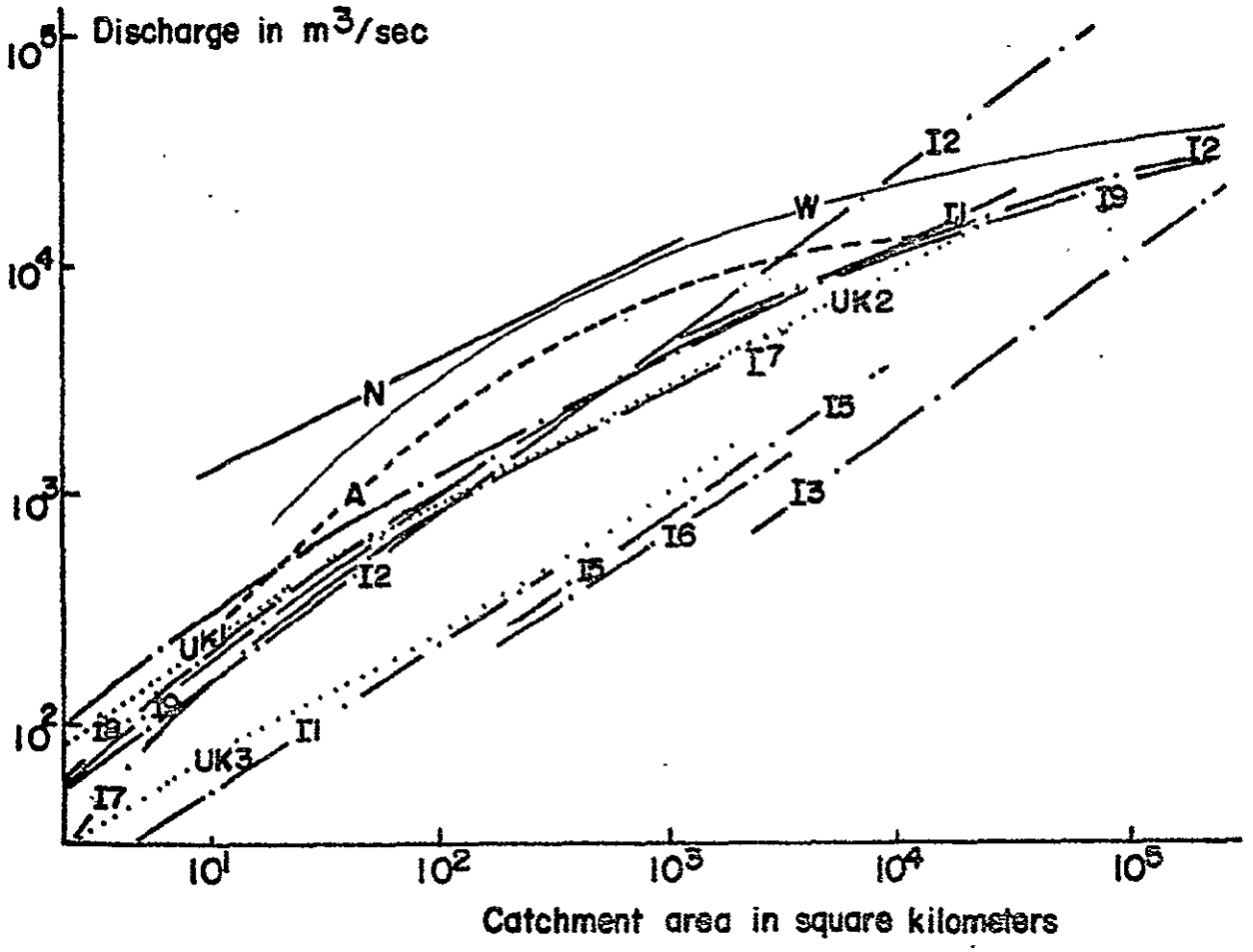

A ----- Australia

I —.—.— India

UK ..... United Kingdom

W _____ World

N ——— New Zealand

FIGURE 3. DIVERGENCE OF PREDICTION BETWEEN PLANNING MODELS

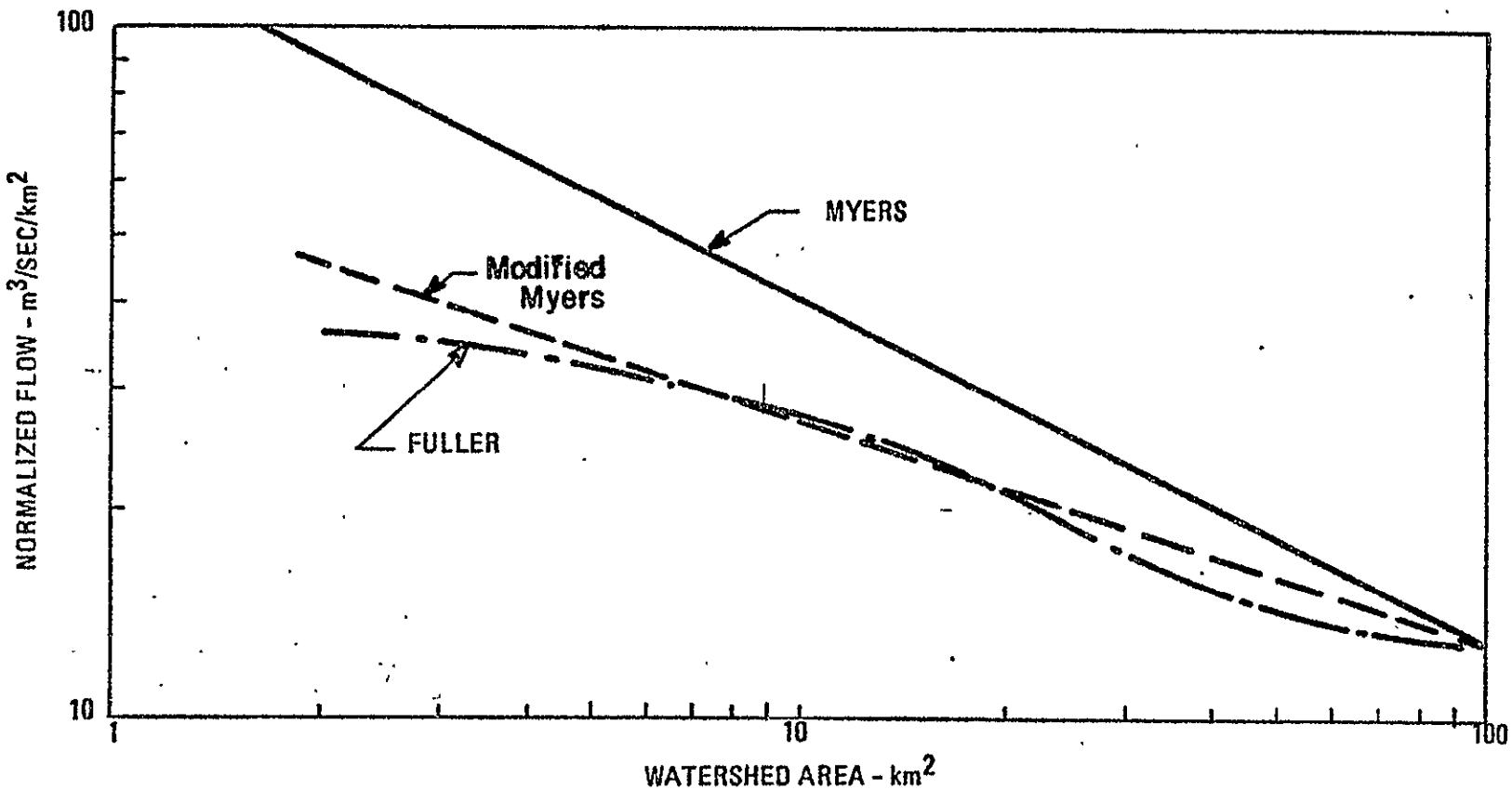

Normalized Watershed, Same Region

FIGURE 4

TYPICAL UNCERTAINTIES IN PREDICTIONS OF CONVENTIONAL PLANNING MODELS FOR GAGED WATERSHEDS

25-year records

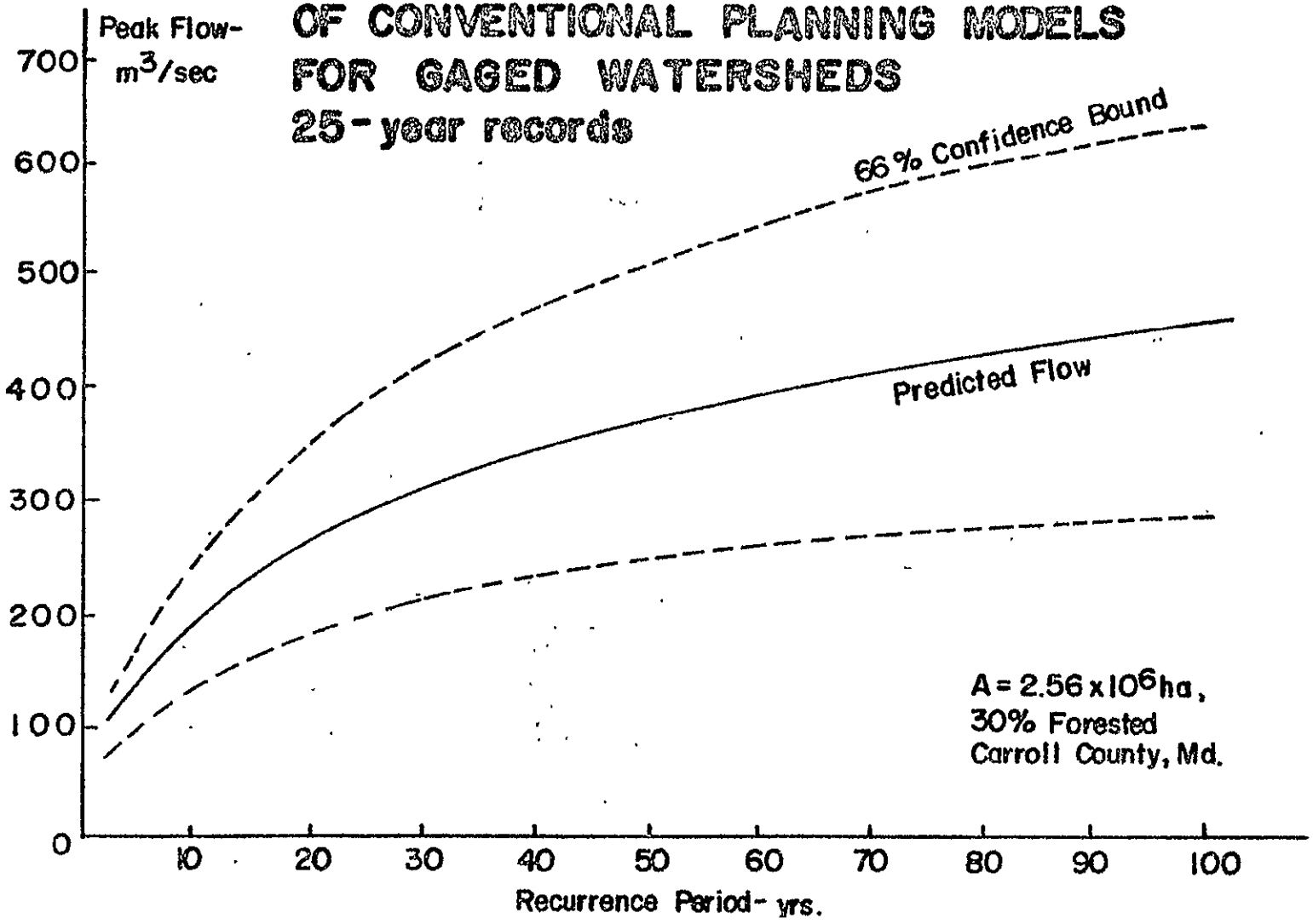

1.1.2 Method 2: The Statistical Approach

If there is a sufficiently long historical record available, the random character of the flow peak can be treated as a stochastic variable. There is an underlying assumption that the controlling random process is stationary, e.g., the character of the event remains unchanged by long term trends or other effects. Using daily records, various statistical parameters such as the mean, the variance, the coefficient of variability, and the skewness can be computed. By assuming a given probability distribution such as Log Pearson III, Gumbel, or log-normal, the probability of the recurrence of a peak event equal to or greater in magnitude than an arbitrary value can be determined.

There are several fundamental problems involved with the purely statistical approach. First, there is the obvious requirement for extensive records in order to achieve a given level of confidence. This dependence is shown in Figure 5, which indicates the sensitivity of the record length in predicting the fifty year event for a particular region in the U.S. Percent of error due to this cause alone decreases from 40% to 16% as the length of record increases from 2 to 20 years at 90% confidence level. This assumes that the watershed has not changed significantly during the period of record.

INTENTIONALLY

LEFT

BLANK

Additionally, there is considerable variation among predictions from the principal statistical models in use and between the model results and actual records. Figure 6 is a comparison between the two principal distributions used in the U.S. and shows the magnitude of the error for two typical watersheds.

In summary, the statistical method is not applicable to ungaged watersheds, and is subject to potentially significant errors in watersheds undergoing change.

1.1.3 Method 3: Semi-Empirical Macro Models - Rational Approach

A useful and logical extension to these wholly empirical models is the addition of the rainfall component $i_{T,d}$. This component is the average rate of rainfall "i" (m/hr) which is observed to occur for a duration "d" (hrs) at a recurrence interval of "T" (years). Since a large number of rainfall records are generally available, it is reasonable to assume that the inclusion of rainfall data should reduce the variance of the results. Semi-empirical methods are useful, although far from precise, where the coefficients relating runoff to rainfall are well-known; however, extrapolation of the coefficients on a regional basis is difficult and the results are subject to considerable uncertainty.

Rational or semi-empirical models have the general form:

$$q = A^n i^m(T) g(T) h(W)$$

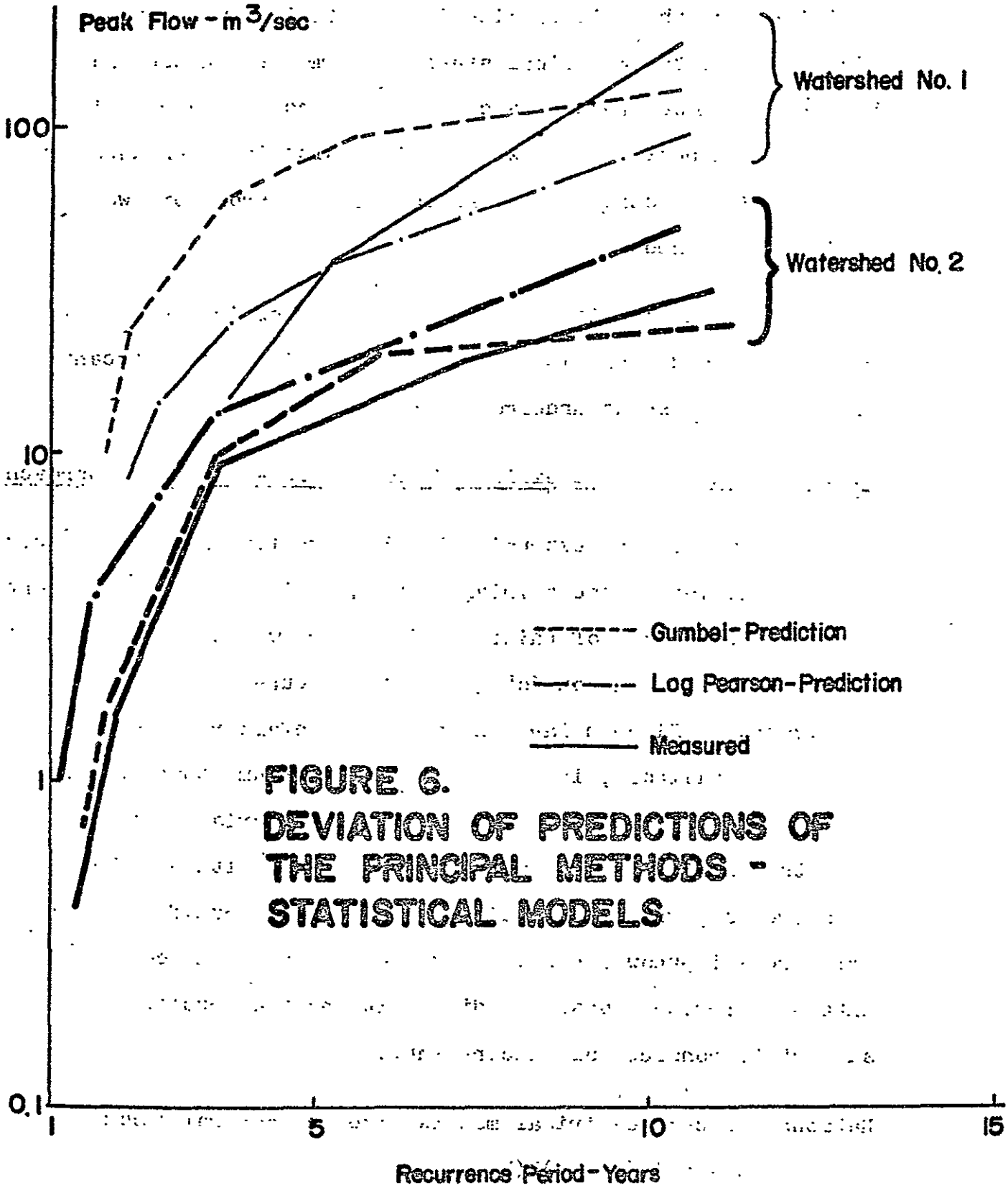

FIGURE 6.
DEVIATION OF PREDICTIONS OF THE PRINCIPAL METHODS - STATISTICAL MODELS

Where:

q = flow per unit watershed area

A = total watershed area

i = rainfall rate of a given duration occurring at a given recurrence period T

W = watershed parameters, e.g. vegetative cover, drainage density, slope, etc.

g,h= functional relationships

n,m= empirically derived coefficients

One explanation of the reason that available rational-type planning models yield significant errors is that in meeting the desiderata for generality and simplicity they in general do not explicitly include critical driver parameters. Further, the functional relationships between the significant drivers are not evaluated as regards various flood regimes, e.g. surface dominant regions, subsurface dominant regions, etc.

It would be possible in theory to utilize a more recent generation of models, the so-called parametric models, as planning models by introducing the data pertaining to the desired recurrence interval. This approach presents three problems:

1. Current parametric models were devised for gaged watersheds. They thus require a feedback correction through streamgage data of at least a few, perhaps five years, duration.
2. Current parametric models are not optimally structured, for good and valid reasons, to exploit to the fullest the capabilities of remote sensing.

3. They are quite expensive in terms of computer time and require relatively large computer facilities, not available to most of the "grass roots" users.

It is these drawbacks which the present effort is intended to alleviate or obviate. Specifically, this effort is directed toward determining which remote sensing observables are most important to the planning of watersheds vis-a-vis peak flow. Concomitantly, it seeks to identify the regions in which surface parameters dominate the hydrologic processes, in order to test the remote sensing model hypotheses.

2.0 GENERAL APPROACH

With the advent of remote sensing, the hydrologist has available a practical tool for developing a new data series which can be input into planning models. In principle, it is now possible to receive synoptic and repetitive information about the watershed and to develop therefrom a sequential profile of the vegetative cover, impervious area, potential infiltration and soil humidity from past potential evapotranspiration. The new data elements are potential drivers for planning models: their incorporation can be expected to reduce the variance of the error.

The thrust of this effort was concentrated in four areas:

1. Determination of driver phenomena.
2. Construction of a generalized hydrologic planning model, primarily involving "observables."
3. Verification of the model with data from existing watersheds.
4. Identification of the role of remote sensing.

The relationship of each of these tasks to the others and their roles in the overall effort are shown in Figure 7.

The first step in the approach was to attempt to isolate those phenomena which "drive" hydrologic planning models. A driver for a planning model for peak flow is defined as any watershed

FIGURE 7 PROGRAM FLOW CHART, NAS8-30539

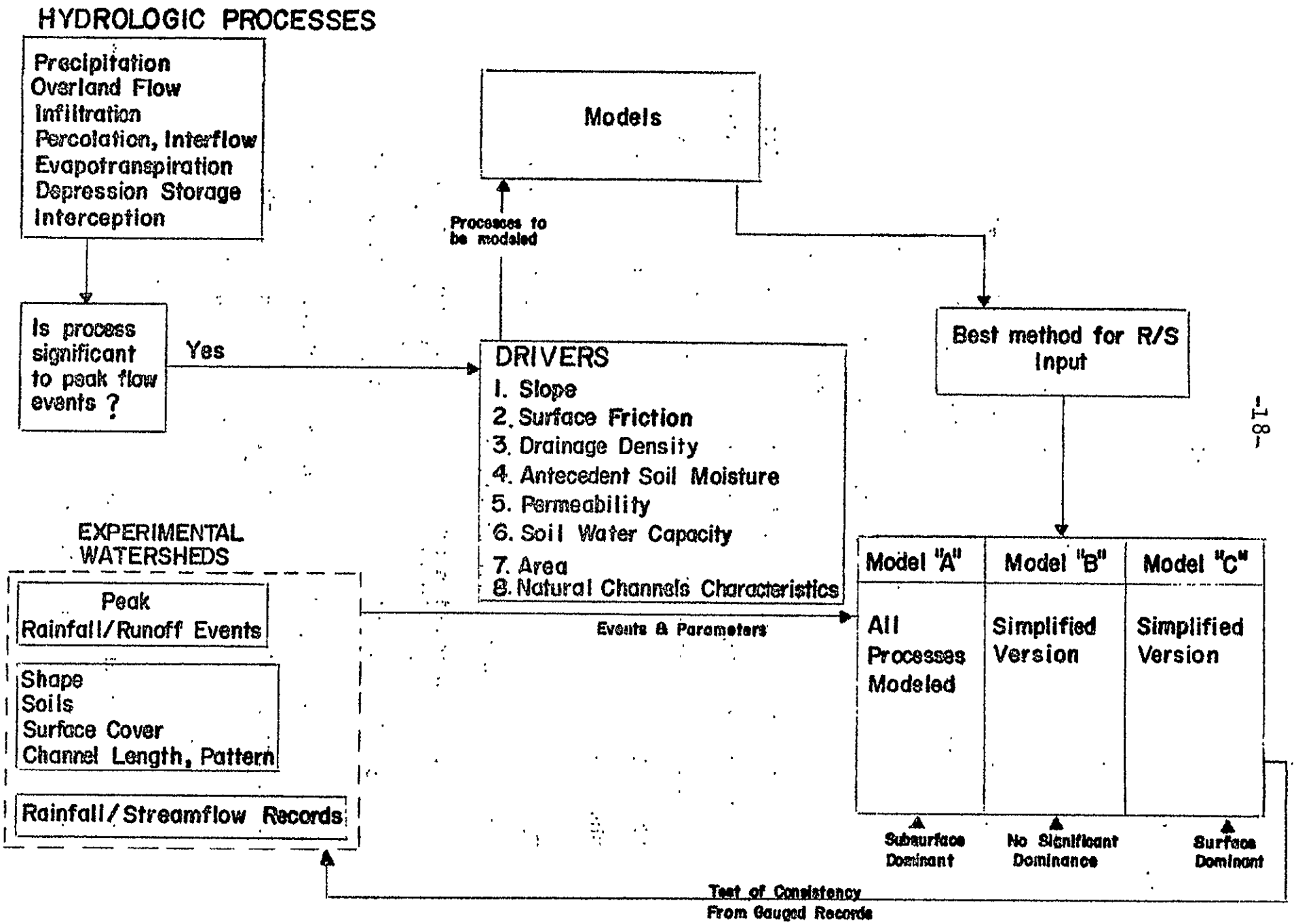

ECOSYSTEMS INTERNATIONAL INC.

condition or parameter which, when modified, causes a significant alteration in the peak runoff.

The driver concept was used to validate three hypotheses:

1. Not all the physical characteristics of watersheds contribute significantly to runoff rate or volume. Therefore, the drivers of peak flow events constitute a relatively small group of watershed parameters.
2. Drivers may be spatially and/or temporally variable. Much of the uncertainty of current hydrologic planning models is due to their inflexibility in accommodating natural and man-induced variations in watershed conditions.
3. After ascertaining the extent of influence of each driver, it is possible to neglect those phenomena whose contributions to the desired end result (peak flow) are minor, i.e., cause an error smaller than a preassigned proportion of the total peak flow.

Once the important drivers were identified, their interrelationships were investigated. This portion of the effort proceeded along two lines. First, the mathematical relationships among processes and drivers were explicitly determined, in order to develop an analytic model. Next, analog computer equivalents were developed. The analytic model was primarily applied to the examination of runoff and its correlation to areal rainfall, while the analog representation was used to test the

sensitivity of hydrologic processes to changes in various basin parameters.

The proposed verification of model results required the assemblage of a data base of physical characteristics and rainfall/runoff records extending over a large number of existing watersheds. The advantages of having access to this data base were twofold:

1. Real information was available during the formulation of the model, to test the accuracy of its results.
2. Since the drivers are spatially variable, a large geographically dispersed sample of basins facilitated the determination of which physical conditions, and therefore which hydrologic processes, were dominant in each location.

Ultimately, the results of this effort should be applicable to the construction of a "modular" model, capable of being tailored easily to the area under study. Referring again to Figure 7, the A, B, and C versions of the model represent what are expected to become unique combinations, each including the minimum number of modules to ensure accurate results.

To assemble the required data base, a geographically representative sample of basins was taken from a group of experimental watersheds operated by the Agricultural Research Service (ARS) for the purpose of studying the effects of agricultural

practices upon hydrologic processes. 158 watersheds were selected from 30 locations in the United States, as shown in Figure 8. The sample included substantially all ARS basins with area greater than 100 acres (40.5 hectares), since benefits from improved peak flow prediction are small in watersheds of lesser area.

Finally, the effort involved the description of the role of remote sensing as it relates to hydrologic modeling. Particular emphasis was placed upon identification of the areas where ERTS-type data is of maximum benefit and specification of the method by which specific parameters may be remotely sensed.

INTENTIONALLY

LEFT

BLANK

3.0 INVESTIGATION OF DRIVER PHENOMENA

Figure 9 illustrates the mechanism by which rainfall becomes peak runoff. The figure depicts a watershed of area A, subject to rain at constant rate, the runoff from which is measured at the watershed outlet. If the watershed were impermeable and the rainfall duration sufficiently long, the outflow would become constant at the instant when runoff rate began to equal rainfall rate. Therefore, the peak outflow rate would equal the product of the rain rate times the watershed area. The time elapsed from the moment the rain starts to the moment at which this peak occurs is termed the time of concentration of the watershed.

Assume, however, that the watershed allows a portion of the water to be abstracted (by infiltration, interception, evaporation, etc.). Then the peak outflow rate will be lower and may be determined by:

$$Q_{peak} = (\dot{P} - \dot{I})A$$

Where:

$\dot{P}$ = rainfall rate

$\dot{I}$ = abstraction rate

A = watershed area

ORIGINAL PAGE IS
OF POOR QUALITY

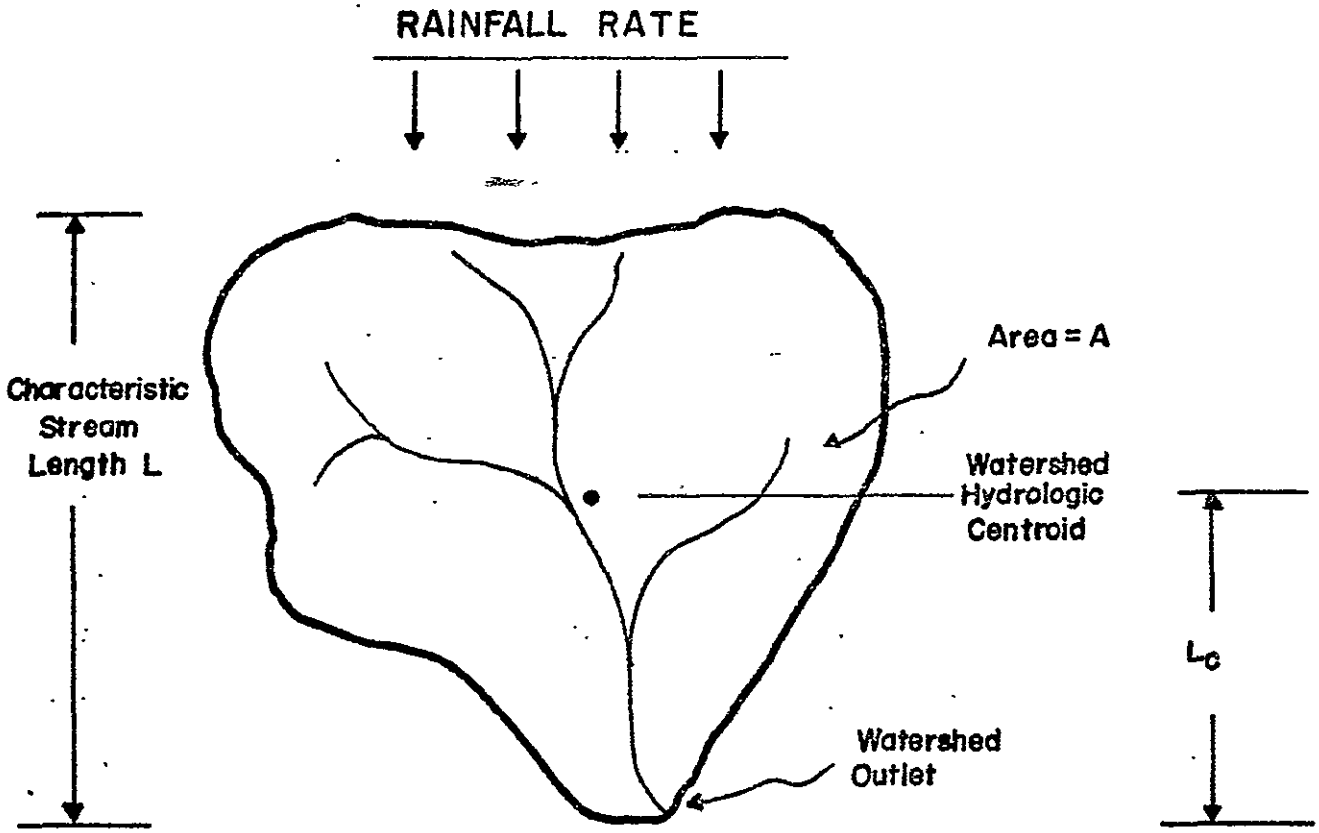

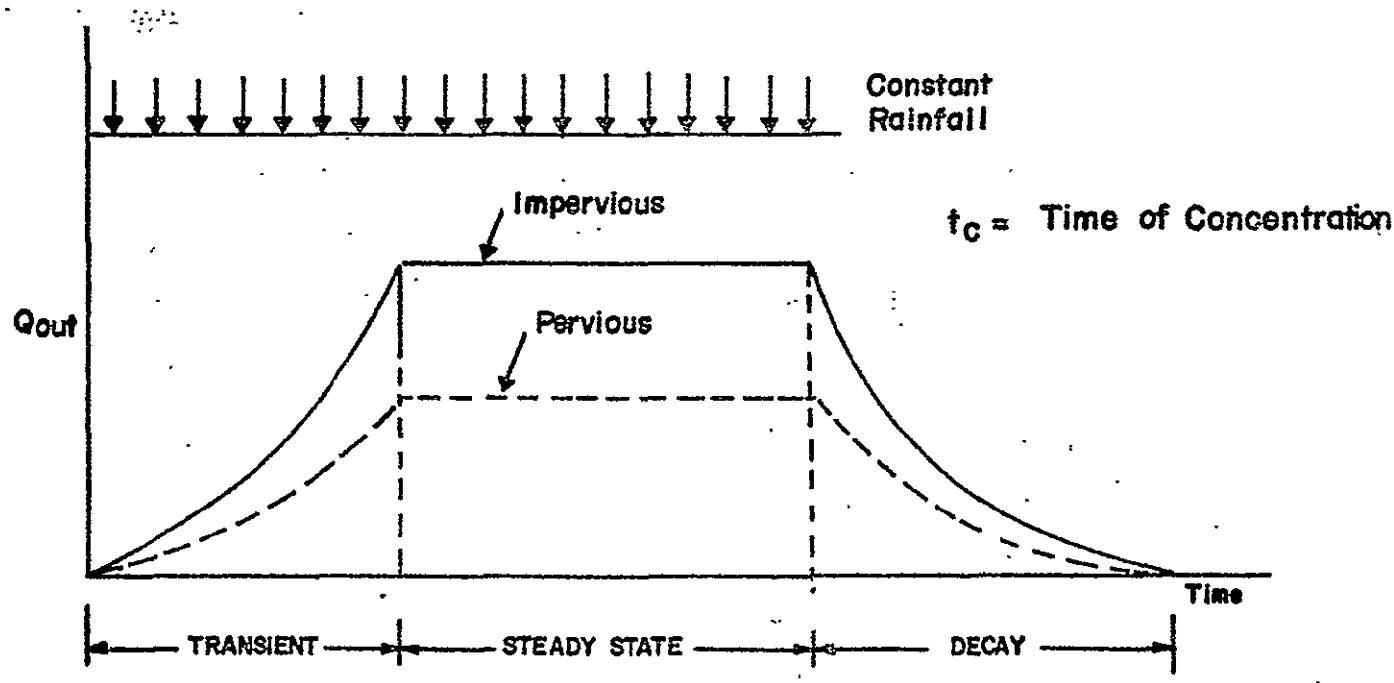

WATERSHED RESPONSE TO CONSTANT AND UNIFORM RAIN

FIGURE 9

In practice, as we shall see, $\dot{I}$ and $\dot{P}$ are not as simply related as the expression above implies. All that can be said at this point is that the peak runoff will increase as rain increases, and decrease as the abstraction increases, but not necessarily in direct proportion to either factor.

Figure 10 graphically illustrates the principal interrelationships among hydrologic processes. Table 2 supplies a brief definition of each process, while Table 3 lists the potentially important drivers for each process. Note that "potentially important" is only a qualitative indicator. The purpose of the discussion which follows is to convert this qualitative into a quantitative measure of each driver's importance.

3.1 Precipitation

Since precipitation is the source of the direct runoff, its properties are the basic input to any hydrologic model. Hydrologic planning models are concerned with the statistical distribution of peak events which are likely to recur within a specified number of years (the 25-year flood, the 50-year event, etc.). Therefore, we are concerned here with the statistical properties of the rainfall, e.g. the rainfall rate-duration relationship.

The statistical properties of rainfall, of interest to planning models, are:

FIGURE 10

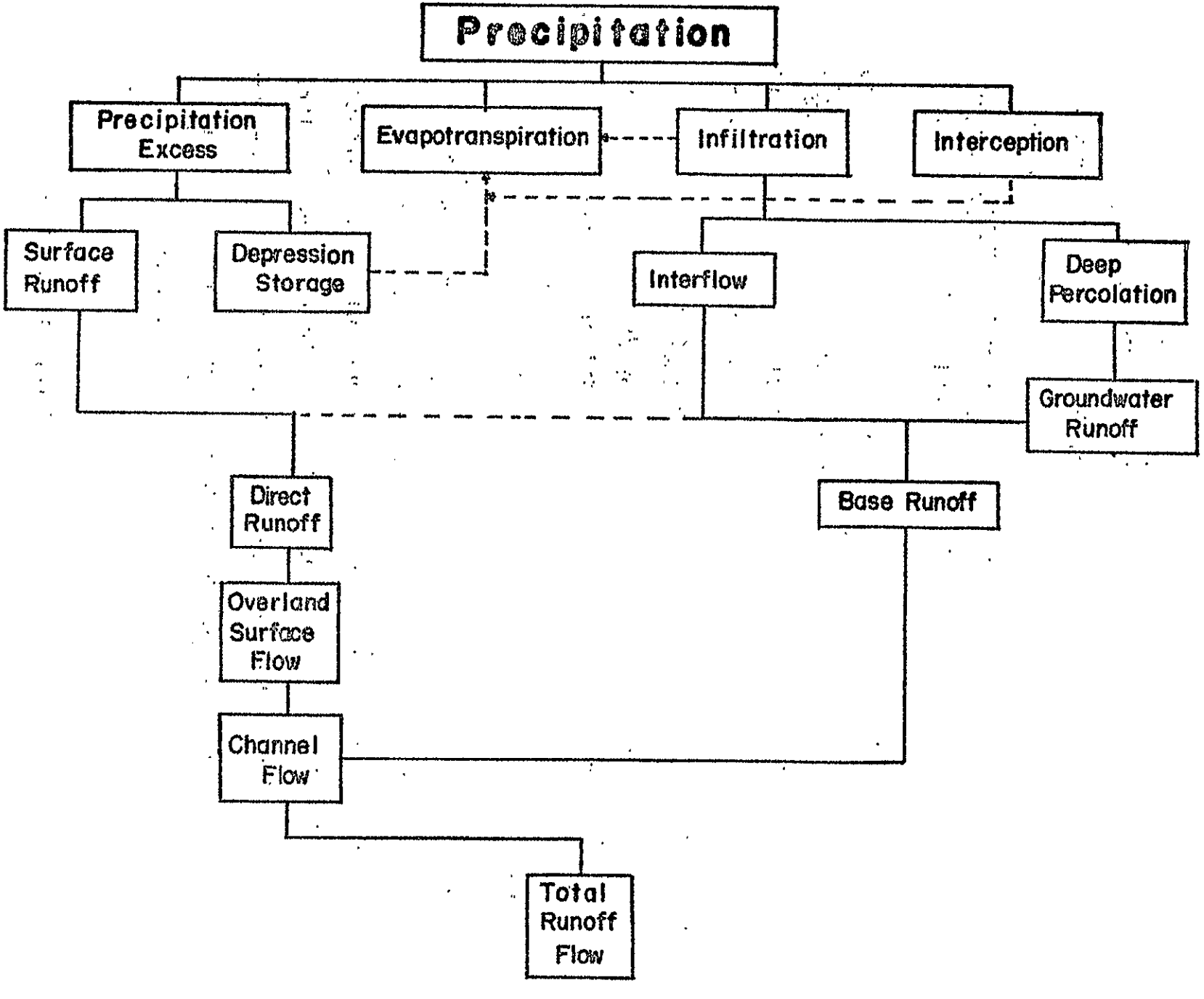
Precipitation
Precipitation Excess
Evapotranspiration
Infiltration
Interception
Surface Runoff
Depression Storage
Interflow
Deep Percolation
Groundwater Runoff
Direct Runoff
Base Runoff
Overland Surface Flow
Channel Flow
Total Runoff Flow

TABLE 2

SUMMARY DESCRIPTIONS OF HYDROLOGIC PROCESSES

HYDROLOGIC PROCESS	DESCRIPTION
Interception	Moisture caught and stored on plant leaves and stems or other impermeable objects; eventually evaporated back into the atmosphere.
Infiltration	Downward movement of water from the surface into the soil.
A) Interflow	Lateral subsurface water movement toward stream channels.
B) Percolation	Downward movement of water through soil to groundwater (area where pores of soil or rock are filled with water).
C) Base Runoff	Water from interflow and percolation which moves underground to the channel.
Evapotranspiration	
A) Evaporation	Upward movement of water in gaseous state from the surface.
B) Transpiration	Movement of water through plants to the atmosphere.
Precipitation Excess	
A) Depression Storage	Retention of excess rainfall in surface depressions.
B) Surface Flow	Uninfiltrated water which flows over land surface to stream channels.
C) Channel Flow	Flow of water in natural channels.
Total Runoff	Sum of runoff from underground processes (base runoff) and overland flow (direct runoff).

TABLE 3

POTENTIALLY IMPORTANT DRIVERS AS RELATED TO HYDROLOGIC PROCESSES

HYDROLOGIC PROCESS	PRINCIPAL DRIVERS	SECONDARY DRIVERS
Overland Flow	*Slope *Roughness of Soil & Cover *Drainage Density & Pattern	— —
Infiltration	*Soil Permeability *Antecedent Soil Moisture Soil Moisture Capacity	*Vegetative Cover *Slope Water Turbidity Temperature
A) Interflow	*Soil Permeability Subsurface Moisture Gradient *Flow Length, Slope	— —
B) Percolation	*Soil Permeability Subsurface Moisture Gradient Soil Depth	— —
Evapotranspiration		
A) Evaporation	Temperature *Antecedent Soil Moisture *Soil Permeability	Water Turbidity Wind
B) Transpiration	Temperature *Solar Radiation *Vegetative Cover *Antecedent Soil Moisture	Wind
Depression Storage & Detention	*Depression Density *Cover Retention	*Slope
Interception	Duration of Rainfall Intensity of Rainfall *Cover Composition, Age, Density	Evaporation Rate

* indicates factors which are potentially remote sensing observable.

1. The magnitude of the peak rain event varies with geographic location, as shown in Figure 11. For the United States, the range of variation is approximately 3.5:1, if unusually dry areas are excluded, such as Death Valley, for example.
2. The rate of the peak rainfall event varies as a function of the length of the event, as shown in Figure 12. The longer the event, the lesser the rate. However, the mass, i.e. the total amount of water precipitated, grows with increasing event duration.
3. For a given region, the rain recurrence-duration-intensity relationships follow the empirical relationship:

$$i = \frac{\alpha_1 T^{\alpha_2}}{(t+d)^{\alpha_3}}$$

Where:

i = rain rate, cm/hr.

T = recurrence internal, years

t = rain duration, hrs.

α_1, α_2

α_3, d = constants for specific location

The constants can be determined from existing rain-gage records. Figure 13 illustrates a typical relationship, related to the curves of Figure 12.

FIGURE 11 TYPICAL PEAK EVENT RAINFALL RECURRENCE
50 Year, 3 Hour Duration

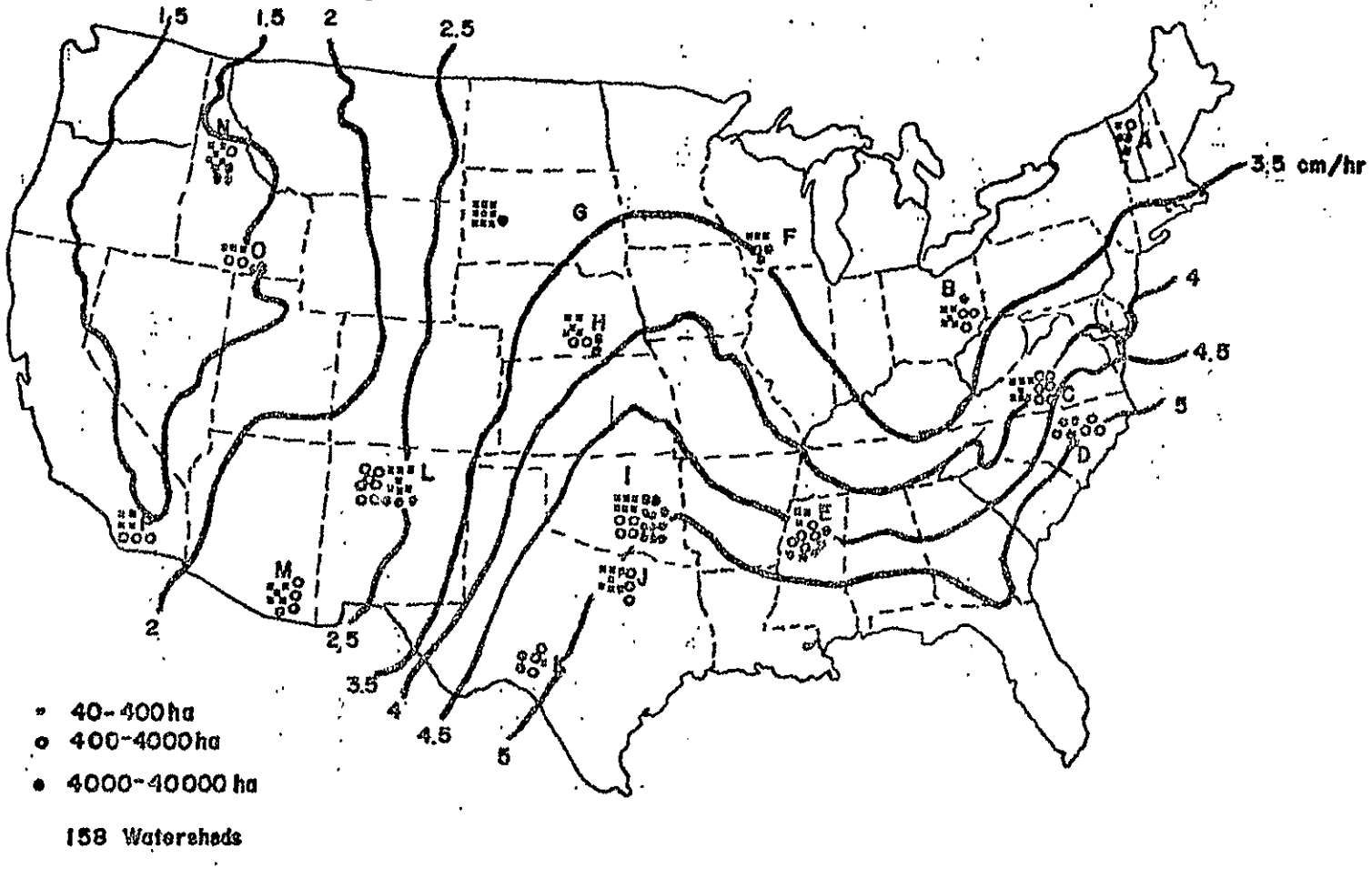

FIGURE 12

RAINFALL RATE / MASS RELATIONSHIP

DANVILLE, VERMONT WATERSHEDS
50 YEAR RECURRENCE RAIN

MAXIMUM RATE AND MASS VERSUS DURATION

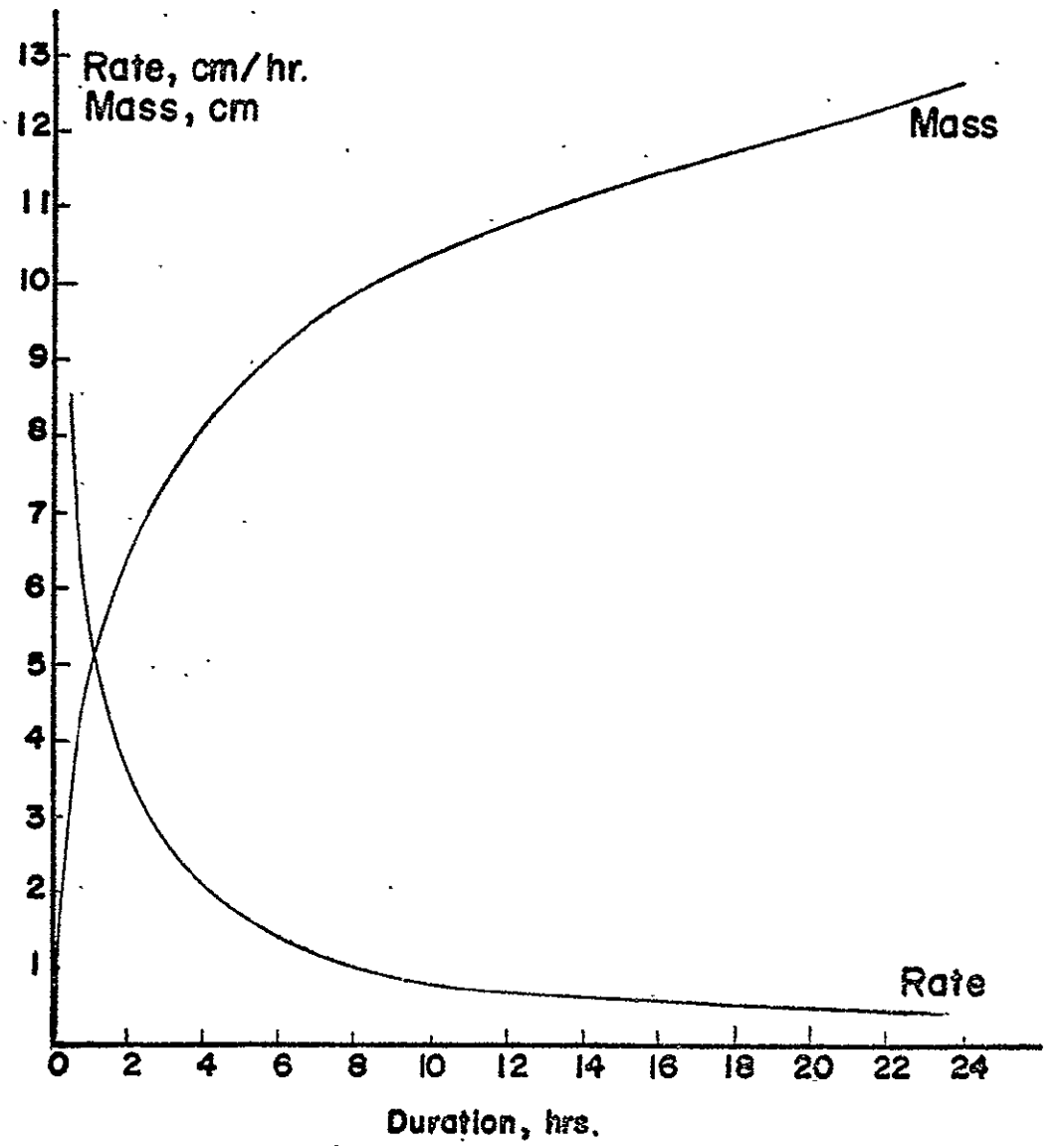

TYPICAL DEPENDENCY OF PEAK RAIN EVENT UPON DURATION AND RECURRENCE

DANVILLE, VERMONT EXPERIMENTAL WATERSHEDS

FIGURE 13

(t) Duration, hrs.	(T) Recurrence, yrs. 25	50	100
.5	7.6 cm/hr	8.6 cm/hr	8.9cm/hr
1	4.6cm/hr	5.3 cm/hr	5.8cm/hr
2	3.1 cm/hr	3.3cm/hr	3.6cm/hr
3	2.0 cm/hr	2.5cm/hr	2.8cm/hr
6	1.3cm/hr	1.5 cm/hr	1.8cm/hr
12	0.79cm/hr	0.84cm/hr	1.1 cm/hr
24	0.48cm/hr	0.53cm/hr	0.58cm/hr

General Formula: $i = \frac{\alpha_1 T^{\alpha_2}}{(t+d)^{\alpha_3}}$

where,

i = rain rate, cm/hr.

T = recurrence interval, years

t = rain duration, hours

$\alpha_1 \alpha_2 \alpha_3 d$ = constants for specific location

For Danville: $i_{cm/hr} = \frac{3.30\ T^{0.16}}{(t+0.2)^{0.77}}$

4. The intensity of rainfall is not uniform within the area rained upon. The larger the area, the greater the reduction in rainfall rate as one progresses from the point of highest rate towards the edges of the area.

   Therefore, when considering watersheds of relatively large extent, a correction factor for rainfall should be employed, as indicated in Figure 14. Note that the areal distribution of rain is only imperfectly known, because the experimental data collected up to now on this phenomenon have been scant. Thus Figure 14 should be taken as indicative only.

The time scale of interest in the abscissa of the curves of Figures 12 and 13 can be approximated by computing the concentration time from existing formulations. The result is only approximate, but sufficient to yield a gross calibration. The computation, whose details are reported in Section 5, is summarized in Figure 15, from which it can be deduced that the times of interest for the watershed sizes, shapes and slopes contained within the 158 ARS test watersheds range from perhaps 10 minutes to upwards of 5 hours.

FIGURE 14

THE EFFECT OF WATERSHED AREA ON THE PEAK RAIN RATE

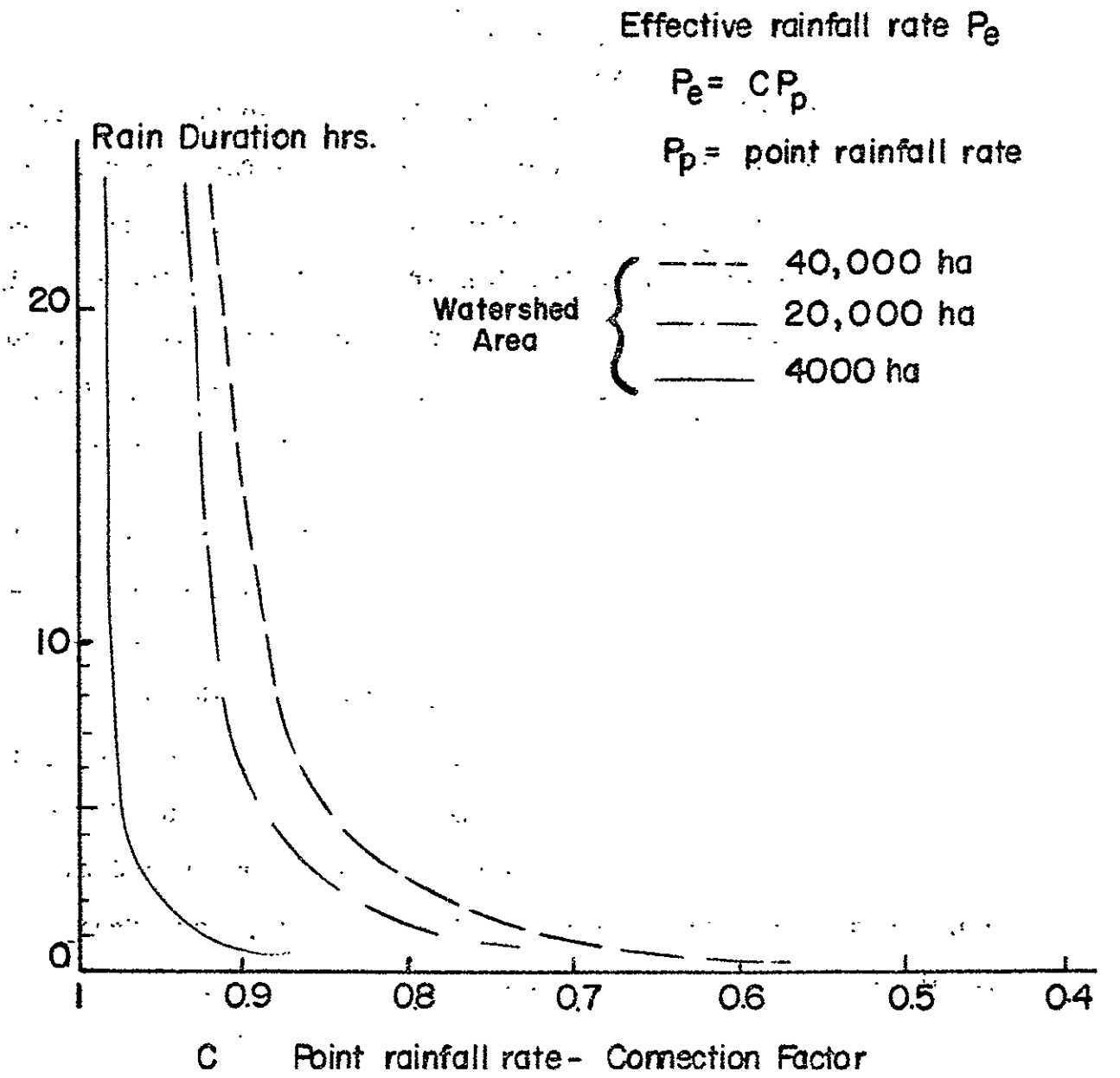

FIGURE 15

TIME OF CONCENTRATION VRS. AREA FOR BASINS OF DIFFERENT GEOMETRIES, SLOPE=0.1

FOR SLOPE=0.01, MULTIPLY T_c BY 2.43

$$T_c = .00013 \frac{(c\sqrt{A})^{.77}}{S^{.385}}$$

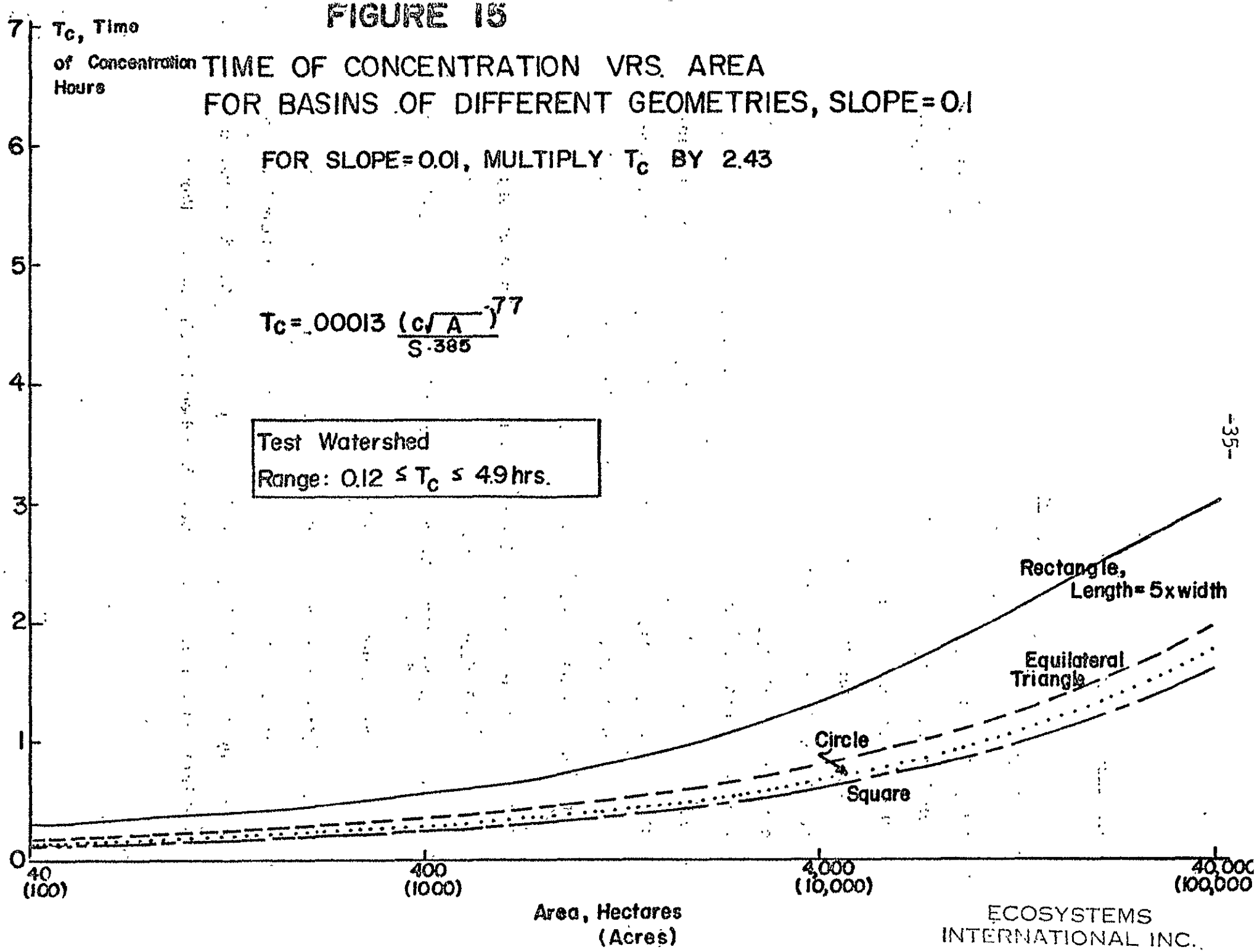

ECOSYSTEMS INTERNATIONAL INC.

3.2 Subsurface Processes

3.2.1 Subsurface Abstraction

A fraction of the rainfall reaching ground level will penetrate or infiltrate into the soil. This fraction -- or at least, the portion thereof that does not evaporate -- eventually becomes runoff via the subsurface flow mechanism. However, as will be shown, the runoff from the subsurface component is almost always considerably delayed with respect to the runoff from the surface component. Thus, except for very special cases, the portion of rainfall which is abstracted to the subsurface does not contribute to peak flow events. The fundamental role of the abstraction is to reduce the magnitude of the peak event. The crucial question, as regards hydrologic planning models, is thus: How much of the peak rainfall is abstracted?

There are three major drivers of subsurface abstraction:

- Soil permeability
- Soil storage capacity, a combination of porosity and soil depth
- Antecedent soil moisture

Permeability is conditioned by the degree of resistance to fluid flow through the soil. It is essentially determined by soil type and humidity. It is defined as a rate, in terms of centimeters per hour of water absorbed by the soil. For a

given type of soil, permeability assumes the largest value when the soil is dry; this is known as the initial permeability. As the soil becomes wet, permeability decreases, until it assumes a steady state value, known as the final permeability. Figures 16 a and b give initial and final permeability or infiltration rates, for the range of soils of interest to most hydrologic planning models.

Porosity, the percent of total soil volume available for water storage, does not per se affect the abstraction rate - also known as infiltration rate - but rather affects the amount of infiltrated water which may be stored. For a given soil porosity, the shallower the soil layer above the impermeable layer, the lesser the capability of the soil to store water. When this layer becomes saturated, infiltration into the soil ceases. If there are several layers of different porosity and depth, the one with the least permeability controls the process. If the soil layer is very deep with respect to the total rainfall, it can be essentially considered as an infinite layer. In this case, the subsurface abstraction is controlled only by the soil's permeability. Figure 16 c shows that highly permeable soils, such as sands and sandy loams, do not retain water well because they have low porosity. Less permeable soils such as clays, however, have higher rates of water retention, due to high percentages of porosity.

REPRESENTATIVE PHYSICAL PROPERTIES OF SOILS

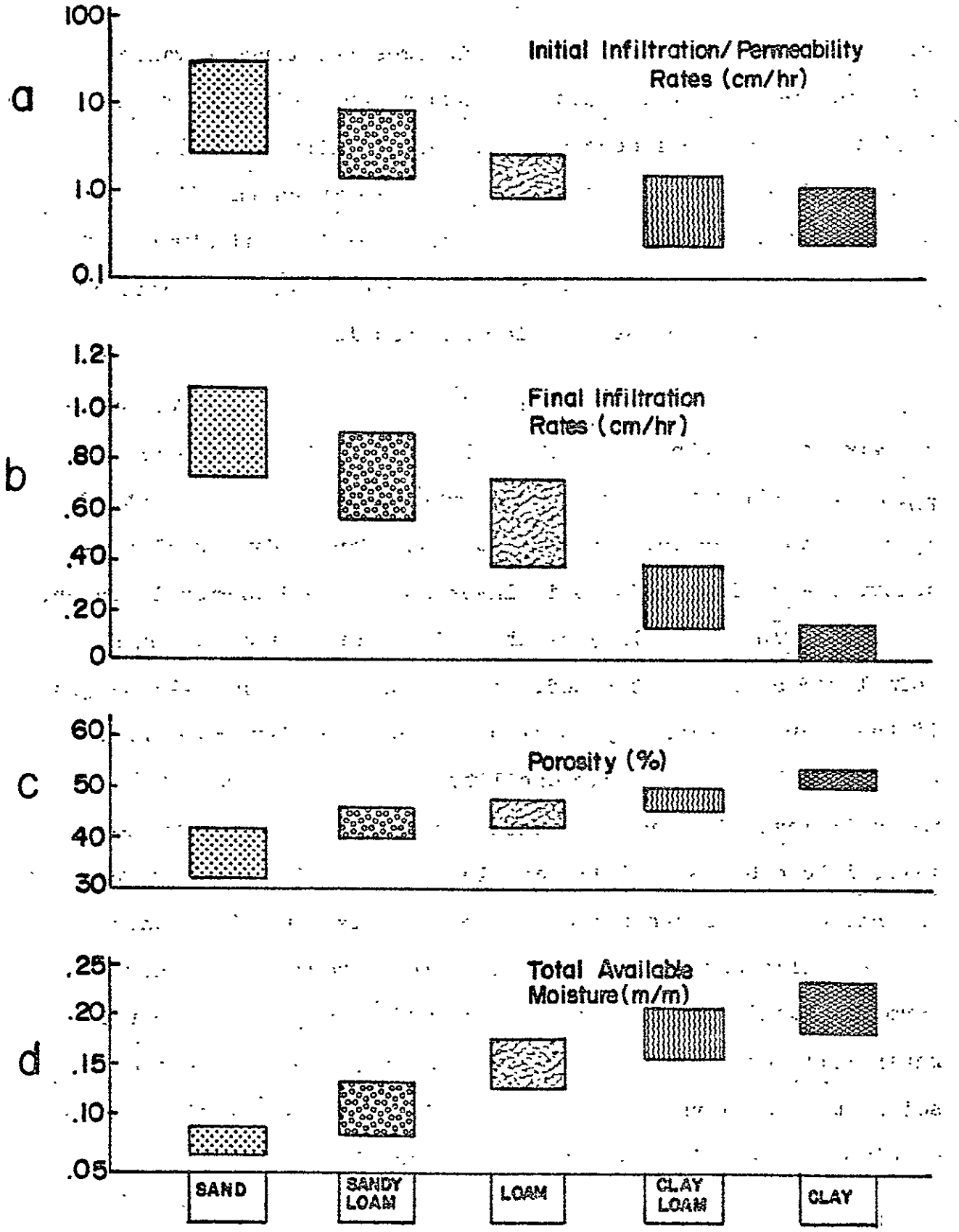

FIGURE 16

Available moisture capacity is the total amount of water which a given depth of a given type of soil can store. It is a measure of the maximum amount of water which can fill all the available pore space. Figure 16 d lists the available moisture capacities for various types of soils. Soils with low infiltration rates and high porosities have larger values of available moisture capacity than do soils with high infiltration rates and low porosity.

Antecedent moisture is the amount of water already present in the soil at the beginning of a rain event, and has the effect of reducing available moisture capacity and infiltration rates. Its net effect upon the peak runoff event is to increase its magnitude, the more so the greater the antecedent moisture. What this means, in effect, is that a peak rain event of a given recurrence does not necessarily generate a peak runoff event of the same recurrence: the 50-year flood does not necessarily correspond to the 50-year rain. It can, in fact, be generated by two lesser rains - for example, 20-year rains - occurring sufficiently close together in time.

In hydrologic management models, antecedent soil moisture is handled by computing the net difference between the water infiltrated into the soil and the water lost through evapotranspiration, over an interval of time preceding the event under study, which interval can range upwards of a few months.

In hydrologic planning models, the antecedent soil moisture must be evaluated by using statistical methods yielding the probability, in a given region, of having a certain sequence of peak rain events, separated by specified time intervals. This investigation is reserved for future phases of this research effort.

Factors such as slope, water turbidity, and temperature also have an effect on subsurface abstraction, but the magnitude of their influence is negligible when compared to the influence of permeability, porosity and antecedent moisture.

Figure 17 shows the effect of soil permeability upon infiltration for two "infinite" soils in Prince George's County, Maryland, derived from an analog computer simulation. For a given rain event, the low permeability of one of the soils (Leonardtown silt loam) causes reduced infiltration and increased runoff mass; the high permeability of the other soil (Croom gravel loam) allows a higher rate of infiltration, and a consequently lower runoff mass. Therefore, a watershed composed of deep Leonardtown silt loam would discharge more runoff and have a shorter time of concentration (i.e., would produce peak runoff faster) than would a similar watershed made up of Croom gravel loam.

Figure 18 illustrates the importance of soil storage capacity (porosity and depth combination) to infiltration and runoff.

FIGURE 17 EFFECT OF INFILTRATION UPON RUNOFF PRINCE GEORGE'S COUNTY 50 YEAR, 3 HOUR RAIN

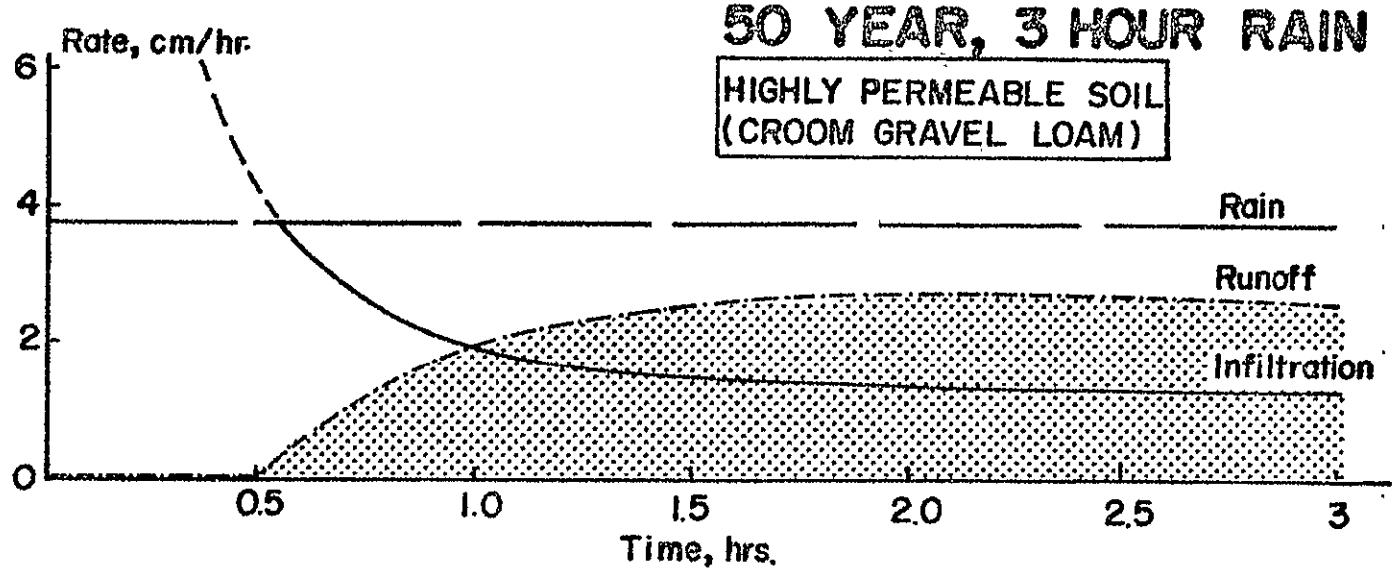

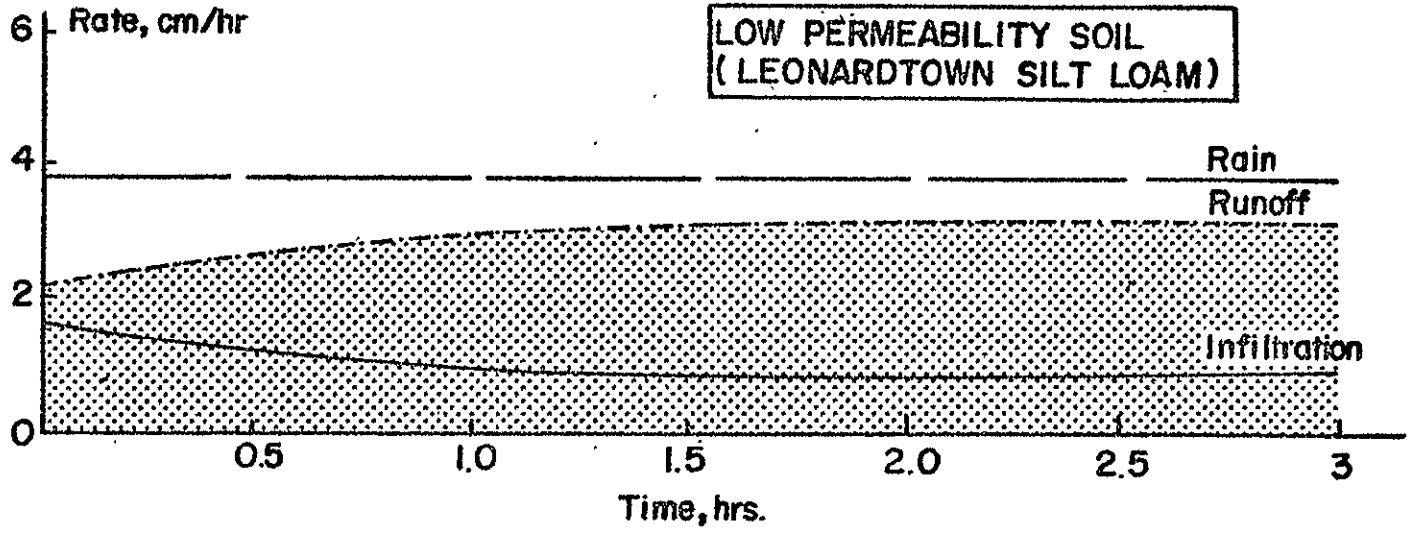

FIGURE 18 INFLUENCE OF SOIL DEPTH UPON RUNOFF

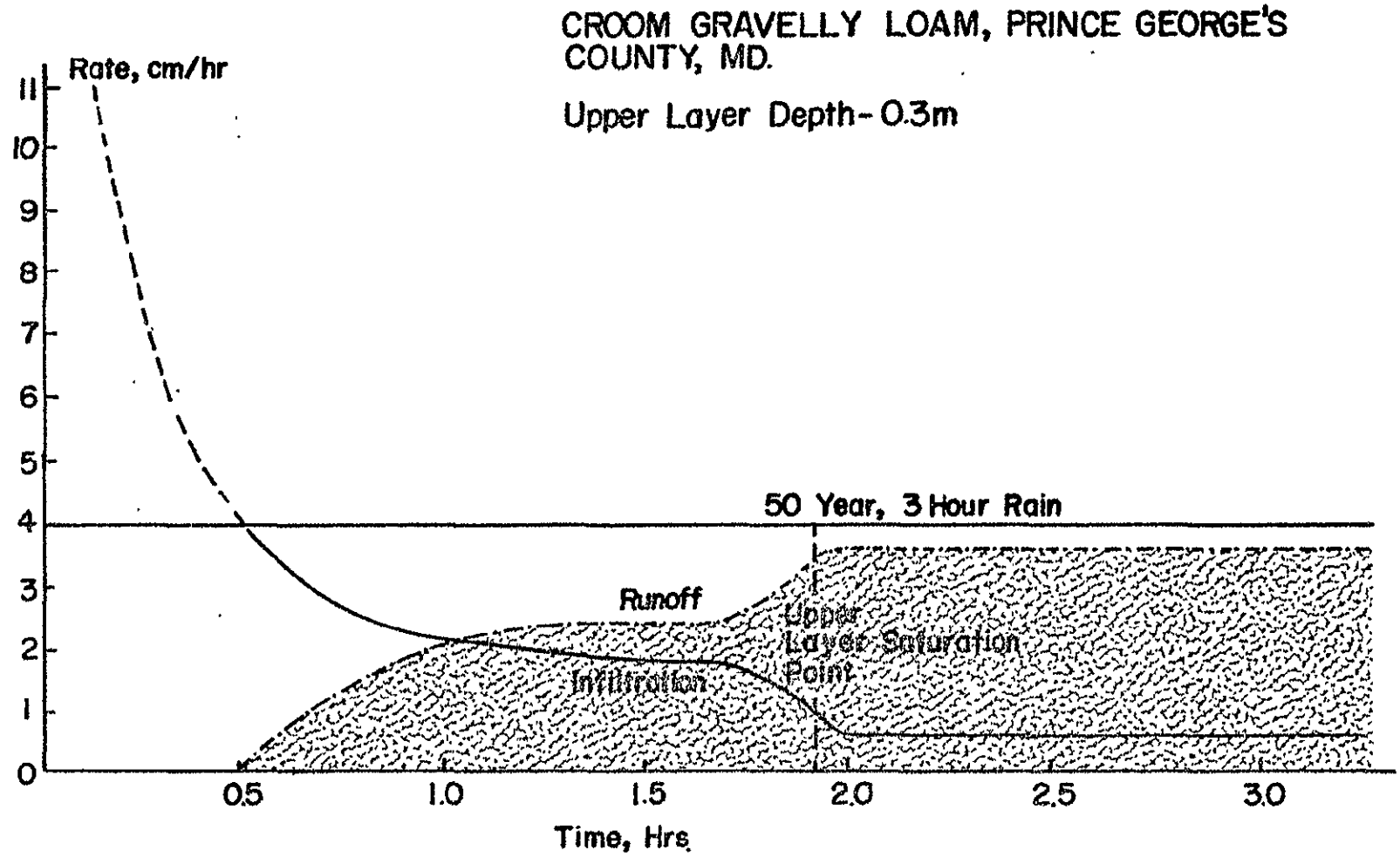

ECOSYSTEMS INTERNATIONAL INC.

Here, the finite depth of the upper layer of soil limits total available storage. When the upper layer becomes saturated, there is a sudden drop in the effective infiltration (or abstraction) rate because there is no more storage available. The water cannot sink as readily into the soil; consequently, the runoff increases.

Figure 19 demonstrates the effect of antecedent soil moisture on infiltration and runoff. Initially dry soil accepts water readily; therefore, time to beginning of runoff is high and runoff mass is low. However, when there is a large percentage of moisture already in the soil, less water infiltrates; the runoff begins earlier in time and mass is larger.

Although a great deal of research has been conducted in the area of subsurface abstraction, no consensus presently exists as to which mathematical formulation best describes the process. Table 4 lists the most widely applied formulations for the effective infiltration. These include the effects of permeability, storage capacity and antecedent soil moisture. Most of the equations basically describe an exponentially decaying function which finally declines to a finite value equal to the saturated conductivity of the soil. The Holtan equation, graphed in Figure 20 using actual data from the Danville, Vermont watershed, is illustrative.

EFFECT OF ANTECEDENT SOIL MOISTURE CONTENT ON INFILTRATION AND RUNOFF

CROOM GRAVELLY LOAM, PRINCE GEORGE'S COUNTY, MD.

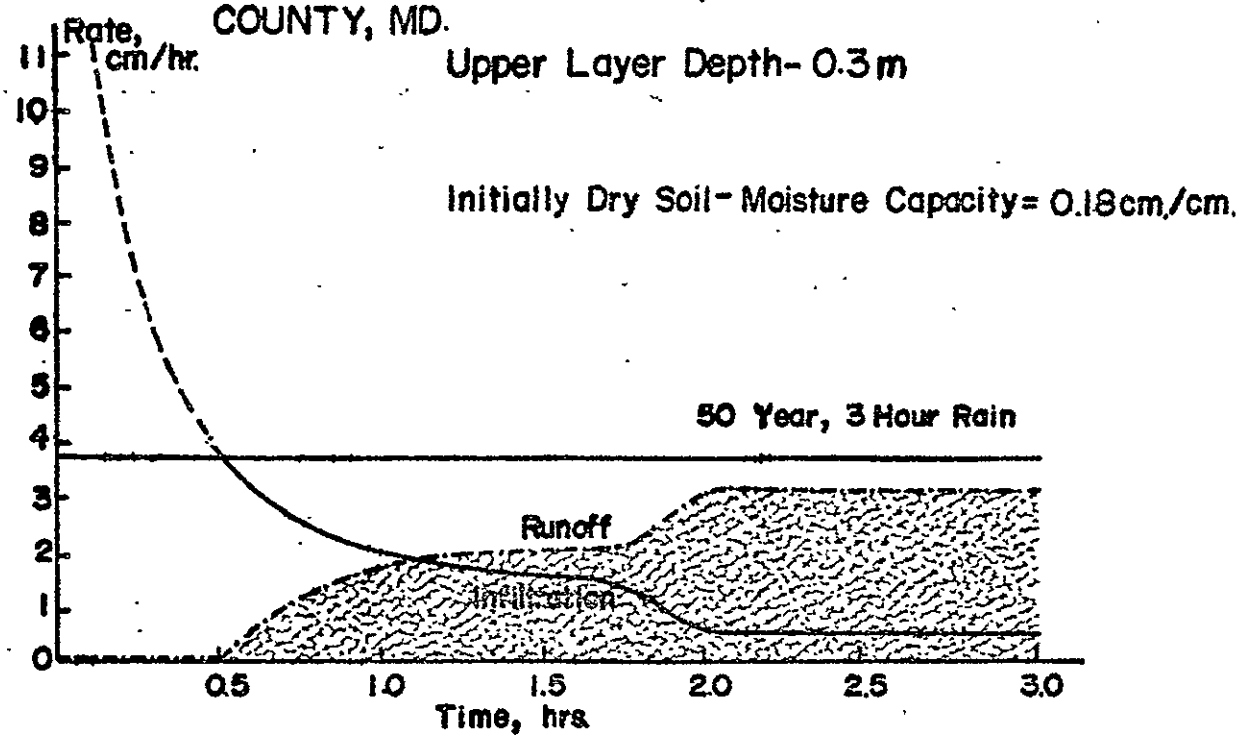

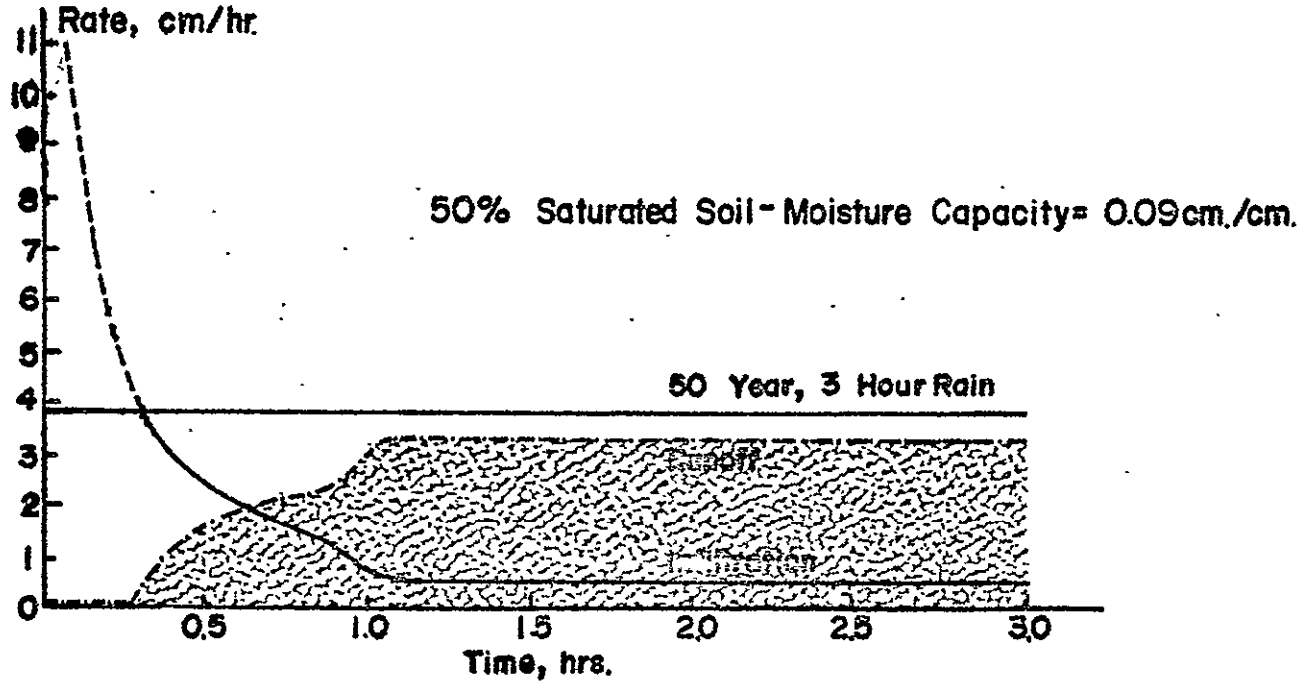

FIGURE 19

Table 4

Principal Infiltration Formulations:

Kostiakov

$I = Kt^{a}$

where K, a = constants, empirically determined; no physical significance

Horton

$$I = \dot{I}_f t + \frac{(\dot{I}_o - \dot{I}_f)}{B}\left[1 - e^{-Bt}\right]$$

$$\dot{I} = \dot{I}_f + (\dot{I}_o - \dot{I}_f)e^{-Bt}$$

where B is dependent on soil and rain characteristics

Green & Ampt

a) $\frac{K}{f}t = {}^{L - \Phi}L\left[\ln\left(\frac{(L + L)}{\Phi L}\right)\right] I = fL$

where L = depth to wetting front

ΦL = matric potential of wetting front

K = soil permeability

f = soil porosity

b) $fp = K_s \; I + (M_d \cdot S/F)$

$$\dot{I} = If + \left(\frac{MdS}{I}\right)\dot{I}f$$

where fp = infiltration capacity

K_s = saturated conductivity $\dot{I}f$

M_d = initial moisture deficit, vol./vol.

S = capillary suction, ins.

F = cumulative infiltration

Phillip

$Q = At^{1/2} + Bt$

$\dot{Q} = 1/2\,At^{-1/2} + B = \dot{I}$

where A, B = empirically determined constants - no physical relation

Holtan

$\dot{I} = .62\,kSr^{1.387} + fc$

where Sr = available porosity = $S_o - F_p$

k = vegetative cover constant

fc = final infiltration rate

Fp = cumulative infiltration to time of fc

numerical constants are empirically determined

Table 4 (cont'd)

Principal Infiltration Formulations:

Holtan; Overton (Huggins & Monk Modification)

$$\dot{I} = \dot{I}f + A\,[(S-I)\,T_p]$$

where A, B = constants characteristic of a given soil & antecedent condition

S = storage potential of soil within infiltration control zone = total porosity - antecedent soil moisture

T_p = total soil porosity

Richards

$$\frac{\partial \theta}{\partial L} = \partial\left[K\left(\frac{\partial H}{\partial x}\right)\right] / \partial x - \frac{\partial K}{\partial x}$$

where θ = water content = $\frac{\text{water volume}}{\text{unit soil volume}}$

K = capillary conductivity

H = height of water column; head

x = depth

FIGURE 20
INFILTRATION RATE vs. TIME FOR DANVILLE, VERMONT WATERSHED

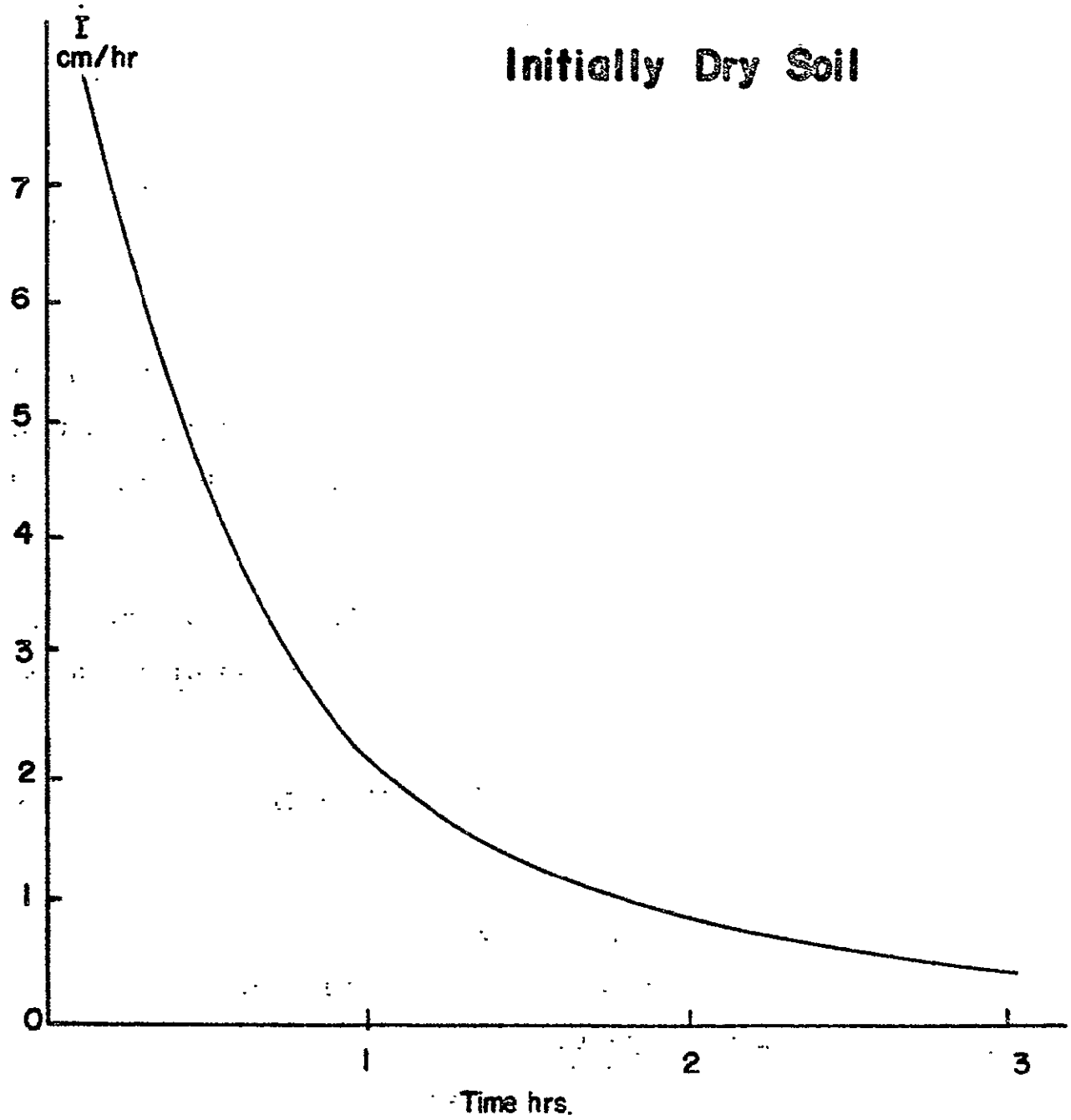

In spite of differences in the mathematical expressions, computations for two of the most widely used formulas (Holtan and Horton), shown in Figure 21, with the same initial and final conditions, indicate that the differences in the results are relatively small. A lesser-used formulation, that of Green and Ampt, yields a different end infiltration when normalized to the same initial conditions as the other two formulations. Conversely, the Green and Ampt formula yields different initial conditions when normalized to the same end-conditions.

Approximately similar overall results can be obtained by deciding, case by case, whether it is more representative to favor initial or terminal conditions. For short rains, for example, initial conditions control.

The Holtan formulation was tentatively and temporarily selected for use in the model on the basis of its suitability to remote sensing:

$$\dot{I} = \bar{a} \cdot GI \cdot (\overline{Sa} - I)^{1.4} + \dot{I}f$$

Where:

$\dot{I}$ = infiltration rate

$\bar{a}$ = average vegetative cover factor

GI = growth index

$\overline{Sa}$ = average available soil moisture capacity

I = cumulative subsurface abstraction

$\dot{I}f$ = final infiltration rate equal to saturated conductivity

FIGURE 21 INFILTRATION FORMULATIONS

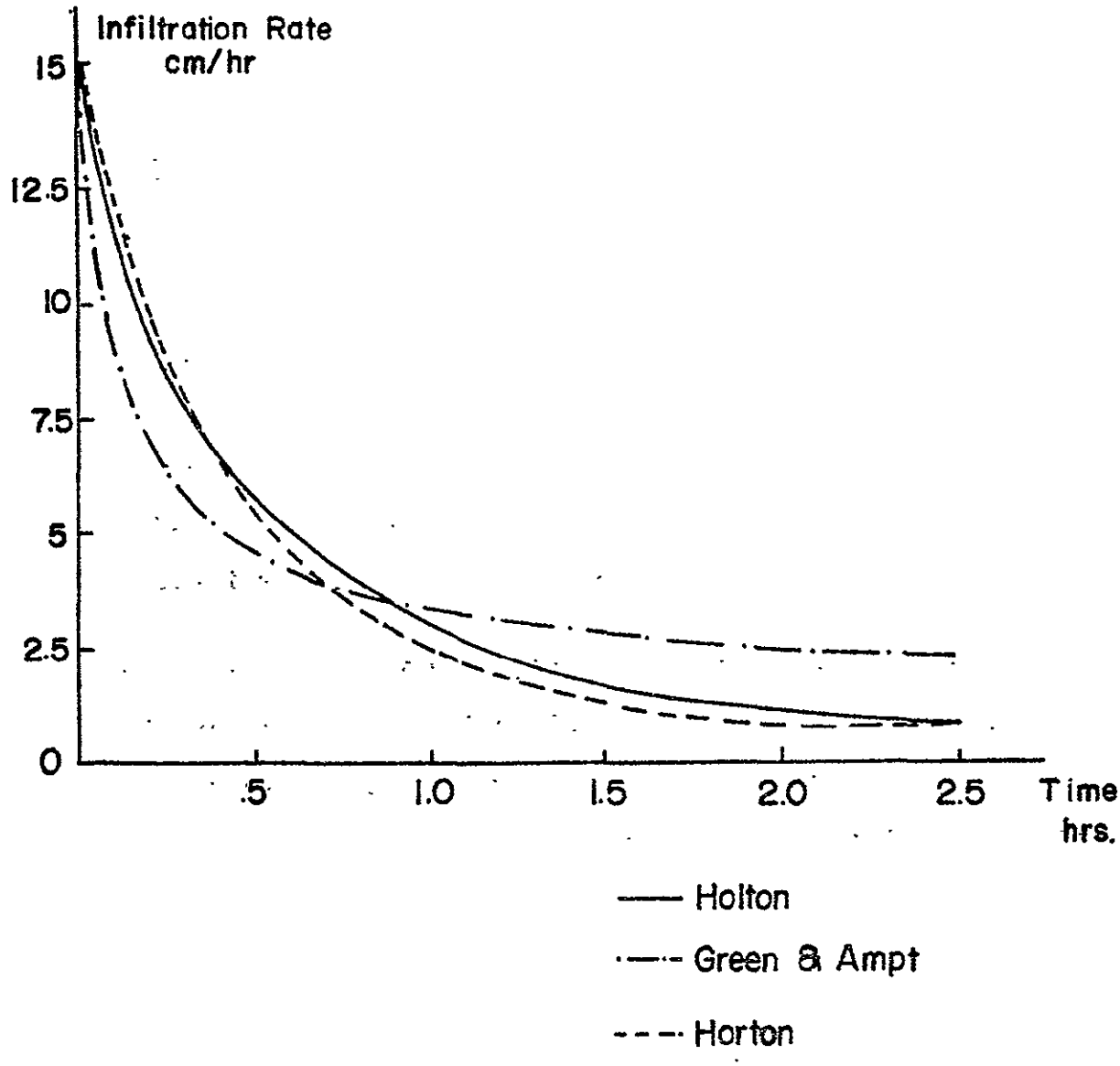

There are two advantages in using Holtan's equation:

1. It includes several of the physical factors which affect infiltration: surface type (determined by vegetative cover), permeability (included in the If term), and available soil moisture capacity.

2. All of the factors included can be determined or at least inferred from surface observations, with $\bar{a}$ and GI being directly measurable. Values of $\bar{a}$ can be determined by identification of the existing cover and GI values in a range of 0 - 1.0 represent the maturity of the agricultural cover or crops present, with a value of 1.0 equalling maturity. Storage capacity and final infiltration rate are both inferrable from soil type and soil moisture.

In conclusion, infiltration rates, given earlier in Figure 16, vary from as low as 0.13 cm/hr to as high as 25 cm/hr, rain rates vary within the same range. Thus effective infiltration rates are a substantial percentage of total rainfall rates. Infiltration is, therefore, a critical driver in any hydrologic planning model.

3.2.2 Percolation and Interflow

The remaining subsurface processes are percolation and interflow. Percolation is the process by which infiltrated water drains deep into the soil to eventually become groundwater. Interflow is the process by which infiltrated

water flows laterally, eventually becoming surface runoff. To have significant impact upon hydrologic planning models, percolation and interflow must be of sufficient magnitude to significantly alter the runoff mass. Also, the water involved must reach the watershed outflow point in time to contribute to the runoff peak.

In real watersheds, with possibly rare exceptions, neither of the above requirements is met. Rates of percolation and interflow are low to negligible compared to those of overland flow, as computed in Table 5 and summarized in Figure 22. This difference in speeds is due partly to the fact that during a peak flow event, the pressure of water flowing in the channel is opposed to the flow of subsurface water, thus retarding the inclusion of subsurface water in the outflow volume.

3.3 Evapotranspiration

Evapotranspiration combines two processes:

- Evaporation - the loss of water to the atmosphere.
- Transpiration - the process by which water is drawn out of the soil and transpired by vegetation.

Evapotranspiration can account for direct losses of precipitation and for losses of stored, infiltrated, and intercepted water.

TABLE 5

AVERAGE INTERFLOW RATES

$$\text{Avg. Interflow} = \frac{(1 - \frac{Q}{P})\,\bar{P}\ \text{in/hr.}}{365 \times 24}$$

Region	$\bar{P}$ in/m	$\bar{Q}$ in/m	$1-\frac{\bar{Q}}{\bar{P}}$	$\overline{\text{Int.}}$ "/hr.	$\overline{\text{Int.}}$ cm/hr	$\frac{\overline{\text{Int.}}}{\text{P100yr, 5hr}}$	$\frac{\overline{\text{Int.}}}{\text{P25yr, 24hr}}$
A	34.7	17.2	.50	.002	.005	.06%	1.0%
B	35.9	11.5	.68	.003	.007	.06%	1.2%
C	36.2	8.2	.78	.003	.008	.06%	1.4%
D	37.5	9.0	.76	.003	.008	.05%	1.1%
E	49.5	14.5	.71	.004	.010	.06%	1.0%
F	48.6	8.8	.82	.005	.012	.08%	1.7%
G	29.1	5.1	.82	.003	.007	.06%	1.4%
H	11.4	0.56	.95	.001	.003	.03%	0.8%
I	25.5	3.7	.85	.002	.006	.04%	1.2%
J	26.6	1.6	.94	.003	.007	.04%	1.0%
K	29.9	4.9	.83	.003	.007	.04%	0.9%
L	19.8	0.42	.98	.002	.006	.03%	0.8%
M	10.4	0.40	.96	.001	.003	.04%	0.9%
N	11.1	0.50	.96	.001	.003	.03%	0.8%
O	17.7	2.8	.84	.002	.004	.08%	1.7%
P	16.9	3.6	.79	.002	.004	.09%	1.8%
Q	no $\bar{P}$ or $\bar{Q}$ records				$\bar{x}$	.05%	1.17%
					σ	.02%	.34%

A, B, C..... = Watershed Location

$\bar{P}$ = Avg. Annual Rainfall

$\bar{Q}$ = Avg. Annual Runoff

$\overline{\text{Int}}$ = Avg. Interflow rate

FIGURE 22

OVERLAND FLOW AND INTERFLOW RATES FOR DIFFERENT SOILS AND COVERS SLOPE = 0.1

SURFACE FLOW - depth of flow = 0.25-0.50cm

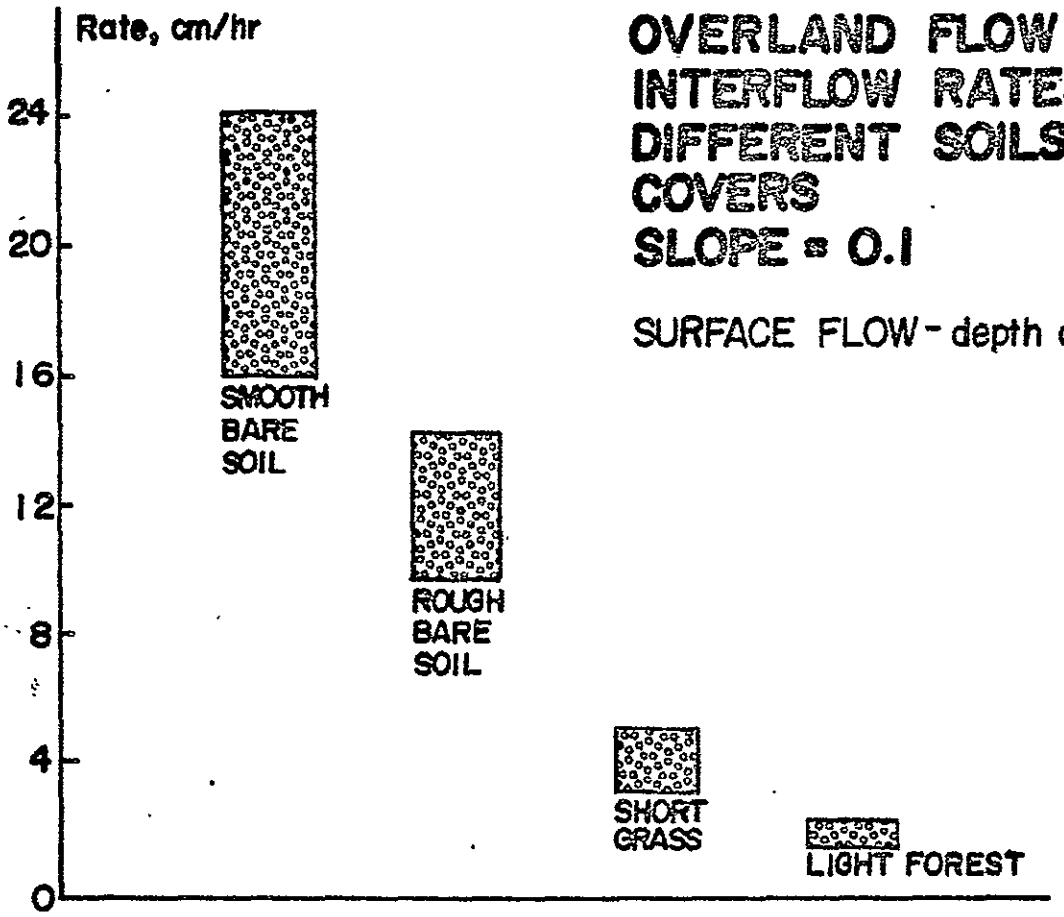

SUBSURFACE FLOW

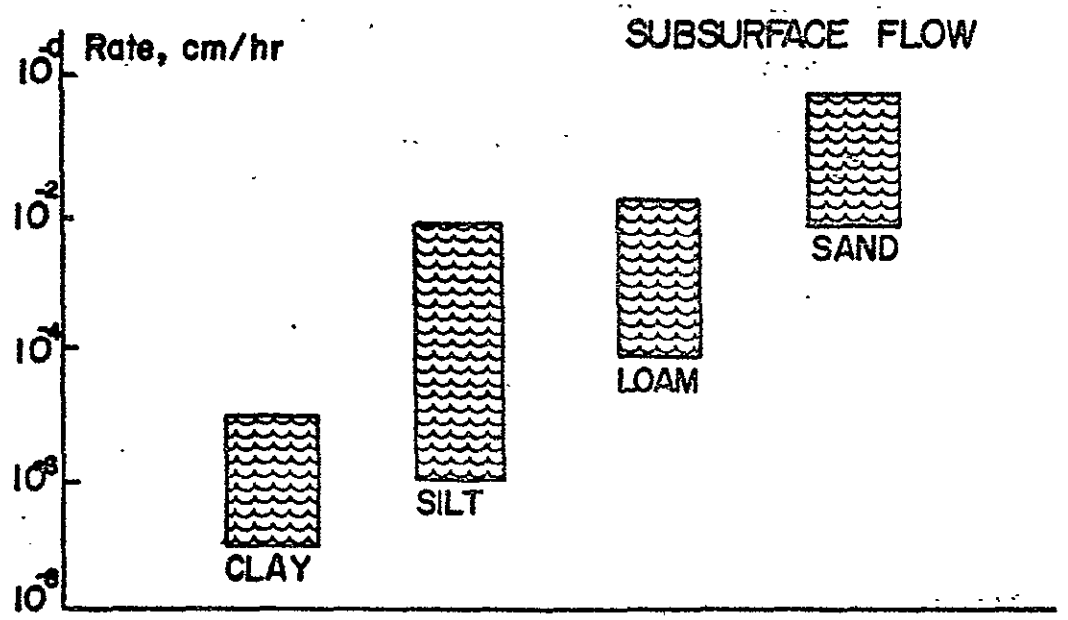

There are five major drivers of evapotranspiration:

- Temperature
- Solar Radiation
- Antecedent Soil Moisture
- Soil Permeability
- Vegetative Cover

Temperature and solar radiation are related since they both function in determining amount of heat present in the air. When the air temperature is high, evapotranspiration rate is also high since available moisture evaporates quickly. When the air is cool water evaporates more slowly and evapotranspiration rate is low.

Evapotranspiration is also affected by antecedent soil moisture, since the process can continue only as long as moisture is present in the soil or on the surface. Once this moisture is depleted, evapotranspiration must necessarily cease, even if other drivers are present.

Soil permeability determines the rate at which water can move upward through the soil, just as it influences the rate of infiltration. Soil permeability, which is determined by soil type, and rate of evapotranspiration are less for clay soils which resist movement of water through the soil than for sandy soils which have low resistance to fluid movement.

ORIGINAL PAGE IS
OF POOR QUALITY

Vegetative cover is important because plants transpire differently. In an area where there are not plants, evapotranspiration involves evaporation only and its rate will be determined solely by the rate of evaporation. However, in an area where vegetative cover is heavy, rate of transpiration must also be considered.

Other factors also influence evapotranspiration. Wind, for example, functions in removing moist air from above vegetation and water turbidity or muddiness slows down the rate of evapotranspiration. However, the influence of these factors is quite small compared to the effect of temperature, solar radiation, antecedent soil moisture, soil permeability, and vegetative cover.

To ascertain the importance of evapotranspiration relative to other parameters, average rates were calculated from the ARS test watershed data, using the Thornewaite equation:

$$\text{Avg. ET} = .022 \left(\frac{10t}{TE}\right)^a$$

Where:

Avg. ET = average evapotranspiration rate, cm/hr.

t = mean monthly temperature, °C

$TE = \sum_{1}^{12} (t/5)^{1.514}$ for each month

$a = .000000675(TE)^3 - .0000771(TE)^2 + .01792(TE) + .49239$

Results are presented in Table 6. The maximum practical value is approximately 0.4 cm/day. When compared to rainfall and infiltration rates, this indicates that evapotranspiration occurring during peak events is unimportant to hydrologic planning models.

However, evapotranspiration preceding peak events is important, because its effect is that of depleting antecedent moisture, thus increasing the subsurface abstraction. For example, in regions where rate of evapotranspiration is high and the rainless period of long duration, antecedent moisture will be greatly reduced. For example, at an average rate of 0.4 cm/day, an area which experiences two storms spaced 8 days apart will lose 3.2 cm in upper soil layer water content between storms, significantly increasing storage capacity in the soil. Therefore, although evapotranspiration is minimal in its influence upon runoff, it is important in its effect upon soil moisture content.

This importance is a function of the available storage capacity. In shallow soils, for example, or in deeper soils with low porosity, the subsurface abstraction is a smaller fraction of the precipitation than for deep, porous soils. Hence, for the former type of soils, the antecedent moisture plays a relatively minor role. As we shall see, it is exactly these soils which are the most amenable to the construction of hydrologic planning models based upon

TABLE 6

AVERAGE EVAPOTRANSPIRATION RATE FOR THE TEST WATERSHED AREAS

Watershed Area	a*	Mean Temp. °C	Avg. Monthly Evaporation, cm	ET Rate (cm/hr)
A	1.25	8.61	3.32	0.005
B	1.69	15.56	5.49	0.008
C	1.72	16.03	5.65	0.008
D	2.21	19.74	7.04	0.010
E	2.51	21.12	7.69	0.011
F	1.42	11.39	4.07	0.006
G	1.36	10.00	3.61	0.005
H	1.57	13.25	4.56	0.006
I	2.31	20.19	7.24	0.010
J	2.51	21.12	7.69	0.011
K	3.20	24.37	10.35	0.014
L	1.44	12.78	4.75	0.007
M	2.21	19.73	7.03	0.010
N	1.48	13.71	5.06	0.007
O	1.17	10.00	4.29	0.006
P	2.43	20.66	7.40	0.010

* Thornwaite temperature efficiency correction

remote sensing techniques.

3.4 Interception

Interception is the process by which rainfall is prevented from reaching the ground to become runoff or infiltration. It is dependent upon duration and intensity of rainfall, upon the species, composition, age and density of vegetation, and upon the season of the year and the geography of the region.

Two factors limit the importance of interception to the hydrologic modeling of peak flow events. First, interception stores only small quantities of water. For example, in a basin completely covered by deciduous forest, and thus of highest interception capacity, interception will claim about 0.35 centimeters of a 3.5 centimeter rain. Thus, in practical cases but little of a peak rain will be subject to interception storage. Second, the time period required to fill interception storage is negligible. During a 1.8 centimeter per hour rain, for example, only approximately 15 minutes are required to saturate interception capacity. Rain intensities of interest to planning models are generally on the order of three to five times greater; saturation times will be proportionately smaller.

3.5 Depression Storage

Depression storage is similar to interception; it is the process by which water is retained at the surface by recesses, or shallow small pools, in the soil. It is determined primarily by depression density and retention of cover.

Like interception, depression storage is not a continuing process; it ceases when a fixed capacity is reached. Typical saturation capacities are 0.5, 0.375, and 0.25 centimeters for sand, loam, and clay soils, respectively. In the Washington, D.C. area, for example, only approximately 4% of the 50-year 1-hour rain would be stored by depression storage.

Depression storage is thus of minor importance to the modeling of peak flow events.

3.6 Overland Flow

During a peak event, the rate at which the excess rainfall over and above the subsurface abstraction contributes to streamflow is determined by the overland flow process. The process is shown schematically in Figure 23. The excess rainfall, i.e. the rainfall less the subsurface abstraction, flows over the surface until it encounters a natural channel. It is then conveyed from the higher-order channels into successive lower-order streams. In the channel, the

FIGURE 23
PRINCIPAL OVERLAND FLOW PARAMETERS

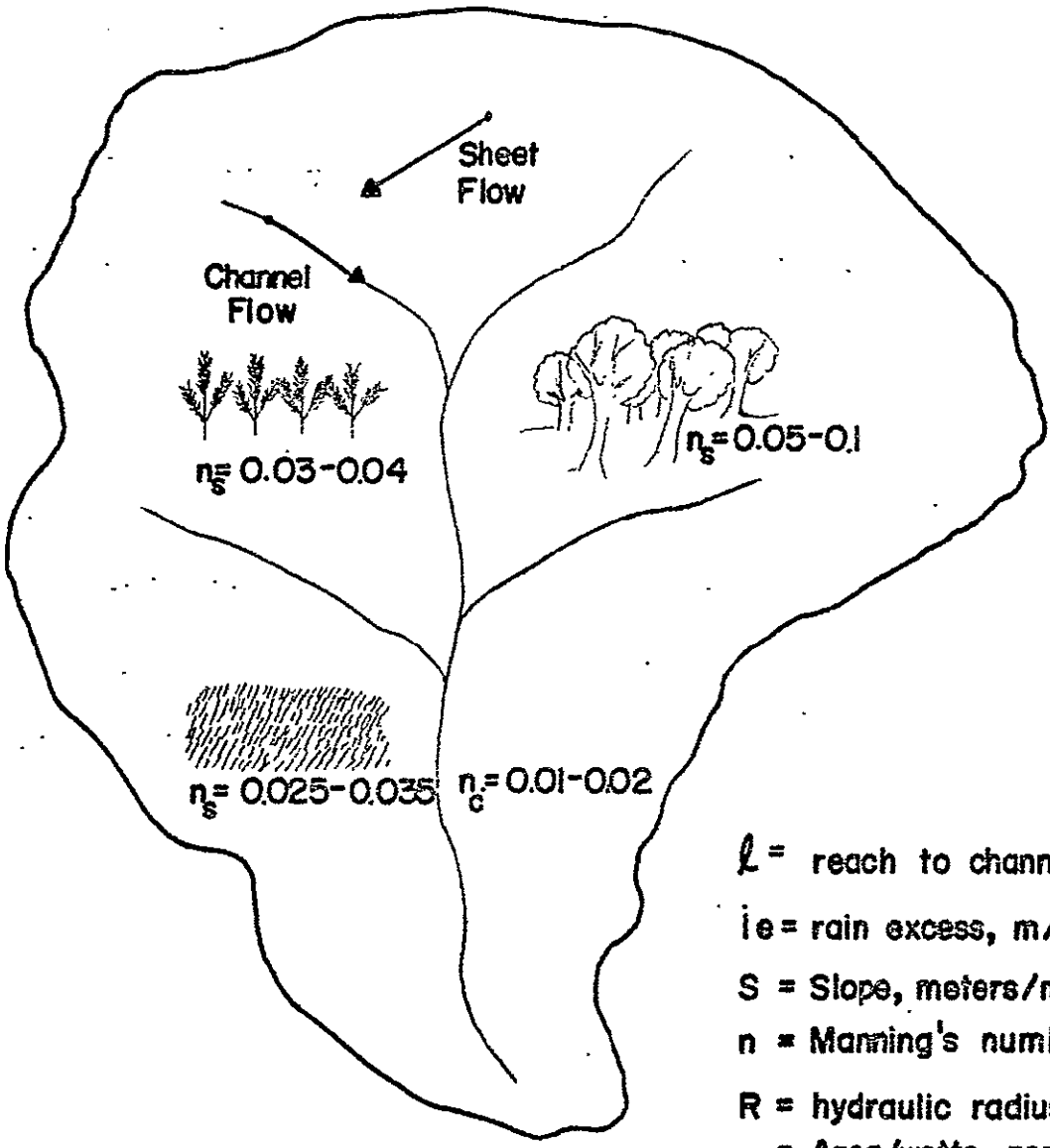

ℓ = reach to channel

ie = rain excess, m/sec

S = Slope, meters/meter

n = Manning's number

R = hydraulic radius =
= Area/wette perimeter

$$\mathcal{V}_{sheet} = \frac{S^{3/10}\ ie^{2/5}\ \ell^{2/5}}{n_s^{3/5}}$$

$$\mathcal{V}_{channel} = \frac{R^{2/3}\ S^{1/2}}{n_c}$$

water generally speeds up since it travels faster in the channels than over the surface, it would be expected that the time of concentration, i.e. the time required for the water to travel from the uppermost reach of the watershed to its outlet, would be shorter the more the number of channels per unit area of the watershed. The total length of the channels divided by the area of the watershed is known as the drainage density. It has been indicated in the literature, and demonstrated in this project, that the drainage density plays an important role in determining the magnitude of the peak flow event.

The rate of overland flow is governed by the following:

- Watershed slope
- Watershed cover
- Drainage density
- Channel pattern

The ground slope determines the magnitude of the gravitational force which induces flow of the water. The type and density of ground cover determines the frictional force opposing flow. Hence the combination of slope and cover is a determinant of flow velocity. The drainage density defines the average distance over which water must travel before reaching the stream. The channel pattern establishes the speed with which water is carried away by the channel

network. In combination with surface flow velocity, this defines the time of concentration.

In the literature, overland surface flow is generally considered to be sheet flow. The reason alleged is that the depth of flow is small, compared to its width, implying that viscous fluid forces predominate over those produced by inertia. Further, overland flow is often considered to be uniform; that is, no change in magnitude or direction takes place over the flow length. In this project, the assumption of sheet or laminar flow was retained as a preliminary working hypothesis, to be analyzed further for correctness if warranted by significant discrepancies between results and predictions from the model.

Overland surface flow can be quantified by assuming the land surface to be approximated by a wide channel. Since channel sides have minimal effect upon velocity when the channel width exceeds ten times the depth of flow, the hydraulic radius for overland surface flow becomes essentially the depth of flow.

Overland surface flow eventually reaches a channel; thence it is discharged into a sequence of ever-larger streams, as it proceeds towards the watershed outlet. The cross sectional geometry of natural channels is a major determinant of flow rate within the channel. Figure 24 graph-

FIGURE 24 COMPARISON OF FLOW OF CHANNELS OF DIFFERENT CROSS SECTIONS, ASSUMING SAME AREA AND TOP WIDTH

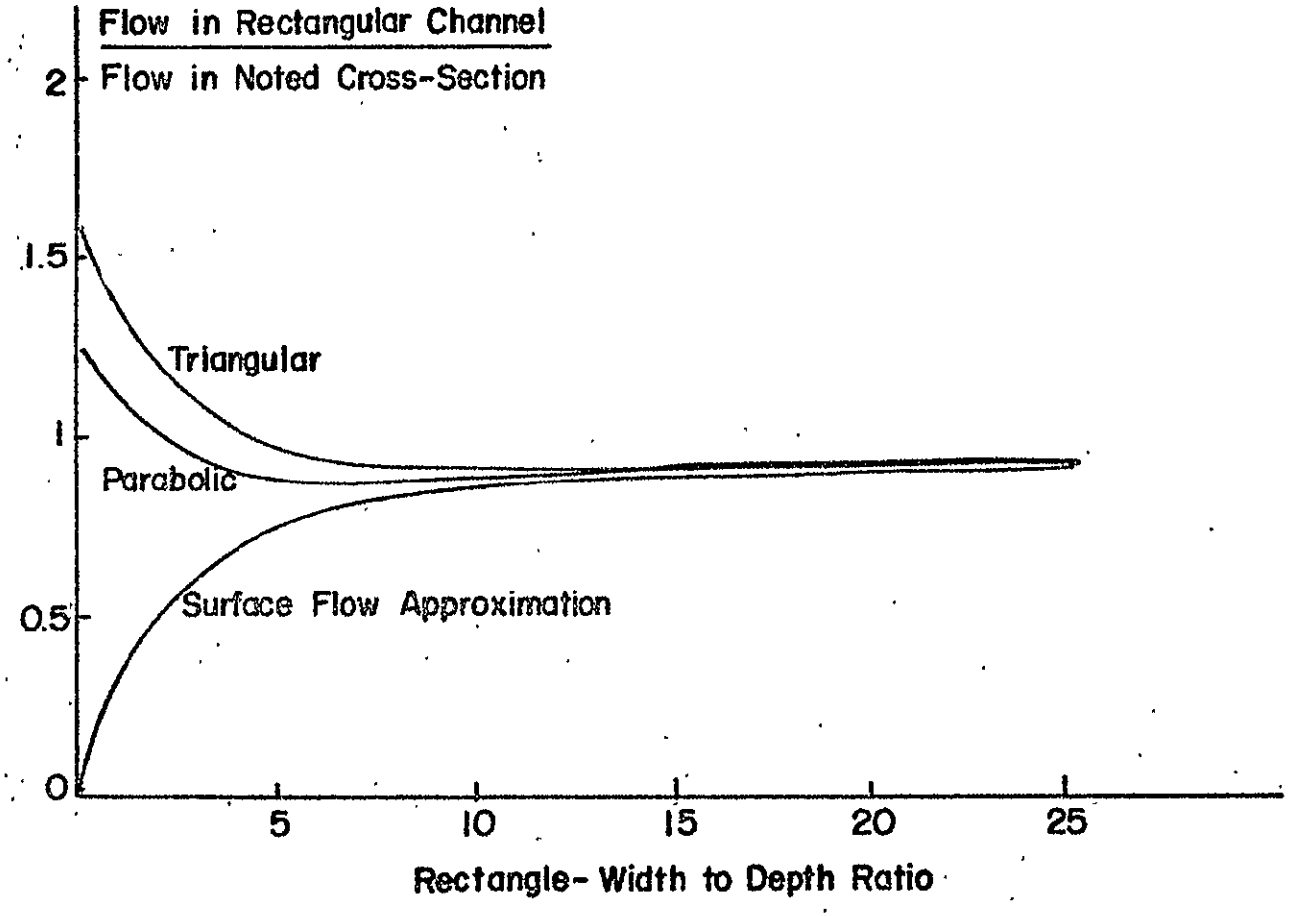

ically demonstrates its effect upon channel flow. As the width to depth ratio increases, the exact channel geometry becomes less important: the hydraulic radius can more and more be approximated by the depth of flow.

The particular cross sectional shape that evolves naturally in a stream is that which best balances the transmission of water and the structural stability of the banks. In channels with firm banks, for example, the shape most efficient to flow is parabolic. However, the cross sections of natural streams are not generally parabolic in shape but appear to be trapezoidal, at least in the stream's straight sections. Empirical evidence has shown that channels in the dry western states are usually wider and more shallow than those in humid areas.

The shape taken by channels is determined by the peak events of a stream rather than by its average flows, possibly because during peak events, the forces acting upon stream beds and banks are the highest. Typically, U.S. rivers carry less than their mean flow 60-75% of the time, and less than half of the mean flow about 25% of the time. Average annual discharge fills the channel to only approximately 1/3 of its bankfull depth. Bankfull discharge occurs about once every 1.5 years; a flood plain is inundated to approximately 1.8 times the bankfull depth of the channel once in fifty years.

The channel cross section changes as a function of its position along the stream axis. Progressing in the downstream direction, for example, discharge increases, causing stream geometry to alter. The channel's top width increases approximately as the square root of discharge. Also, because of higher flows, bed roughness tends to diminish. The trapezoidal shape becomes progressively more rectangular, since stream width increases faster than depth.

The Manning equation provides a good description of the relationship between the hydraulic parameters, roughness and mean channel velocity:

$$\underset{m/sec}{\text{Velocity}}\ (v) = \frac{1}{n} R^{2/3} S^{1/2}$$

Where:

R = hydraulic radius, m

S = slope, m/m

n = Manning's roughness coefficient, $m^{-1/3}$ sec

The hydraulic radius, defined as the cross sectional area of flow divided by the wetted perimeter, varies with channel geometry, as shown in Table 7. In natural channels, the variations are usually small. Since the top width is typically of the order of, or greater than, 10 times the depth, the hydraulic radius for all common cross sections may be approximated by the depth of flow without significant loss of accuracy.

Section	Area A	Wetted perimeter P	Hydraulic radius R
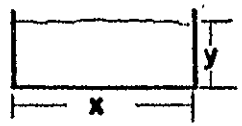	xy	$x + 2y$	$\frac{xy}{x+2y}$
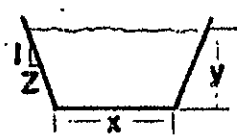	$(x+zy)y$	$x+2y\sqrt{1+z^2}$	$\frac{(x+zy)y}{x+2y\sqrt{1+z^2}}$
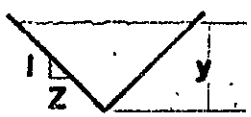	zy^2	$2y\sqrt{1+z^2}$	$\frac{zy}{2\sqrt{1+z^2}}$
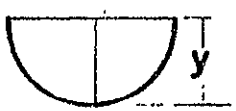	$\frac{\pi y^2}{2}$	πy	$y/2$
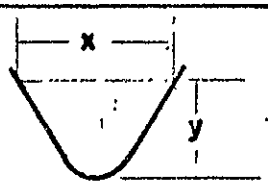	$2/3\,xy$ *	$x+\frac{8}{3}\frac{y^2}{x}$ *	$\frac{2x^2y}{3x^2+8y^2}$ *
Surface Flow 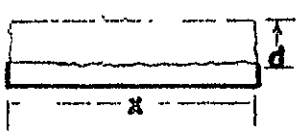	xd	x	d

* Approximate

TABLE 7 HYDROLOGIC PARAMETERS FOR DIFFERENT CHANNEL CROSS-SECTIONS

Thus, Manning's equation, for both overland surface flow and wide channels, becomes:

$$\text{Velocity } (v) = \frac{1}{n} d^{2/3} S^{1/2}$$

Where:

d = depth of flow, m

S = slope, m/m

n = Manning's roughness coefficient, $m^{-1/3}$ sec.

The corresponding equation for the flow is:

$$\text{Flow } (Q) = Av$$

m^3/sec

Where:

A = cross sectional area of flow, m^2.

Manning's roughness coefficient (n) is a measure of the frictional resistance of the surface to flow, due to the watershed's surficial characteristics. The roughness coefficient is a combination of the effects of various surface factors. The value of n for channel flow is influenced by the following factors:

- Roughness
- Presence of vegetation
- Irregularities
- Channel alignment
- Silting and scouring

- Obstructions
- Stage and discharge
- Seasonal change
- Suspended material and bed load

Similar effects are present in overland flow, although the magnitude and importance of each differs. Surface roughness, vegetation and seasonal change, for example, are much more important to overland flow than they are to channel flow, while silting and scouring, stage and discharge, suspended material and bed load are more important to channel flow.

Manning's n then can be written as:

$$\bar{n} = m\sum_{i}(n_i)$$

$\bar{n}$ = the effective Manning's n

n_i = contribution of roughness factors to n

m = meander factor

Typical values of the n_i and m are given by Vente Chow, Handbook of Hydrology, and are reproduced in Table 8.

For example, $\bar{n}$ for a gradually varying coarse gravel channel with minor irregularities, negligible obstructions, high vegetation, and minor meandering would be:

$$\bar{n} = (0.028 + .005 + .000 + .037)\ 1$$

$$= 0.07$$

Typically, $\bar{n}$ can range from 0.03 to 0.29.

Table 8

Channel conditions			Values
Material Involved	Earth	n_0	0.020
	Rock cut		0.025
	Fine gravel		0.024
	Coarse gravel		0.028
Degree of Irregularity	Smooth	n_1	0.000
	Minor		0.005
	Moderate		0.010
	Severe		0.020
Variations of Channel cross section	Gradual	n_2	0.000
	Alternating occasionally		0.005
	Alternating frequently		0.010-0.015
Relative Effect of Obstructions	Negligible	n_3	0.000
	Minor		0.010-0.015
	Appreciable		0.020-0.030
	Severe		0.040-0.060
Vegetation	Low	n_4	0.005-0.010
	Medium		0.010-0.025
	High		0.025-0.050
	Very high		0.050-0.100
Degree of Meandering	Minor	m_5	1.000
	Appreciable		1.150
	Severe		1.300

VALUES FOR THE COMPUTATION OF THE ROUGHNESS COEFFICIENT

ORIGINAL PAGE IS
OF POOR QUALITY

Typical values of n for different overland surfaces are given in Table 9. It is clear from these figures that land cover is significant in determining runoff. Differences in surface roughness can cause overland flow velocity to vary up to approximately eight times its minimum value.

Routing the runoff mass to the basin outlet involves consideration of both overland and channel flow. The difference between the two types of flow determines the amount of water stored on the surface or built up on the channel, and, therefore, the depth of flow and its rate.

3.7 Important Processes and Drivers for Hydrologic Planning Models

Figure 25 summarizes graphically the relative magnitudes of the principal hydrologic processes. The ranges of values shown in Figure 25 represent the ranges encountered in the 158 ARS test watersheds.

It is clear that the primary hydrologic processes which dominate peak flow events, and whose representation, therefore, must be included in a generalized watershed planning model, are rainfall, infiltration or subsurface abstraction, and overland flow. Secondarily, according to the region under consideration, the statistical behavior of antecedent moisture condition as it relates to peak rain-

Table 9

MANNING'S ROUGHNESS COEFFICIENT FOR OVERLAND FLOW FOR VARIOUS SURFACE TYPES

Watershed Surface	Manning's "N"
Smooth Asphalt	0.013
Concrete (Trowel Finish)	0.013
Rough Asphalt	0.016
Concrete (Unfinished)	0.017
Smooth Earth (Bare)	0.018
Firm Gravel	0.020
Cemented Rubble Masonry	0.025
Pasture (Short Grass)	0.030
Pasture (High Grass)	0.035
Cultivated Area (Row Crops)	0.035
Cultivated Area (Field Crops)	0.040
Scattered Brush, Heavy Weeds	0.045
Light Brush and Trees (Winter)	0.050
Light Brush and Trees (Summer)	0.060
Dense Brush (Winter)	0.070
Dense Brush (Summer)	0.100
Heavy Timber	0.100
Idle Land	0.030
Grass Land	0.032

FIGURE 25 RATES OF HYDROLOGIC PROCESSES

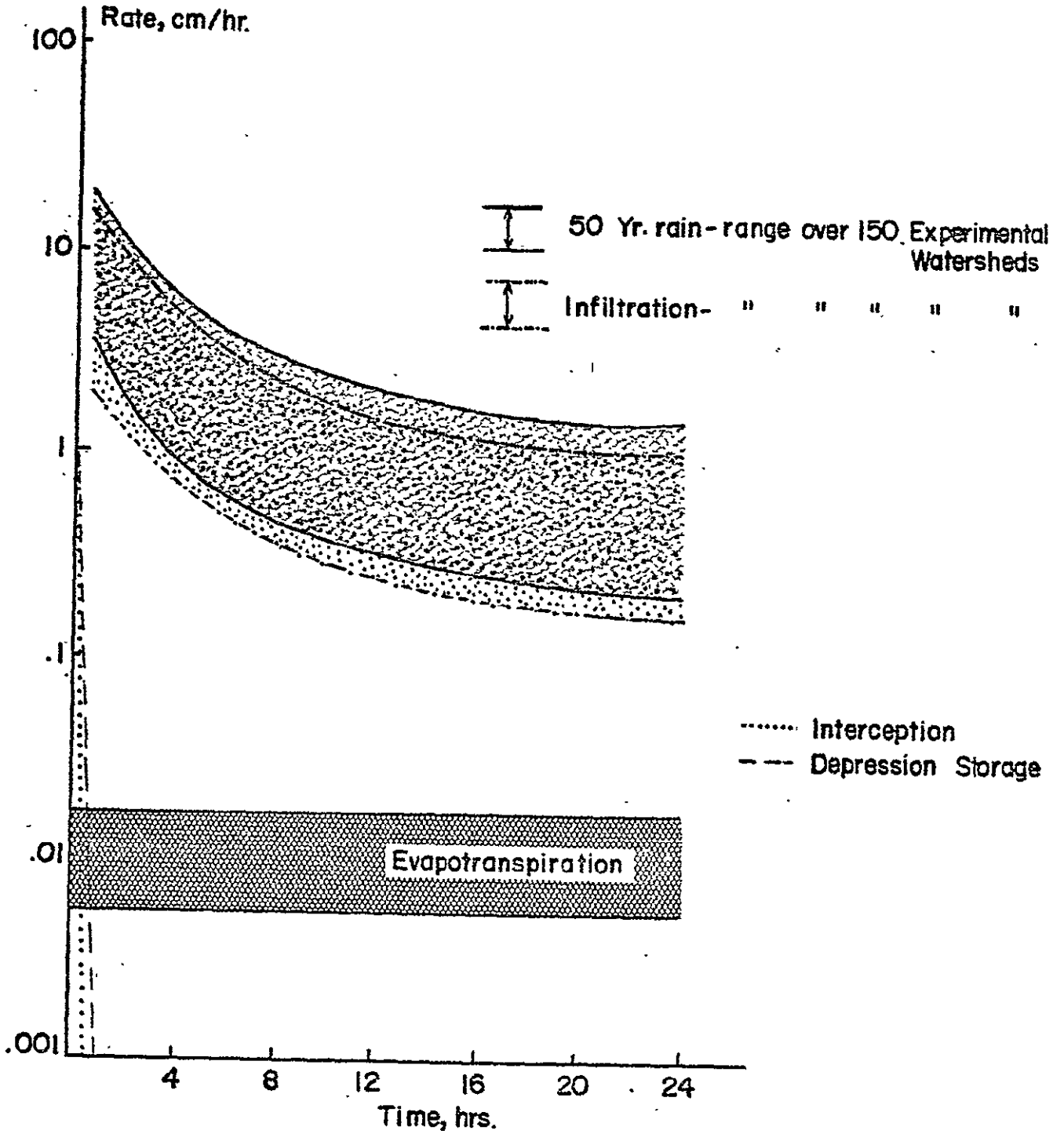

fall events must be included.

Rainfall is the principal causative factor defining the magnitude of the peak flow. Its important characteristics are the recurrence statistics, determined by empirical correlation of regional rainfall records.

Infiltration governs the portion of the rainfall which contributes to the direct runoff peak. It can be evaluated from watershed soil records, abundantly available.

The overland flow process and channel flow determines the timing of the peak. The timing in turn determines the rainfall rate and mass for a given recurrence frequency, and hence determines the peak flow. The overland flow can be modeled from knowledge of the surface characteristics of the watershed, which are directly amenable to remote sensing.

The key drivers of peak flow, in addition to rainfall statistics are:

1. Soil Permeability - high permeabilities mean high acceptance of water and smaller runoff mass.
2. Soil Water Capacity - a soil having a greater water water capacity will retain more rainfall and produce less runoff.
3. Antecedent Soil Moisture - as soil moisture rises, the soil becomes saturated, slowing infiltration

ORIGINAL PAGE IS
OF POOR QUALITY

rates, reducing total soil moisture capacity, and increasing the runoff volume.

4. Slope - flow velocity varies directly but non-linearly with slope.

5. Surface Friction - velocity varies inversely (and non-linearly) with surface friction.

6. Drainage Density and Pattern - defines the relative distances that water will flow overland and in the channel; in combination with slope and surface friction, defines concentration time.

A first-cut quantification of the sensitivity of the runoff volume, or of hydrologic quantities impacting runoff volume, to variations in these drivers is presented in Table 10.

Areas which are dominated by surface processes (i.e., produce the most surface water per volume of precipitation) will in general derive the most benefits from hydrologic planning models. Also, regions which are surface dominated are the best served by remote sensing.

The influence of temporal variations of watershed parameters - for example, caused by urbanization - well amenable to remote sensing, is more prominent in surface dominated regions.

Table-10 Sensitivity of Runoff to the Principal Drivers

Driver	Practical Range	Computed Effect Upon Runoff
Slope	0.01 to 1.0 m/m	10 x increase in flow rate (Manning)
Surface Friction	0.01 to .10 $m^{-1/3}$ sec	10 x decrease in flow rate (Manning)
Drainage Density	1/100 to 1/10000 m/m^2	Up to approx 10x decrease in flow velocity
Antecedent Soil Moisture	0 to 100% of available capacity	Up to 2x decrease in runoff volume
Soil Water Capacity	0 to 60% of upper soil layer volume	Up to 2x decrease in runoff volume
Soil Permeability	0.0025 to .25 m/m	Up to 10x decrease in rate of precipitation excess buildup

Data acquired from the 158 test watersheds, a summary of which is contained in the Appendix, provides the basis for partitioning the United States into areas possessing either surface-dominated or subsurface-dominated hydrologic regimes. From rainfall and runoff data, average annual precipitation ($\overline{P}$) and average annual discharge ($\overline{Q}$) were calculated for all test basins over the period of record. $\overline{Q}$ divided by $\overline{P}$ yields a first-cut measure of the propensity of a watershed to discharge. Figure 26 gives $\overline{Q}/\overline{P}$ numbers for the regions in which the test watersheds are located. On the basis of these calculations, an initial partition of the United States into 3 categories of hydrologic regimes appears as in Figure 27. The three regions are:

1. Heavily Surface Dominant - Where the percentage of rainfall to runoff significantly exceeds the percentage of rainfall to infiltration.
2. Surface Dominant - Where more rainfall runs off than infiltrates.
3. Subsurface Dominant - Where more rainfall infiltrates than runs off.

It is interesting to note that the regions which are surface dominated are also those which have historically experienced the greatest flood damage.

FIGURE 26

AGRICULTURAL RESEARCH BASINS 100-100,000 ACRES

Average Annual Runoff ÷ Average Annual Precipitation

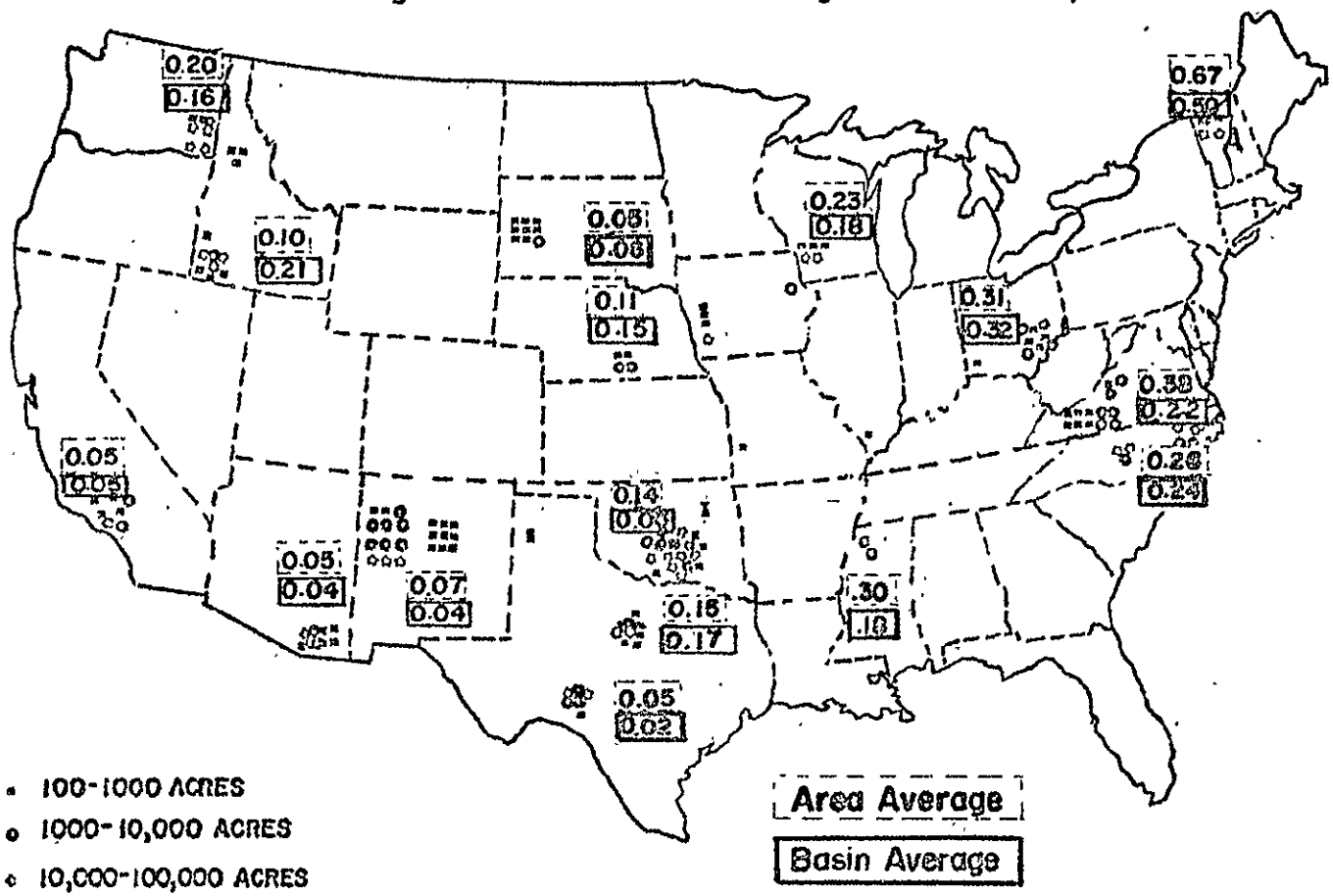

INITIAL PARTITION
BASED UPON
AGRICULTURAL RESEARCH BASINS 100-100,000 ACRES

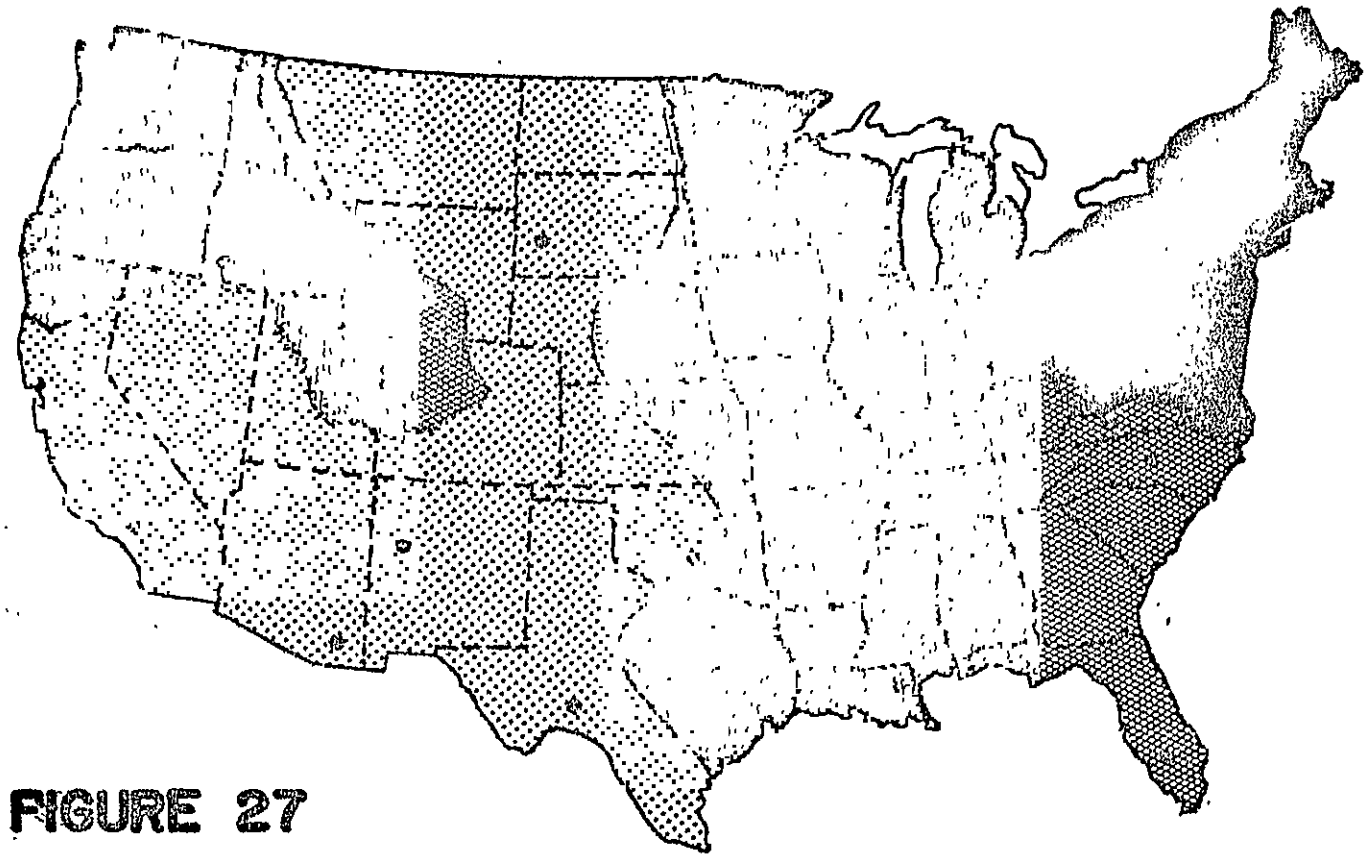

FIGURE 27

Heavily Surface Dominant

Surface Dominant

Subsurface Dominant

4.0 GENERALIZED HYDROLOGIC PLANNING MODEL

This project attained two milestones towards the achievement of a hydrologic planning model:

1. An overall framework was formulated.
2. A number of segments, or modules, were constructed, each modeling a distinct hydrologic process.

What remains to be done is to connect and integrate the various modules into a single model.

The modules consist of, and the integrated model is expected to consist of, analytic expressions suitable for digital or analog computer programming.

The analytic procedure was supplemented by an analog computer simulation, which was oriented primarily at establishing the sensitivities of the runoff to variations in the important watershed parameters: soil permeability, antecedent soil moisture and total storage capacity (soil depth). The advantages of the analog simulation were found to be:

1. Flexibility and ease of variation of rates and magnitudes of the physical parameters.
2. Adequacy in representing the physical phenomena, yet with relatively small computer hardware.

Figure 28 is a block diagram of the analog computer model developed.

FIGURE 28 ANALOG CIRCUIT FOR

CONSTANT RAIN WITH EXPONENTIALLY DECAYING INFILTRATION; CONSTANT ET

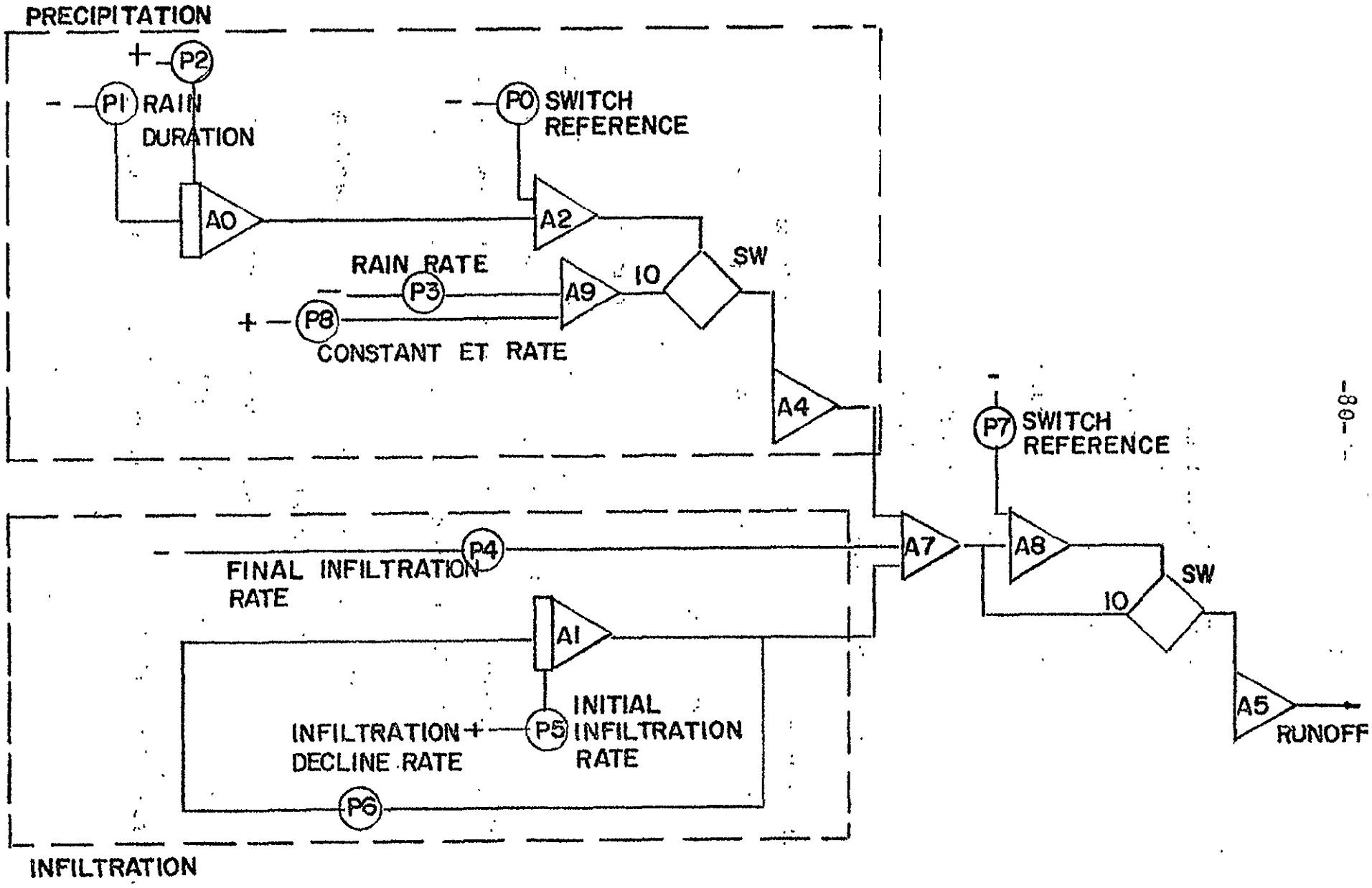

It lends itself to simulating rain events of varying characteristics: rates, durations, and rate variations within the rainfall period. It also simulates the subsurface abstraction process with varying parameters: initial and final infiltration rates, infiltration decline rate. Derived parameters which can be simulated are soil depth, soil storage capacity, antecedent moisture. The output is the total runoff. The overland flow computation is performed analytically, although an analog simulation is quite feasible and is contemplated for future phases of this effort.

Since, as has been shown, the effects of interflow, percolation, and depression storage are minimal during peak events, they are not included explicitly. They can, however, be factored in through potentiometer P8 of Figure 28, as a constant small rate. Abstractions from evapotranspiration can be factored in similarly. Although, as has been shown in the preceding section, the abstraction from evapotranspiration is generally small with respect to rainfall and to subsurface abstractions, there may exist combinations of meteorological and physical watershed parameters which may warrant its inclusion. For example, evapotranspiration consideration should be included when one of the following conditions exist: the watershed to be modeled is contained in an area of high evapotranspiration potential (dry sunny climate); it contains highly evaporative vegetation; the peak recurring rains are not very intense; the times of concentration are long (large watersheds with high surface friction); or the precision desired in the model's output is very high. In most practical cases, however,

the evapotranspiration component can be neglected.

Consideration of evapotranspiration becomes important when the peak flow event is produced by multiple sequential rainfall events. In this case, if the statistical distribution of the inter-event intervals shows that they can be relatively long, evapotranspiration becomes important in determining the statistics of antecedent humidity. Although multi-storm analysis was not performed in this phase of the project, analog simulation circuits were devised to provide the capability for such a study at a later time. The circuit is depicted in Figure 29. It simulates a sequence of rain events of arbitrary intensity, duration, and inter-event period.

The period of the rain function can be set to match diurnal or seasonal intervals of high and low evapotranspiration potential. The circuit will act to increase the time to soil saturation or to raise the infiltration rate. Over this long term, time variations in the infiltration rate can be ignored since the time required for it to fall to the final value is much shorter than the evapotranspiration period. For the complete model, a recurring rainfall with a period equal to the desired time between storms could be combined with the evapotranspiration and infiltration circuits described above.

By this means, a rain event could be initiated, then stopped and a second event restarted. During the interim, the evapotranspiration circuit would deplete soil moisture.

ANALOG CIRCUIT FOR SINUSOIDAL PRECIPITATION AND EVAPOTRANSPIRATION WITH CONSTANT INFILTRATION RATE

FIGURE 29

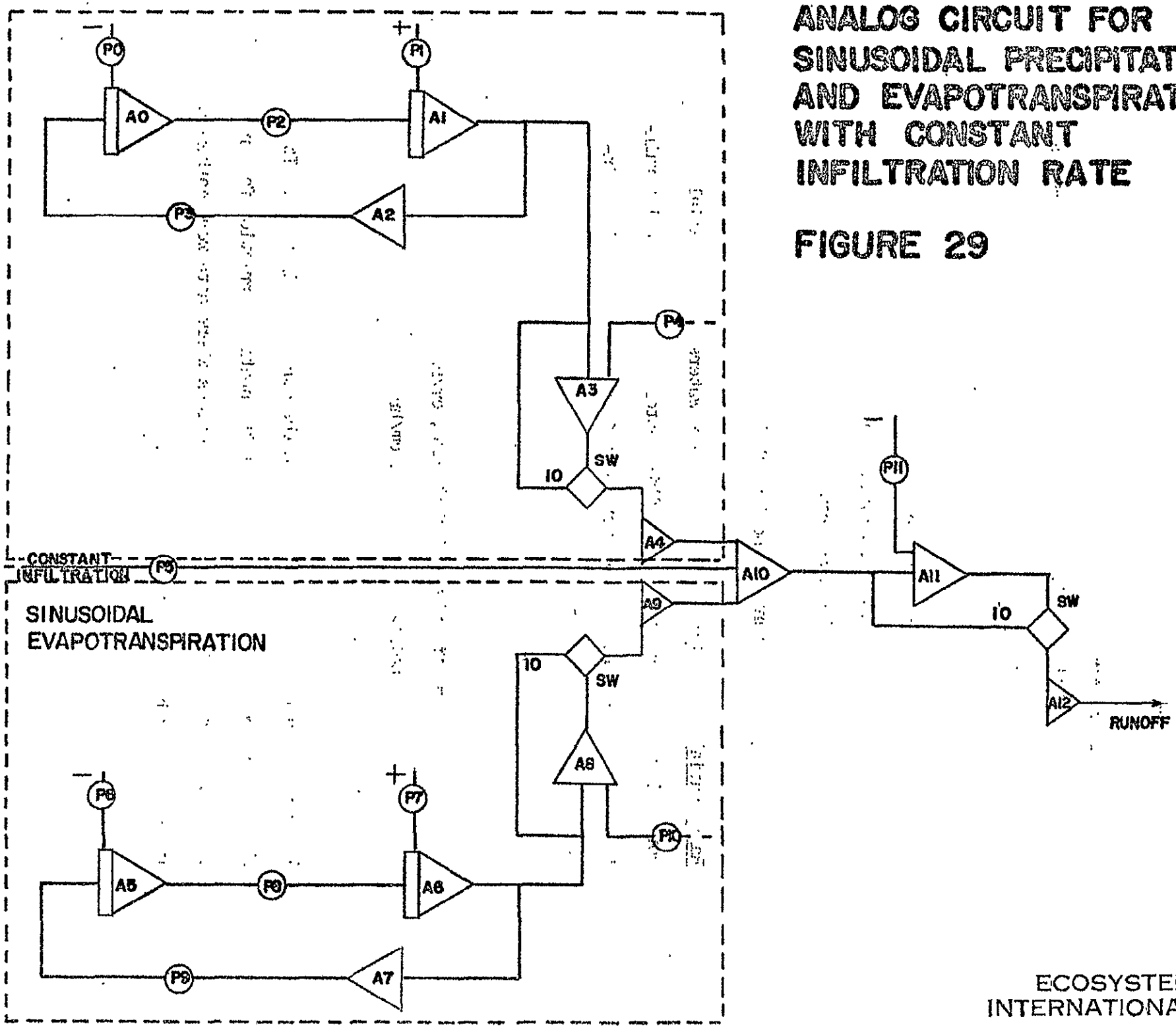

ECOSYSTEMS INTERNATIONAL INC.

The analytic model is composed of the following modules:

Rain recurrence module: This is an empirical formulation, derived from analysis of the rainfall records of the 158 ARS test watersheds:

$$i = \frac{\alpha_1 T^{\alpha_2}}{(t + d)^{\alpha_3}}$$

Where:

i = rain rate, m/sec

T = recurrence interval, years

t = rain duration, hours

α_1, α_2
α_3, d = constants, function of the location.

Rain spatial correction module: For large watersheds, a spatial correction factor is introduced. This factor converts the point rainfall rate at the center of the watershed to a lesser effective rainfall rate:

$$P_e = cP$$

Where:

P_e = effective rainfall rate, cm/hr

P = point rainfall rate, cm/hr

c = correction factor.

The correction factor c is derived from the curves of Figure 30. It should be noted that the reliability of the spatial correction factor is as yet unproven for more than a few regions where data were gathered. It should thus be used with reservation.

FIGURE 30

CURVE FOR COMPUTING THE SPATIAL CORRECTION FACTOR

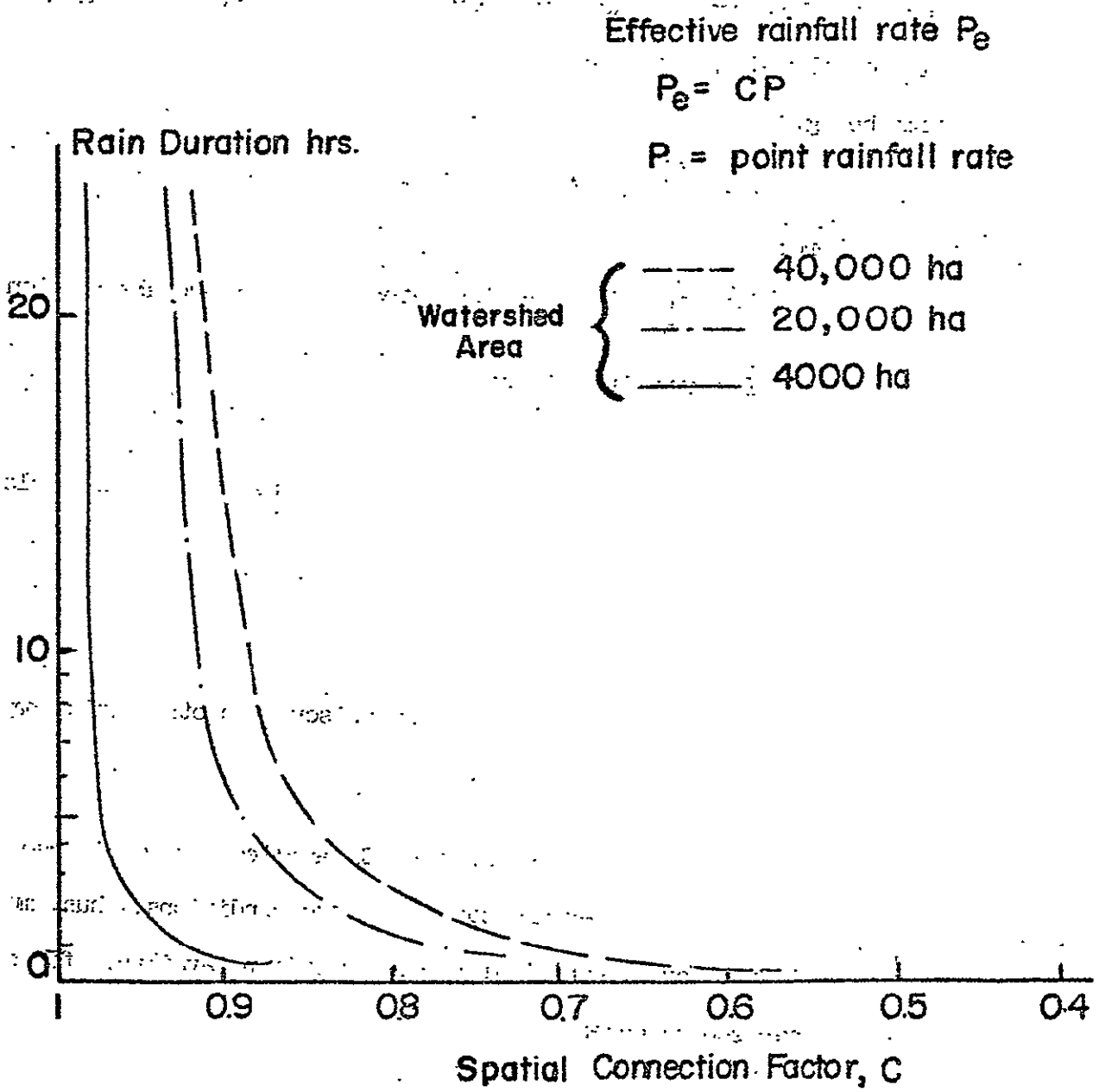

ORIGINAL PAGE IS
OF POOR QUALITY

Subsurface abstraction module: Since initial infiltration rates are typically two to ten times the final rate occurring at the time of concentration and the processes are non-linear, accurate results require that the process be modeled over time, rather than relying upon some "average" value. The expression for subsurface abstraction developed by Heggie Holtan of the ARS has been employed for the time being:

$$\dot{I} = GI \cdot \bar{a} \cdot (\overline{Sa} - I)^{1.4} + \dot{I}f$$

Where:

$\dot{I}$ = total infiltration rate (or subsurface abstraction rate)

GI = maturity of cover

$\bar{a}$ = average vegetative cover factor

$\overline{Sa}$ = average available water capacity = total available storage - initial moisture content

I = cumulative infiltration = $\int_0^t \dot{I} dt$

$\dot{I}f$ = final infiltration rate

This formulation was selected after comparison with other existing formulations because:

1. Holtan's equation is being widely applied over a diverse spectrum of cover and soil types and conditions; thus, much in the way of empirical results should be available for comparison purposes.

2. It is a complete formulation; it includes both surface (cover composition and condition) and subsurface (soil type

and antecedent moisture) phenomena.

3. Its results do not differ excessively from those of other widely used formulations, as shown in Section 3.2.

4. It explicitly includes surface observables (the $\bar{a}$ and GI factors) which are potentially remotely sensible.

Overland and channel flow module: As will be remembered, the peak outflow from the watershed will occur at the time of concentration, assuming a rain of at least this duration and of constant intensity. At the time of concentration, all points of the watershed are contributing to the runoff.

The initial analytic model for overland flow assumes the watershed schematic configuration shown in Figure 31. A single channel flows down the centerline of the watershed. Note that the single channel hypothesis is essentially valid for subwatersheds of the highest order (the smallest in area); for larger watersheds, composed of several aggregates of subwatersheds, the contribution of each subwatershed can be calculated with this model and the aggregate contribution is then computed by routing.

With reference to Figure 31, consider the watershed subdivided into strips of unit width and extending perpendicular to, and from the channel to the edge of the watershed. The total amount of water falling on such a unit strip must be released to the stream:

$\bar{\ell}$ = Average overlandflow length, meters

N = friction coeff.

S = Slope, meters/meter

t = Rain duration, hrs.

T = Recurrence interval, years

$\alpha_1 \alpha_2 \alpha_3$ = Regional rainfall coefficients, derivable from rainfall records

$\xi = \alpha_1 T^{\alpha_2}$

L = Channel length, m

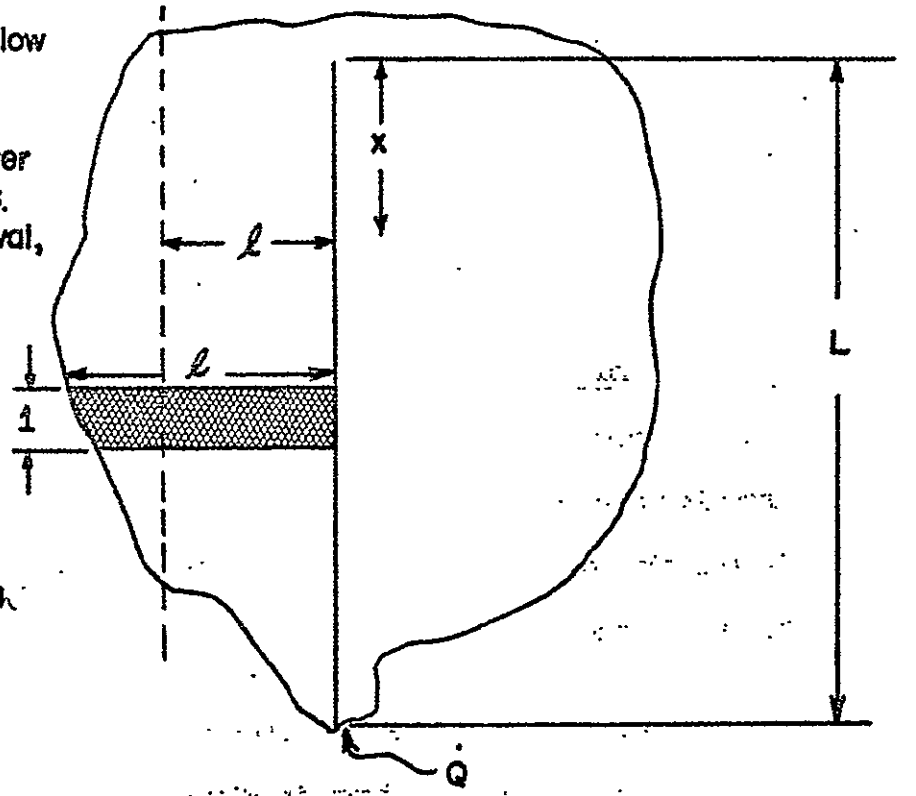

$$i_{max} = \frac{\alpha_1 T^{\alpha_2}}{(t + d)^{\alpha_3}}$$

$$\dot{Q}_{max} = 2 L \bar{\ell} \xi \left[\frac{(\bar{\ell} N)^{3/5}}{3600\, S^{3/10} \xi^{2/5}} \right]^{\frac{1}{2/5 - \frac{1}{\alpha_3}}}$$

PEAK FLOW FOR SURFACE-DOMINATED WATERSHEDS-OVERLAND FLOW CONTRIBUTION

FIGURE 31

C. 2

$$q = il \tag{1}$$

Where:

q = outflow, m^3/sec

i = rain rate, m/sec

l = flow length, m

The flow velocity, which equals outflow divided by cross section of flow, will be, maintaining the assumption of unit width:

$$v = \frac{q}{a} = \frac{il}{d} \tag{2}$$

Where:

d = depth of flow, m

v = velocity, m/sec

a = cross section of flow, m^2

Equating this result to the Manning equation, which also describes flow velocity, yields:

$$v = \frac{il}{d} = \frac{r^{2/3} s^{1/2}}{\bar{n}} \tag{3}$$

Where:

r = hydraulic radius

s = slope

$\bar{n}$ = average surface friction factor

Since, for overland (shallow) flow, the hydraulic radius equals the depth of flow, equation (3) becomes:

$$\frac{il}{d} = \frac{d^{2/3} s^{1/2}}{\bar{n}} \tag{4}$$

Whence:

$$d = \left(\frac{\bar{n}il}{s^{1/2}}\right)^{3/5}$$

Substituting expression (4) into the original equation for velocity (3) yields:

$$v = \frac{il}{d} = \frac{(il)^{2/5} s^{3/10}}{\bar{n}^{3/5}} \qquad (5)$$

Calling "first time of concentration," T_c, the time required by the flow to traverse the entire unit strip of width l:

$$T_{c(sec)} = \frac{l}{v} = \frac{(l\bar{n})^{3/5}}{i^{2/5} s^{3/10}}$$

Converting time units to hours:

$$T_{c(hrs)} = \frac{(l\bar{n})^{3/5}}{i^{2/5} s^{3/10} (3600)} \qquad (6)$$

Substituting the formula from the rainfall module for i in equation (6) yields:

$$T_c = \frac{(l\bar{n})^{3/5}}{\left(\frac{\alpha_1 T^{\alpha_2}}{T_c^{\alpha_3}}\right)^{2/5} s^{3/10} (3600)} \qquad (7)$$

If $(\alpha_1 T^{\alpha_2})$ is set equal to ξ, then:

$$T_c = \left[\frac{(l\bar{n})^{3/5}}{\xi^{2/5} s^{3/10} (3600)}\right]^{\frac{1}{1-2\alpha_3/5}} \qquad (8)$$

Replacing the t term in the formula from the rainfall module by equation (8), and assuming d to be small (as it is in most cases),

yields the rain rate for the time of concentration duration:

$$i = \frac{(\alpha_1 T^{\alpha_2})}{T_c^{\alpha_3}} = \xi T_c^{-\alpha_3}$$

Or:

$$i = \xi \left[\frac{(\overline{ln})^{3/5}}{\xi^{2/5} s^{3/10} (3600)} \right]^{\frac{1}{2/5 - 1/\alpha_3}} \tag{9}$$

For a watershed with a central channel, such as that of Figure 31, the total overland flow length for the unit-width strip will equal $2 \cdot l$. In equation (1), then,

$$q = 2il \tag{10}$$

Substituting equation (9) into (10) and summing along the channel length L gives:

$$Q = 2\overline{l}L\xi \left[\frac{(\overline{ln})^{0.6}}{\xi^{0.4} s^{0.3} (3600)} \right]^{\frac{1}{0.4 - 1/\alpha_3}} \tag{11}$$

Where:

L = channel length, m

$\overline{l}$ = average overland flow length, m

It is clear that this initial model assumes that the overland surface flow is much slower than the channel flow. This assumption turns out not to be overly in error, as the following more complete version of the model shows.

To add the effect of channel flow, consider the geometry depicted in Figure 32. The total concentration time, which is now the sum of the times required by surface flow and channel flow, is:

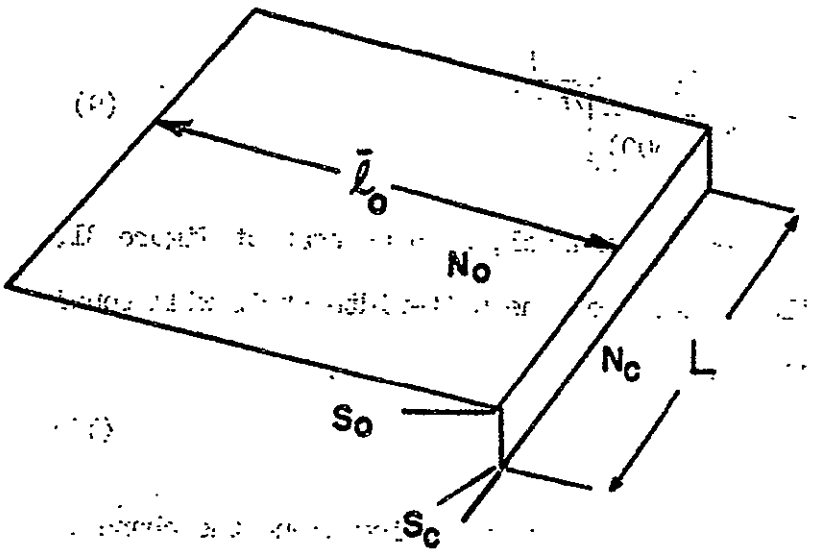

$\bar{\ell}_o$ = Average overland flow length, m

N_o = friction coefficient, overland

N_c = " " , channel

L = length of channel, m

S_o = overland slope, m/m

S_c = channel slope, m/m

Tco = concentration time, overland

R_c = channel hydraulic radius, m

d = depth of overland flow, m

$$T_{tot} = T_{co}\left[1 + \frac{\left(\frac{L}{\bar{\ell}_o}\right)\left(\frac{N_c}{N_o}\right)}{\left(\frac{R_c}{d}\right)^{2/3}\left(\frac{S_c}{S_o}\right)^{1/2}}\right]$$

FIGURE 32

ADDITIONAL DETENTION TIME CAUSED BY CHANNEL

$$T_{c_{total}} = \frac{l_o}{V_o} + \frac{L}{V_c}$$

$$= \frac{l_o\, n_o}{d^{2/3} s_o^{1/2}} + \frac{L n_c}{R_c^{2/3} s_c^{1/2}}$$

$$= T_{c_{overland}} \left[1 + \frac{\left(\frac{L}{l_o}\right)\left(\frac{n_c}{n_o}\right)}{\left(\frac{R_c}{d}\right)^{2/3} \left(\frac{s_c}{s}\right)^{1/2}} \right] \qquad (12)$$

Where the subscript "c" refers to the channel, and "o" refers to the surface:

R_c = hydraulic radius, m

d = depth of overland surface flow, m

The other parameters are as defined previously. The formulation (11) for the flow Q changes accordingly.

The sensitivity of this model to observable phenomena is shown in Figure 33 for watersheds with various typical types of surface cover and varying drainage density.

Point of flooding module: In most practical applications, the user of a hydrologic planning model is interested not only in the accurate value of the peak flow, but in the coordinate where, along its length, the stream or channel will actually begin to flood. The stream begins to flood when the water level equals the height of the banks. Flooding does not necessarily have to occur at the watershed's outlet; it is a function of channel shape, slope and roughness.

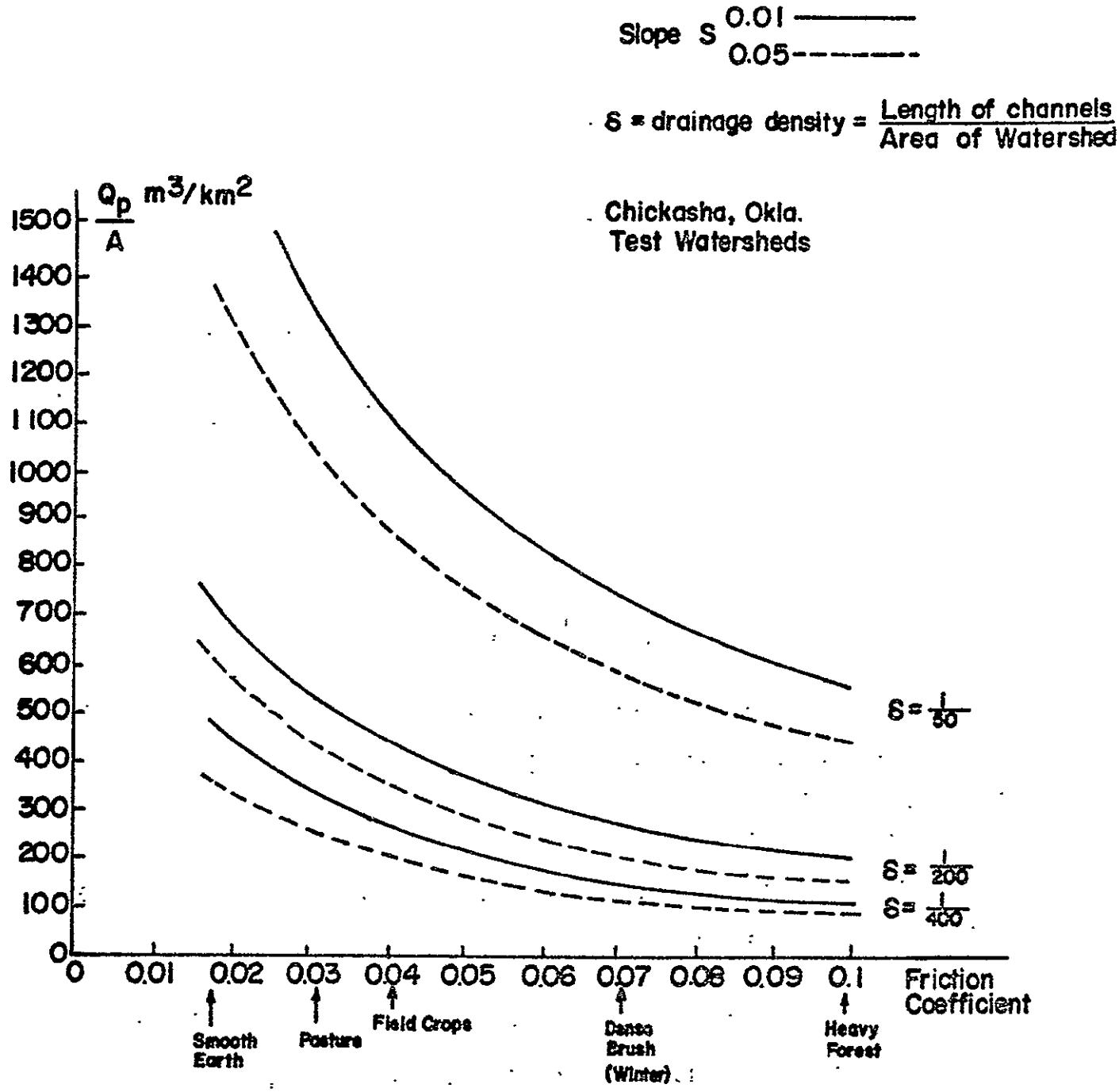

FIGURE 33

SENSITIVITY OF THE MODEL TO SURFACE OBSERVABLES

These factors are conveniently combined into a single formulation expressed in terms of the most easily observable parameter, namely channel width, for a simplified linearly increasing channel. Flooding begins to occur when channel width (w_c) at any point along the channel is less than:

$$w_c < \frac{L_c^{3/8} \xi^{3/8} Y_o^{5/8}}{\left(\frac{k^{5/2}}{1+2k}\right)^{1/4}}$$

Where:

L_c = channel length, m

ξ = roughness ratio surface/channel

k = channel geometric correction factor

Y_o = depth of overland flow, m

w_c = channnel width at distance L_c from beginning of channel

Figure 34 supplies an example for typical values of the parameters.

The modules described above obviously cannot be simply connected. As is apparent almost from inspection, there are strong feedback factors between modules. The connection is thus best performed by programming the modules and their interconnections on a computing machine, analog or digital.

Nevertheless, an analytical interconnection, using simplifying hypotheses carefully checked for validity, was performed for a set of nine ARS test watersheds, chosen at random. The results of this comparison are presented in the next section.

THE EFFECT OF OVERLAND FLOW ON FLOOD CONDITIONS

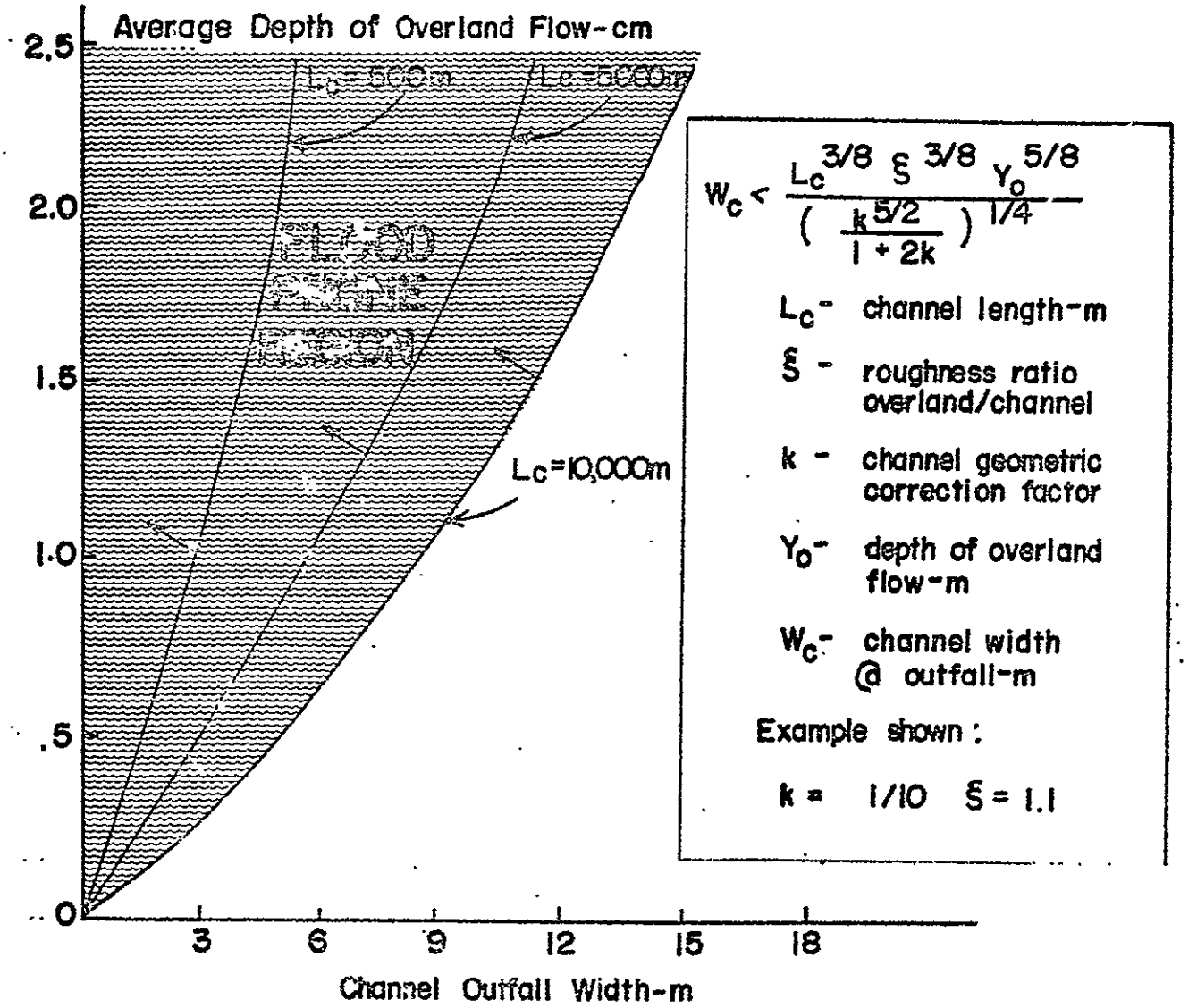

FIGURE 34

5.0 DATA ANALYSIS AND MODEL VERIFICATION

The modules of the hydrologic planning model described in the previous section were interconnected analytically, using simplifying but carefully checked assumptions. This was done on a randomly selected sample of the 158 ARS watersheds, to gage the model's applicability and accuracy and to test the hypothesis that valid predictions of peak flow events can be made using remotely sensed data inputs. The sample consisted of nine watersheds distributed throughout the U.S. The output of the model, e.g. peak flow, was then compared: 1) to actual flow records and 2) to the predictions from the most popular current ungaged models.

Three criteria were used to select the sample from the 158 watersheds. First, a diversity of geographic and physical characteristics was desired. Watersheds were selected from different areas of the country so that climate, vegetative cover, soil type, and other key factors governing watershed behavior would vary as widely as possible. Second, it was desired to include watersheds with the largest number of years of record. Thirdly and finally, watersheds were selected for which the most detailed topographic information was available.

A list of the 9 watersheds, their locations and surface

areas follows:

No. Assigned	Watershed Nomenclature	Location	Area km.^{2}
1	Watershed W-1	N. Danville, Vt.	42.9
2	Watershed 194	Coshocton, Ohio	.76
3	Thorne Creek Watershed W-1	Blacksburg, Va.	12.3
4	Watershed W-10	Oxford, Miss.	22.3
5	Watershed W-1	Fennimore, Wisc.	1.3
6	Watershed 121	Chicasha, Okla.	532.1
7	Watershed D	Waco, Texas	4.5
8	Watershed W-1	Safford, Ariz.	2.1
9	Reynolds Creek Watershed W-1	Reynolds, Idaho	233.2
		Average:	94.6
		Standard deviation σ:	180.1

It is obvious from the above list that the selected watersheds vary widely in location and area. These two factors alone have great influence upon watershed behavior: location determines vegetative cover, soil type, topography, and amount of rainfall; area affects drainage density and time of concentration.

5.1 Analytical Procedure

It should again be emphasized that the simplified analytical procedure hereinafter described is not intended to replace ulimately the construction of the complete model

ORIGINAL PAGE IS
OF POOR QUALITY

containing all modules properly interconnected and integrated. The simplified analytical procedure was here used simply as a substitute for complete interconnection, which is scheduled for subsequent phases of this project. In spite of this shortcoming, significant and most encouraging results were achieved, as will become apparent from the sections that follow. To determine capability to predict peak flow events from remote sensing data and to compare the new model against existing models, the selected 9 watersheds were analyzed in detail by means of the step-by-step procedure which follows.

1. The percentages of each type of soil within the watershed, by infiltration class, were determined. To this end, Soil Conservation Service soil data were used. SCS publishes a listing of the general classification of all soils in the United States. The SCS classifies soils into four general classes, designated A, B, C and D:

   Class A denotes soils with high infiltration rates even when thoroughly wetted, and, therefore, with low runoff potential. These soils consist chiefly of deep, well-to-excessively drained sands or gravels.

Class B denotes soils having moderate infiltration rates when thoroughly wetted. They consist chiefly of moderately deep to deep, and moderately well to well-drained, soils with moderately fine to moderately coarse textures.

Class C includes soils having low infiltration rates when thoroughly wetted. They consist chiefly of soils with a layer which impedes downward movement of water, or soils with moderately fine to fine texture.

Class D represents soils with very low infiltration rates when thoroughly wetted, and, therefore, with high runoff potential. These soils consist chiefly of clay soils, soils with a permanent high water table, soils with a clay layer at or near the surface layer and shallow soils over nearly impervious material.

An average watershed soil class was determined by computing a weighted average of the above data. For example: for Coshocton, 86% of the soils are type C, while 14% are type B. Therefore, average soil class for Coshocton is approximately C. This average is used later in the conventional prediction formulas.

2. An average infiltration rate was calculated for each watershed by means of the subsurface abstraction module. This was done by first computing final infiltration rate ($\dot{I}f$) for each type of soil, then taking a weighted average. Values for final infiltration rates by soil class, presented in Table 11, were taken from the USDA HL 74 model, authored by H. N. Holtan, G. J. Stiltner, W. H. Henson, N. C. Lopez, of the ARS (Reference 1). The character of the soil vis-a-vis layers of soil which constitute an impediment to flow are used to determine the choice of the value within the range. A low value for impeding layer of clay; a mid value for loam; and a high value for sand.

3. After average final infiltration rate was calculated, available water storage per unit depth was computed. Values of available storage capacity were assigned on the basis of soil type, according to Table 12. A weighted average was taken to determine the available storage capacity ($\overline{S}a$).

4. An average vegetative factor ($\overline{a}$) was computed for the watershed. First, the distribution of cover was determined from the data base (for example, 11% cultivated, 58% grassland, etc . .). Then each type of cover was assigned a value according to Table 13. A weighted average was computed, according

Table 11

Soil Class	Final Infiltration Rate Range (cm/hr)
A	1.14-.76
B	0.76-.38
C	0.38-.12
D	0.12-.00

Table 12

Soil Type	Available Storage Capacity m/m
Sand	0.29
Sandy Loam	0.29
Loam	0.25
Clay Loam	0.22
Silty Clay	0.20
Clay	0.18

Table 13
VEGETATIVE COVER FACTORS (a) FOR HOLTAN'S EQUATION

COVER	GOOD CONDITION	POOR CONDITION
Fallow	0.30	0.10
Row Crops	0.20	0.10
Small Grains	0.30	0.20
Hay (legumes)	0.40	0.20
Hay (sod)	0.60	0.40
Pasture (bunch grass)	0.40	0.20
Temporary Pasture (sod)	0.60	0.40
Permanent Pasture (sod)	1.0	0.80
Woods and Forests	1.0	0.80

to percentage of each type of vegetative cover in the watershed.

5. The average infiltration $\dot{I}$ over time was then calculated from the equation:

$$\dot{I} = GI \cdot \bar{a} \cdot (\bar{S}a - I)^{1.4} + \dot{I}f$$

6. To enable comparison of results with the SCS procedure outlined in reference 2, an average SCS curve number was computed. Curve number values were taken from Table 14 according to average soil group. (The determining factor in choosing a curve number is vegetative cover). A weighted average yielded a final curve number.

7. The approximate time of concentration was computed applying the empirical equation developed by Kerby (reference 7) to each of the 9 watersheds:

$$t_c = \left[\frac{2Ln}{3\sqrt{S}}\right]^{.47}$$

Where:

t_c = time of concentration

L = distance from the most remote point in the basin to the channel, in a direction parallel to the slope

S = slope

n = retardance coefficient, according to Table 15.

Table 14
SCS CURVE NUMBERS

Land Use or Cover	Treatment or practice	Hydrologic Condition	Hydrologic Soil group			
			A	B	C	D
Row crops	Straight row	Poor	72	81	88	91
	Straight row	Good	67	78	85	89
	Contoured	Poor	70	79	84	88
	Contoured	Good	65	75	82	86
Small grain	Straight row	Poor	65	76	84	88
	Contoured	Good	61	73	81	84
Legumes or rotation	Contoured	Good	55	69	78	83
Native pasture or range		Fair	49	69	79	84
		Good	39	61	74	80
Woods		Fair	36	60	73	79
		Good	25	55	70	77

Table 15

RETARDANCE COEFFICIENT – KERBY'S EQUATION

Type of Surface	Value of n
Smooth impervious surface	0.02
" bare packed soil	0.10
Poor grass, cultivated row crops or moderately rough bare surface	0.20
Pasture or average grass	0.40
Deciduous timberland	0.60
Conifer timberland, deciduous timberland with deep forest litter or dense grass	0.80

8. The surface friction coefficients (Manning's "n") were derived from Table 9 (see Section 3) and a weighted average calculated which included the effects of the vegetative cover of the watershed.

9. A rainfall intensity-frequency-duration relation was developed from NOAA published rainfall records by empirically fitting to each watershed the rainfall module curve:

$$i = \frac{\alpha_1 T^{\alpha_2}}{(t+d)^{\alpha_3}}$$

Where:

i = rain rate, m/hr.

T = recurrence interval, years

t = rain duration, hrs.

$\alpha_1, \alpha_2, \alpha_3, d$ = constants which vary with region.

As will be shown in Section 5.2.1, this formulation permits the determination of the intensity of a rain event of any recurrence and any duration with a high degree of accuracy, to serve as the input into the hydrologic planning model.

10. Peak discharge rates per unit of watershed area were calculated from three models in wide current usage, plus the new model, in order to assess their relative accuracies. These models were:

ORIGINAL PAGE IS
OF POOR QUALITY

a. Rational formula method (Reference 3)

$Q = CiA$

Where:

Q = outflow, m^3/sec

C = constant based on soils and cover, dimensionless

i = rain rate with a duration of T_c and x-year recurrence, m/sec.

A = watershed area, m^2

b. Cook's method (Reference 4)

$Q = f(A, R, I, C, S, P)$

Where:

f = an empirically derived function

Q = outflow, m^3/sec

A = watershed area, m^2

R = watershed relief factor, dimensionless

I = infiltration capacity factor, dimensionless

C = vegetative cover factor, dimensionless

S = surface storage factor, dimensionless

P = precipitation factor, dimensionless

Soil Conservation Service method (Reference 2)

$Q = f(A, C, S, T_c)$

Where:

f = an empirically derived function

Q = outflow, m^3/sec.

A = watershed area, m^2

C = vegetative cover factor, dimensionless

S = soil type factor, dimensionless

T_c = time of concentration, sec

d. Ecosystems method described previously.

The results of these four methods were compared with the 50-year recurrence flow (Q_{50}), derived from the statistics of the actual records using the Gumbel extreme value distribution (Reference 5).

5.2 Results of the Analysis

The map of Figure 35 shows the location of the 9 test watersheds selected for detailed evaluation. Two watersheds among the nine - - Reynolds, Idaho (No. 9) and Chickasha, Oklahoma (No. 6) - - are very large, having areas greater than 200 km^2. They are composed of numerous subwatersheds and, therefore, do not precisely fit within the framework of the simplified model described previously. As indicated in Section 3, watersheds composed of a significant number of subwatersheds require additional routing techniques to produce good accuracies. Their detailed analysis is reserved for future phases of this effort.

FIGURE 35
NINE WATERSHED SAMPLE

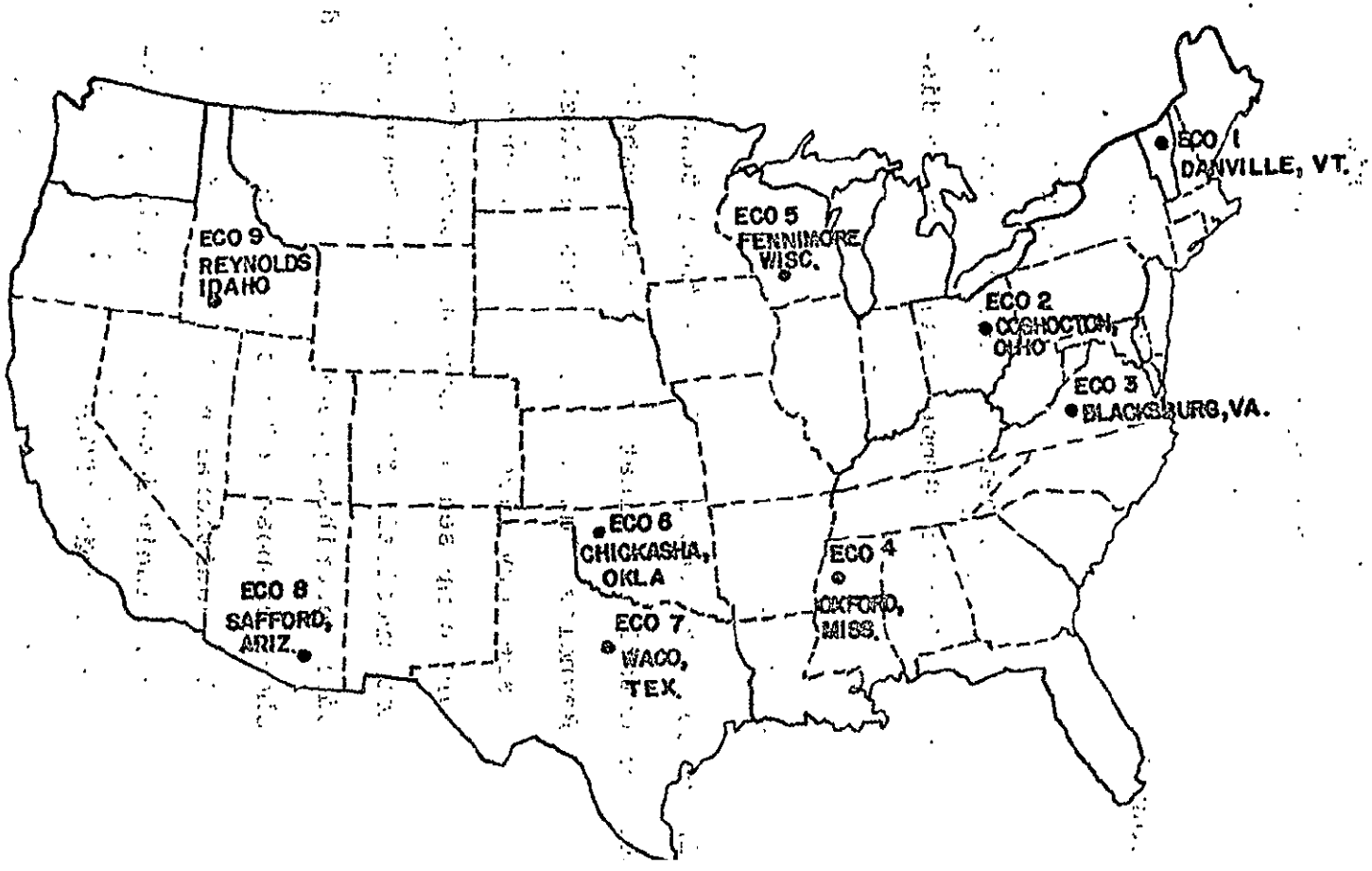

ORIGINAL PAGE IS OF POOR QUALITY

5.2.1 Recurrence Rainfall

For peak events, as previously described, the rain duration chosen was the watershed's time of concentration. Therefore, a rainfall intensity for a given recurrence period can be computed.

The results of the empirical fits of NOAA rainfall data (Reference 6) to the rainfall module formulation for each of the nine watersheds are shown in Tables 16a through i. Table 17 summarizes the results for the nine watersheds. The average error for the nine watersheds was 2.58%. This is well within the bounds of the errors of the other measurements.

5.2.2 Watershed Physiography, Vegetative Cover, and Soils

The physiography for each watershed was developed from USGS 7.5 minute quadrangle maps. It included the physical quantities: area, slope, channel length and drainage density. The capability of remote sensing techniques to determine these physical quantities will be covered in Section 6. Table 18 summarizes the data for the nine watersheds shown in Figures 36 a-i.

The vegetative cover and soil distributions were developed for each watershed as a weighted average using descriptive data provided by the USDA-ARS. The utilization of remote

Table 16a

Rainfall Duration-Recurrence Data- DANVILLE, VERMONT

Duration-Hrs.	RECURRENCE 25 yrs	50 yrs	100 years
0.5	3in/hr .076m/hr	3.4in/hr .086m/hr	3.5in/hr .089m/hr
1.0	1.8in/hr .046m/hr	2.1in/hr .053m/hr	2.3in/hr .058m/hr
2.0	1.2in/hr .030m/hr	1.3in/hr .033m/hr	1.4in/hr .036m/hr
3.0	0.8in/hr .020m/hr	1.0in/hr .025m/hr	1.1in/hr .028m/hr
6.0	0.5in/hr .013m/hr	0.6in/hr .015m/hr	0.7in/hr .018m/hr
12.0	0.31in/hr .0079m/hr	0.33in/hr .0084m/hr	0.42in/hr .0107m/hr
24.0	0.19in/hr .0048m/hr	0.21in/hr .0053m/hr	0.23in/hr .0058m/hr

General Formula

$$i = \frac{.033\,T^{.16}}{(t+.2)^{.77}}$$

where
i = intensity, /hr.
T= recurrence, years
t = duration, hrs.

Table 16b Rainfall Duration-Recurrence Data- COSHOCTON, O.

Duration-Hrs.	RECURRENCE 25 yrs	50 yrs	100 years
0.5	3.4"/hr. .086m/hr	3.6"/hr. .091m/hr.	4.2"/hr. .107m/hr.
1.0	2.1"/hr. .053m/hr	2.3"/hr. .058m/hr.	2.6"/hr .066m/hr
2.0	1.2"/hr. .031m/hr	1.4"/hr. .036m/hr.	1.5"/hr. .038m/hr.
3.0	.93"/hr. .024m/hr.	1.0"/hr. .025m/hr.	1.1"/hr. .028m/hr.
6.0	.55"/hr .014m/hr.	.58"/hr. .015m/hr.	.63"/hr. .016m/hr.
12.0	.30"/hr. .0076m/hr.	.33"/hr. .0084m/hr.	.38"/hr. .0097m/hr.
24.0	.17"/hr. .0043m/hr.	.19"/hr. .0048m/hr.	.21"/hr. .0053m/hr.

eral formula $i = \frac{.039\,T^{.15}}{(t+.2)^{.83}}$

Where,
i = intensity, m/hr.
T = recurrence, yrs.
t = duration, hrs.

Table 16c Rainfall Duration-Recurrence Data- BLACKSBURG, VA.

Duration-Hrs.	RECURRENCE 25 yrs	50 yrs	100 years
0.5	4.0"/hr. .102 m/hr.	4.4"/hr. .112m/hr	5.0"/hr. .127 m/hr.
1.0	2.5"/hr. .064 m/hr.	2.9"/hr. .074m/hr	3.3"/hr. .084 m/hr
2.0	1.5"/hr. .038m/hr.	1.8"/hr. .046m/hr.	2.0"/hr. .051 m/hr.
3.0	1.13"/hr. .029m/hr.	1.3"/hr. .033m/hr.	1.4"/hr. .036 m/hr.
6.0	.67"/hr. .017m/hr	.75"/hr. .019m/hr.	.82"/hr. .021m/hr
12.0	.41"/hr. .010m/hr.	.42"/hr. .011m/hr	.50"/hr. .013m/hr.
24.0	.21"/hr. .0053m/hr.	.25"/hr. .0064m/hr.	.27"/hr. .0069 m/hr

$$i = \frac{.040\ T^{.19}}{(t+.2)^{.80}}$$

where

i = intensity, m/hr.
T = recurrence, yrs.
t = duration, hrs.

Table 16d Rainfall Duration-Recurrence Data- OXFORD, MISS.

Duration-Hrs.	RECURRENCE 25 yrs	50 yrs	100 years
0.5	4.4in/hr. .112m/hr	5.0in/hr .127m/hr	5.4in/hr .137m/hr
1.0	2.8in/hr. .071m/hr	3.1in/hr .079m/hr	3.4in/hr. .086m/hr
2.0	1.75in/hr .044m/hr	1.85in/hr .047m/hr	2.15 in/hr. .055m/hr
3.0	1.27in/hr .032m/hr	1.43in/hr .036m/hr	1.57in/hr. .040m/hr.
6.0	.77in/hr .019m/hr	.87in/hr .022m/hr.	.97in/hr. .025m/hr
12.0	.48in/hr. .012m/hr	.52in/hr .013m/hr	.57in/hr .014m/hr
24.0	.28in/hr .0070m/hr	.31in/hr .0078m/hr.	.33in/hr .0085m/hr

General Formula

$$i = \frac{.049T^{.14}}{(t+.1)^{.75}}$$

where:

i = intensity, m/hr
T = recurrence, years
t = duration, hrs.

Table 16e Rainfall Duration-Recurrence Data- FENNIMORE WISC.

Duration-Hrs.	RECURRENCE		
	25 yrs	50 yrs	100 years
0.5	3.8 in/hr. .097m/hr.	4.2in/hr. .107m/hr.	4.6 in/hr. .117m/hr.
1.0	2.4in/hr. .061m/hr	2.7in/hr. .069m/hr.	2.8in/hr. .071m/hr
2.0	1.4in/hr .036m/hr	1.6 in/hr. .039m/hr	1.8 in/hr. .044m/hr.
3.0	1.03in/hr .026m/hr	1.17in/hr. .0 30m/hr.	1.23in/hr .031 m/hr
6.0	.58in/hr .015m/hr	.67in/hr .017m/hr	.75 in/hr .019m/hr
12.0	.36 in/hr .009m/hr	.39in/hr .010m/hr	46 in/hr .012m/hr
24.0	.21in/hr .005m/hr.	.23in/hr .006m/hr	.26in/hr .007m/hr

General Formula

$$i = \frac{.041\ T^{.14}}{(t+.1)^{.78}}$$

where:

i = intensity, m/hr
T = recurrence, years
t = duration, hrs

Table 16f Rainfall Duration-Recurrence Data- CHICKASHA, OKLA.

Duration-Hrs.	RECURRENCE		
	25 yrs	50 yrs	100 years
0.5	5.0 in/hr .127 m/hr	5.8 in/hr .147 m/hr	6.4 in/hr .163 m/hr
1.0	3.2 in/hr .081 m/hr	3.6 in/hr .091 m/hr	4.1 in/hr .104 m/hr.
2.0	1.85 in/hr .047 m/hr	2.2 in/hr .056 m/hr	2.45 in/hr .062 m/hr
3.0	1.43 in/hr .036 m/hr	1.57 in/hr .040 m/hr	1.8 in/hr .046 m/hr
6.0	.83 in/hr .021 m/hr	.93 in/hr .024 in/hr	1.1 in/hr .027 m/hr
12.0	.49 in/hr .012 m/hr	.54 in/hr .014 m/hr	.63 in/hr .016 m/hr
24.0	.283 in/hr .0072 m/hr	.321 in/hr .0081 m/hr	.358 in/hr .0091 m/hr

General Formula:

$$i = \frac{.055T^{.17}}{(t+.2)^{.82}}$$

where:
i = intensity, m/hr
T = recurrence, years
t = duration, hrs.

Table 16g Rainfall Duration-Recurrence Data- WACO, TEXAS

Duration-Hrs.	RECURRENCE		
	25 yrs	50 yrs	100 years
0.5	5.4 in/hr .137 m/hr	6.2 in/hr .157 m/hr	6.6 in/hr .168 m/hr
1.0	3.4 in/hr .086 m/hr	3.9 in/hr .099 m/hr	4.2 in/hr .107 m/hr
2.0	2.10 in/hr .053 m/hr	2.35 in/hr .060 m/hr	2.65 in/hr .067 m/hr
3.0	1.6 in/hr .041 m/hr	1.77 in/hr .045 m/hr	1.9 in/hr .048 m/hr
6.0	.967 in/hr .025 m/hr	1.07 in/hr .027 m/hr	1.18 in/hr. .030 m/hr
12.0	.567 in/hr .014 m/hr	.642 in/hr .016 m/hr	.73 in/hr .019 m/hr
24.0	.33 in/hr .008 m/hr	.371 in/hr .009 m/hr	.413 in/hr .010 m/hr

General Formula

$$i = \frac{.054\,T^{.17}}{(t+.1)^{.78}}$$

where:

i = intensity, m/hr.
T = recurrence, years
t = duration, hrs.

Table 16h Rainfall Duration-Recurrence Data- SAFFORD, ARIZONA

Duration-Hrs.	RECURRENCE		
	25 yrs	50 yrs	100 years
0.5	2.8 in/hr .071 m/hr	3.4 in/hr .097 m/hr	3.7 in/hr .094 m/hr
1.0	1.9 in/hr .048 m/hr	2.2 in/hr .056 m/hr	2.5 in/hr .064 m/hr
2.0	1.13 in/hr .029 m/hr	1.25 in/hr .032 m/hr	1.40 in/hr .036 m/hr
3.0	.80 in/hr .020 m/hr	.92 in/hr .023 m/hr	1.03 in/hr .026 m/hr
6.0	0.48 in/hr .012 m/hr	0.50 in/hr .013 m/hr	0.58 in/hr .015 m/hr
12.0	0.25 in/hr .006 m/hr	0.31 in/hr .008 m/hr	0.34 in/hr .009 m/hr
24.0	0.150 in/hr .0038 m/hr	0.180 in/hr .0046 m/hr	.188 in/hr .0048 m/hr

General Formula:

$$i = \frac{.027\,T^{.19}}{(t+.1)^{.8}}$$

where:

i = intensity, m/hr.
T = recurrence, years
t = duration, hrs.

Table 16i Rainfall Duration-Recurrence Data- REYNOLDS, IDAHO

Duration-Hrs.	RECURRENCE 25 yrs	50 yrs	100 years
0.5	1.0 in/hr .025m/hr	1.2 in/hr .030m/hr	1.5 in/hr .038m/hr
1.0	.66in/hr .017 m/hr	.8 in/hr .020m/hr	.9 in/hr .023m/hr
2.0	.38in/hr .010m/hr	.47 in/hr .012m/hr	.55 in/hr .014m/hr
3.0	.33in/hr .008 m/hr	.40 in/hr .010m/hr	.43in/hr .011 m/hr
6.0	.21 in/hr .0053m/hr	.23in/hr .0058m/hr	.26 in/hr .0066m/hr
12.0	.125 in/hr .0032 m/hr	.146 in/hr .0037 m/hr	.167 in/hr .0042m/hr
24.0	.075 in/hr .0019 m/hr	.088in/hr .0022m/hr	.100 in/hr .0025m/hr

General Formula:

$$i = \frac{.008\,T^{.25}}{(t+.1)^{.71}}$$

where:

i = intensity, m/hr.
T = recurrence, years
t = duration, hrs

Table 17

SUMMARY OF THE RESULTS OF EMPIRICAL FIT OF RAINFALL-RECURRENCE DATA FOR THE TEST WATERSHEDS

ECO NO.	LOCATION	α_1	α_2	α_3	d	Average Error (%)
1	Danville, Vt.	0.033	0.16	0.77	0.2	3.09
2	Coshocton, O.	0.039	0.15	0.83	0.2	3.34
3	Blacksburg, Va.	0.040	0.19	0.80	0.2	1.80
4	Oxford, Miss.	0.049	0.14	0.75	0.1	1.37
5	Fennimore, Wisc.	0.041	0.14	0.78	0.1	1.76
6	Chickasha, Okla.	0.055	0.17	0.82	0.2	1.69
7	Waco, Tex.	0.054	0.17	0.78	0.1	3.31
8	Safford, Ariz.	0.027	0.19	0.80	0.1	3.45
9	Reynolds, Ida.	0.008	0.25	0.71	0.1	3.40
				Grand Average		2.58

General Formula

$$\frac{\alpha_1 \; T^{\alpha_2}}{(t+d)^{\alpha_3}}$$

Where:

i = rain rate, cm/hr

T = recurrence period, years

t = rain duration, hrs

α_1, α_2

α_3, d = empirical constants

$$\text{Average Error} = \frac{1}{n} \Sigma e, \text{ where } = \left| \frac{\text{predicted} - \text{observed}}{\text{observed}} \right|$$

TABLE 18 PHYSIOGRAPHIC DATA SUMMARY FOR THE NINE TEST WATERSHEDS

ECO NO.	LOCATION	AREA km^2	m/m AVG. SLOPE	SHAPE	m CHANNEL LGTH.	m/m^2 DRAINAGE DENSITY
1	Danville Vt.	42.9	0.12	Triangle	40,300	1/1065
2	Coshocton Ohio	0.76	0.172	Square	1,491	1/510
3	Blacksburg Va.	12.3	0.123	Ellipse L=2.6W	26,900	1/460
4	Oxford Miss.	22.3	0.114	Triangle	20,273	1/1100
5	Fennimore Wis.	1.3	0.08	Ellipse L=2.1W	2,364	1/550
6	Chickasha Okla.	532.1	0.058	Ellipse L=2W	76,014	1/7000
7	Waco Texas	4.5	0.021	Wedge L=2W	6,618	1/680
8	Safford Ariz.	2.1	0.020	Rectangle L=5.3W	6,195	1/339
9	Reynolds Ohio	233.2	0.176	Wedge L=1.9W	164,177	1/1420

FIGURE 36a

NORTH DANVILLE VERMONT ECO I

Area 42.9 Km^2
Slope .120 m/m
Shape-Triangle
Length of Channel 40.3 Km^2
Drainage Density 1/1065 m/m^2

$$i = \frac{.033\,T^{.16}}{(t+2)^{.77}}$$

Cover
64% Cultivation
17% Pasture
15% Idle land
3% Homesteads
1% Roads

Soils
33% Stony silt loam
18% Calais loam
18% Royalton loam
16% Rocky loam
7% Fine sandy loam
4% Colrain fine sandy
3% Peacham silt loam
1% Misc. soils

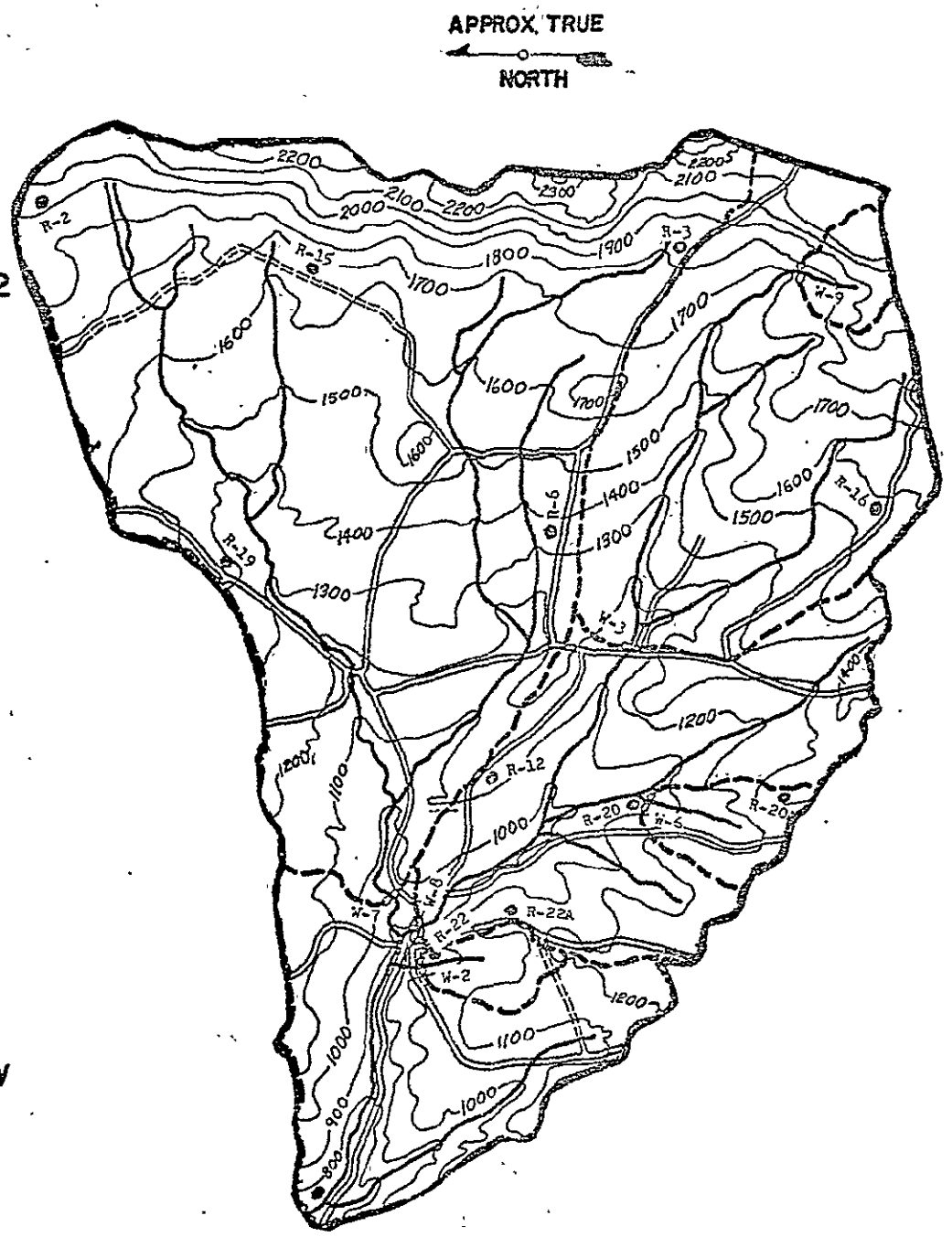

ORIGINAL PAGE IS
OF POOR QUALITY

FIGURE 36b

COSHOCTON OHIO ECO-2

Area = .76 km^2

Slope = .172 m/m

Shape = Square

Length of Channel - 1491 m

Drainage Density = 1/510 m/m^2

$$i_{m/m} = \frac{.039\ T^{.15}}{(t + .2)^{.83}}$$

Cover

- 23% Hardwood Forest
- 58% Grassland
- 11 % Cultivated
- 8 % Miscellaneous

Soils

- 33% Muskingum silt loam
- 19% Keene shallow loam
- 17% Keene silt loam
- 17% Mixed silt loam
- 14% Muskingum stony loam

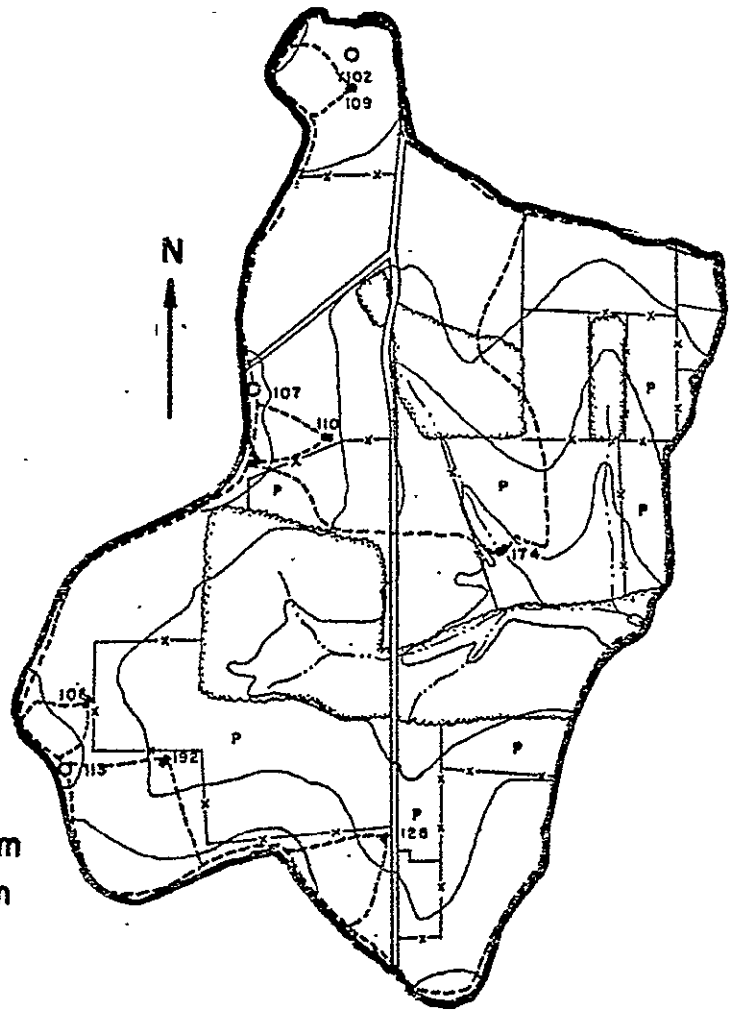

THORNE CREEK AT BLACKSBURG, VIRGINIA ECO-2

FIGURE 36c

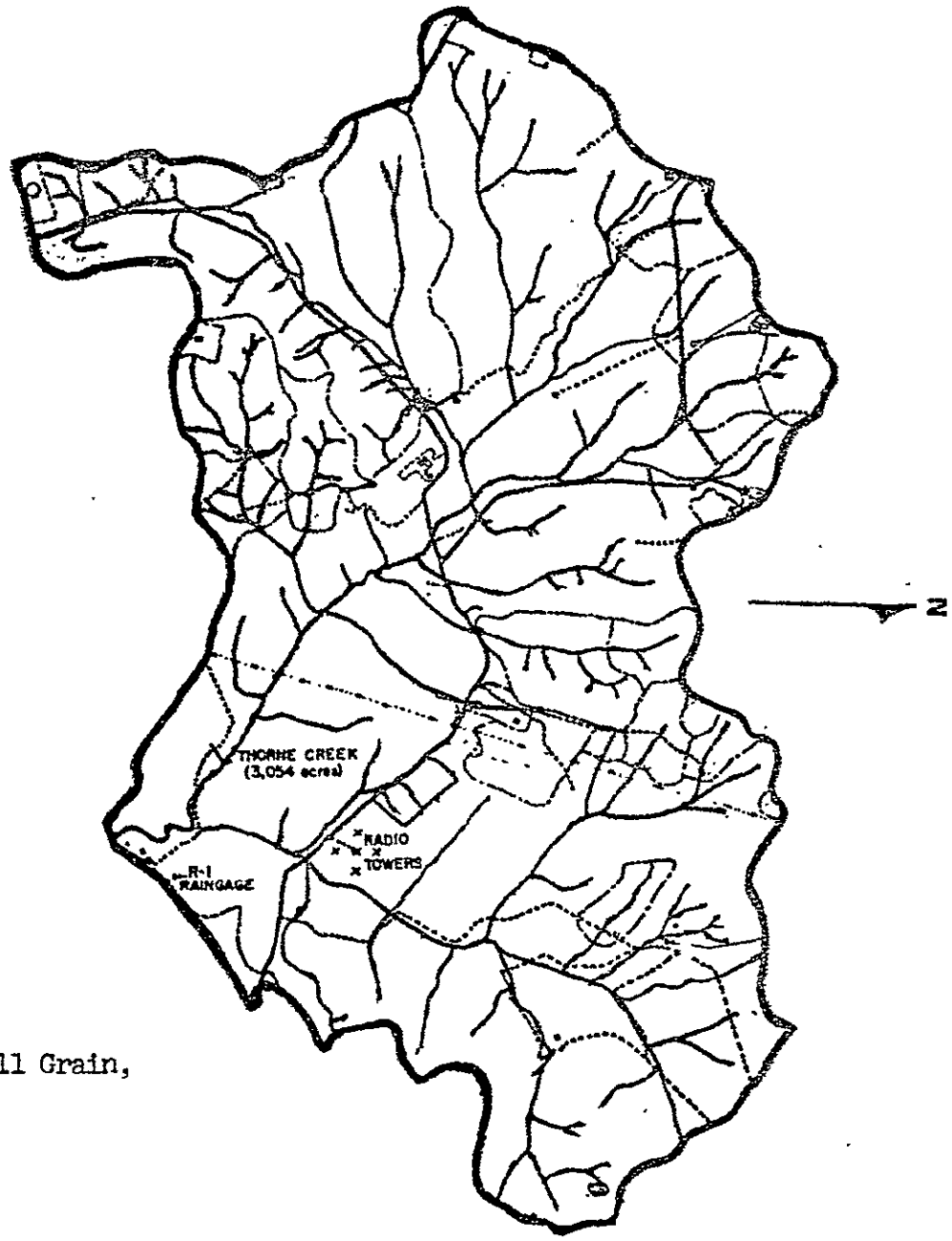

Area = 12.3 Km^2

Slope = .123 m/m

Shape = Ellipse; L=2W

Drainage Density = 1/460 m/m^2

Length of Channel = 26.6 km

$$i = \frac{.040T^{.19}}{(t + .2)^{.80}}$$

Cover
- 61% Pasture
- 32% Cultivated (Corn, Small Grain, Hay Crops)
- 4% Trees
- 2% Idle Land
- 1% Roads

Soils
- 30% Groceclose Silt Loam
- 17% Lodi Loam
- 14% Frederick Silt Loam
- 12% Litz Silt Loam
- 8% Greendale Silt Loam
- 19% Other Silt Loams

FIGURE 36d

OXFORD MISS
ECO 4

Area 22.3 Km^2

Slope .114 m/m

Shape-Triangle

Length of Channel 20.4 Km^2

Drainage Density 1/1100 m/m^2

$$i = \frac{.049^{.14}}{(t+.1)^{.75}}$$

Cover

23% Cotton, corn & soybeans
35% Pasture & idle land
40% Woods
2% Bare gullies

Soils

50% Ruston Ind. sandy loam to clay loam
16% Collins
14% Providence silt loam
12% Loring silt loam to silty clay loam
8% Grenada silt loam

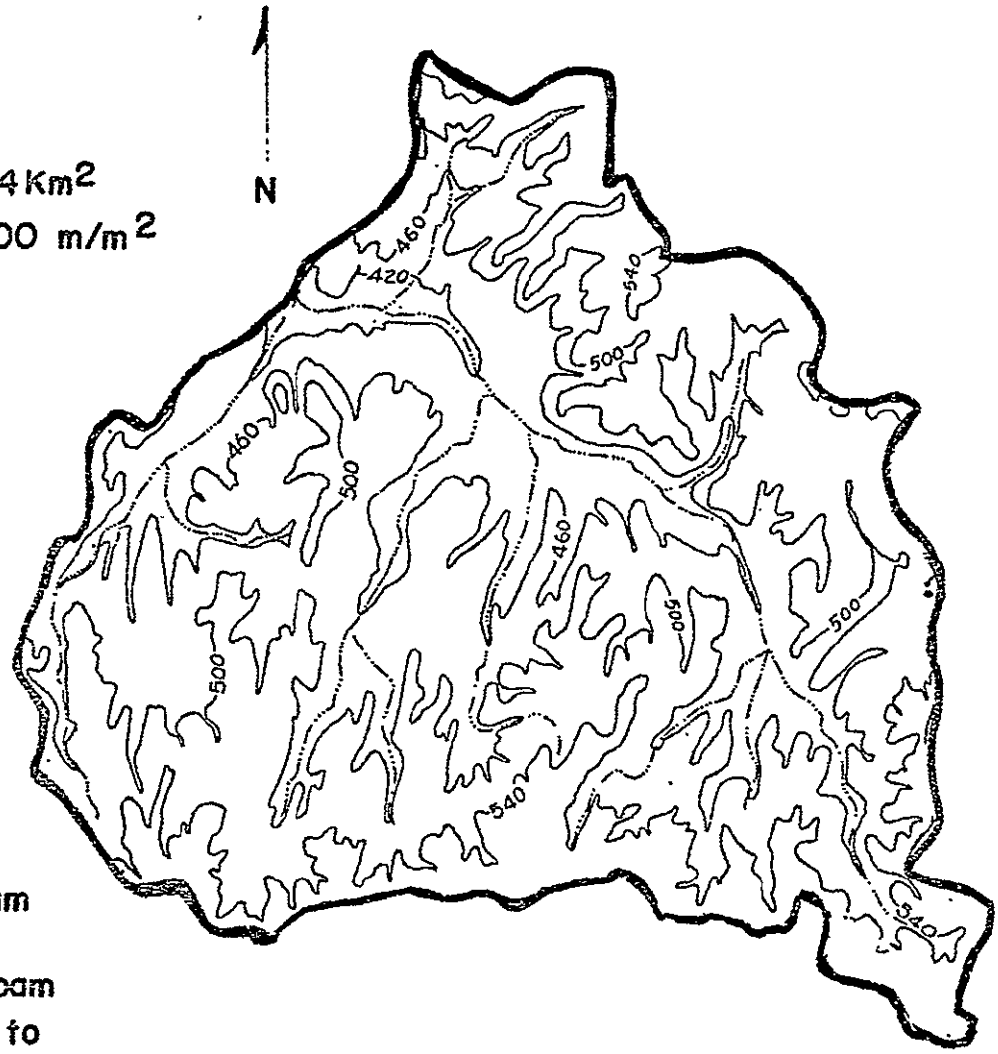

FIGURE 36e

Area = 1.3 Km^2

Slope = .08 m/m

Shape = Rectangle: L=2.44

Drainage Density = 1/550 m/m^2

Length of Channel = 2.44 km

$$i = \frac{.041T^{.14}}{(t+.1)^{.78}}$$

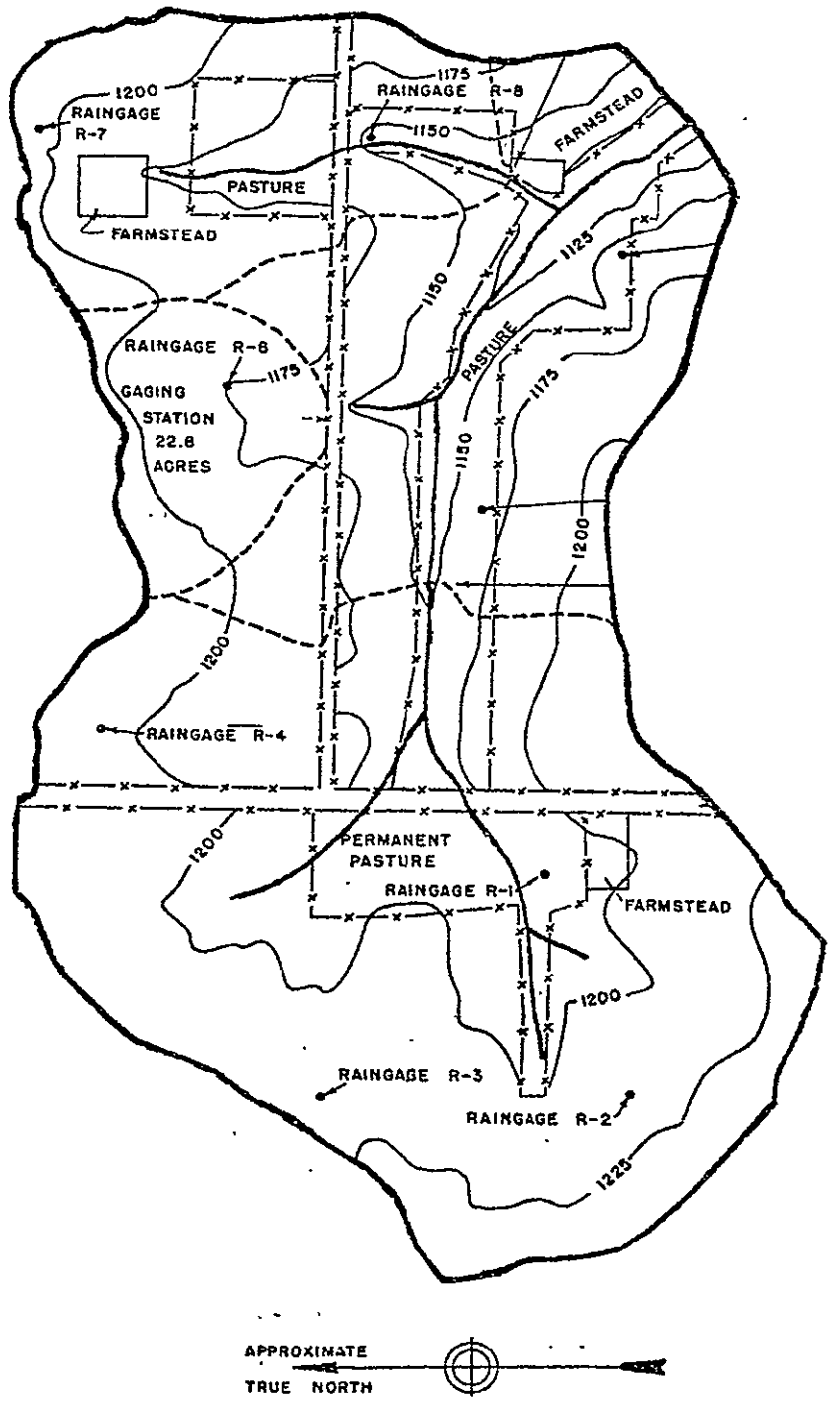

Cover
- 23% Corn
- 10% Grain
- 21% Hay
- 23% Pasture
- 16% Idle
- 7% Roads

Soils
- 50% Tama Silt Loam
- 19% Dubuque Silt Loam
- 23% Dodgeville Silt Loam
- 8% Judson Silt Loam

ORIGINAL PAGE IS
OF POOR QUALITY

CHICKASHA, OKLAHOMA ECO-6

FIGURE 361

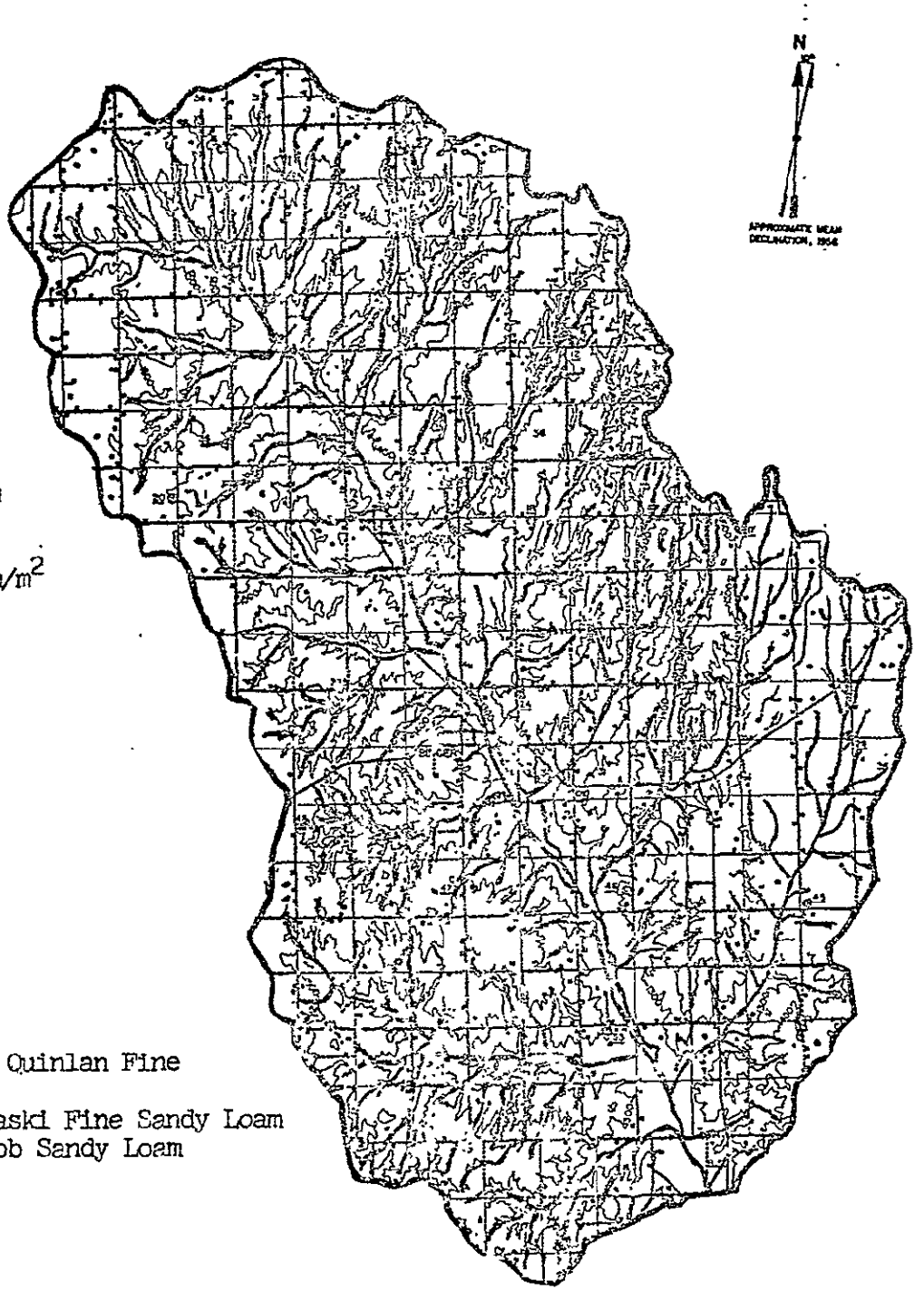

Area = 532.1 Km^2

Slope = .058 m/m

Shape = Ellipse; L=2W

Length of Channel = 74.4 km

Drainage Density = 1/7000 m/m^2

$$i = \frac{055T^{.17}}{(t + .2)^{.82}}$$

Cover
- 8% Alfalfa
- 48% Sowed Crops
- 44% Row Crops

Soils
- 40% Noble Cobb Loam
- 36% Darnel Woodward Quinlan Fine Sandy Loam
- 16% Port-Yahola Pulaski Fine Sandy Loam
- 8% Noble Vanoss Cobb Sandy Loam

ORIGINAL PAGE IS
OF POOR QUALITY

FIGURE 36g

RIESEL (WACO) TEXAS ECO-7

Area 4.5 Km^2

Slope .021 m/m

Shape W L = 2W

Length of Channel 6.6 Km^2

Drainage Density 1/680 m/m^2

$$i = \frac{.054\,T^{.17}}{(t+.1)^{.78}}$$

Cover

60% Pasture
6% Small grain
3% Corn
7% Cotton
9% Row grains
2% Gravel & paved roads
13% Other, mostly weeds

Soils

66% Wilson clay loam
24% Burleson Heiden clay
4% Frio clay loam
3% Crockett loam
2% Burleson clay
1% Houston Black clay

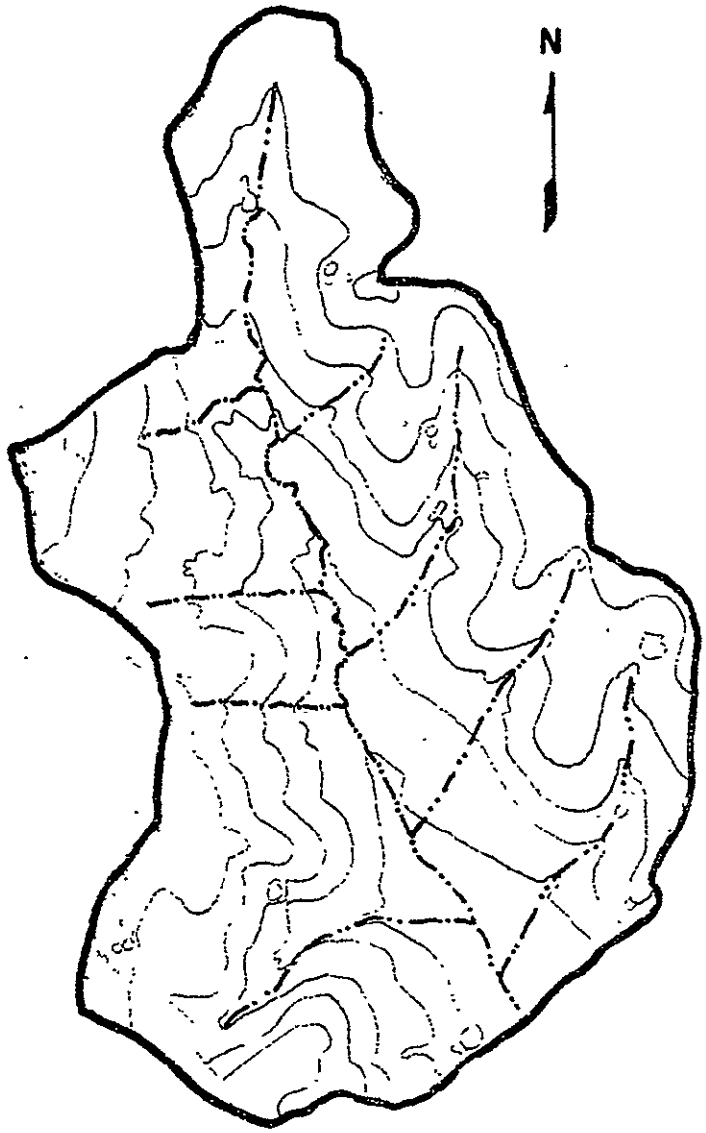

FIGURE 36h

SAFFORD, ARIZONA ECO-8

Area 2.1 Km^2

Slope .020 m/m

Shape Rectangle L= 5.3 W

Length of Channel 6.2 Km^2

Drainage Density 1/339 m/m^2

$$i = \frac{.027\ T^{.19}}{(t + .1)^{.8}}$$

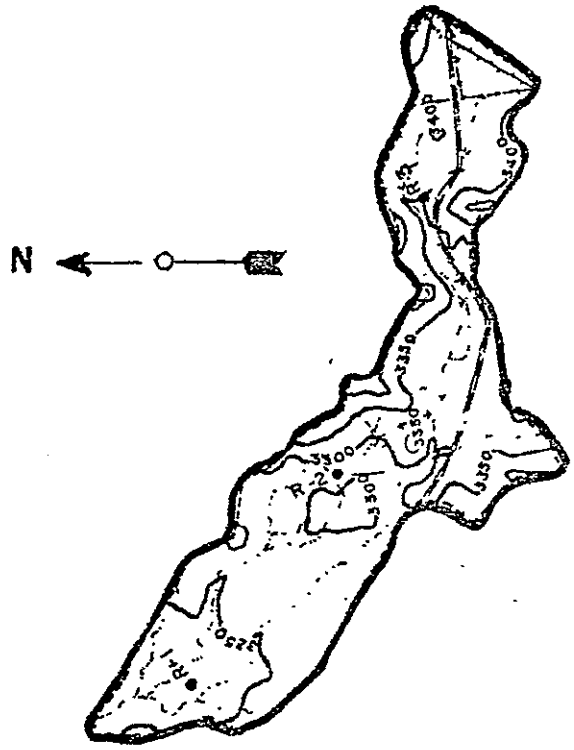

Cover

85% Bare
15% Grasses

Soils

47% Trague
4% Gilman
3% Laveen
46% Luzena

FIGURE 36i

REYNOLDS CREEK IDAHO ECO-9

Area 233.1 Km^2
Slope .176 m/m
Shape-Wedge L=1.9W
Length of channel 164.6 Km

Drainage Density - 1/1420m/m^2

$$i = \frac{.008T^{.25}}{(t+.1)^{.71}}$$

Cover

95% Sagebrush & Rangeland
2% Small stands forest
3% Alfalfa

Soils

12.65% Reywat
10.68% Harmell
8.73% Bakeoven
8.33% Gabeca
7.62% Ruclick
6.87% Takeuchi
5.04% Nannyton
3.75% Lasimer
3.71% Gemid
3.08% Babbington
3.01% Searla
2.95% Glasgow
2.90% Farrot
2.81% Kanlee
2.19% Castle Valley
2.14% Nettleton
13.55% Additional

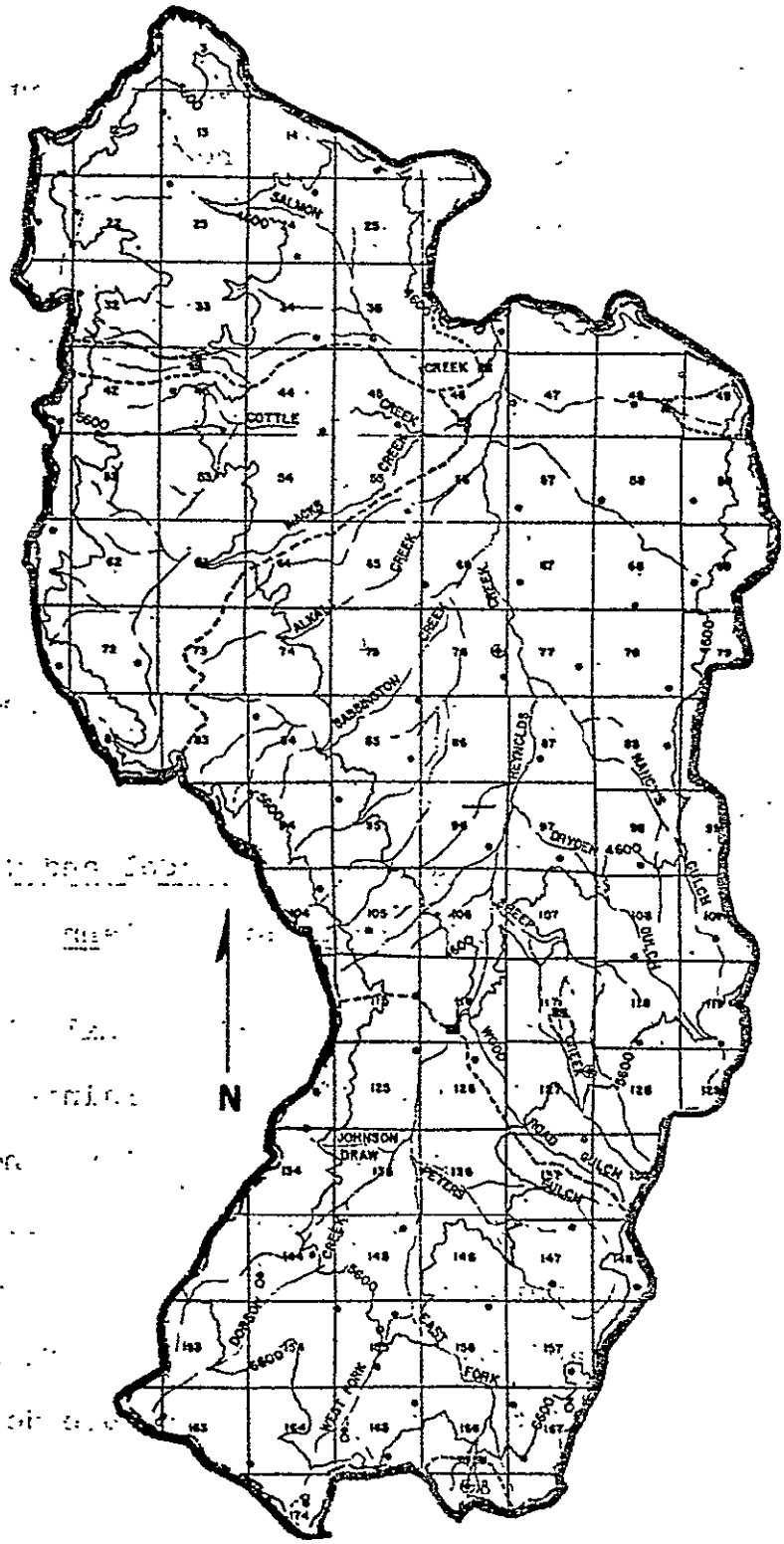

ORIGINAL PAGE IS
OF POOR QUALITY

sensing for the development of this information is discussed in Section 6. The data for each of the basins analyzed is presented in Table 19.

Using the above data, the pertinent parameters for the four models to be compared were computed by the procedure presented in section 5.1. The parameters computed were:

1) the time of concentration;
2) the average infiltration;
3) the average surface friction; and
4) the average subsurface abstraction

Additionally, some of the four models, specifically the SCS model, required the computation of other parameters. A summary of the results of these computations is given in Table 20.

5.3 Results of the Model and Comparison with Actual Records and Existing Planning Models

Having thus determined analytically the values characteristic of the recurring rainfall, and having approximated the subsurface abstraction, the difference between the two became available as the excess rainfall, which is the generator of the overland flow. The overland flow itself and the corresponding peak flow was then computed by means of the overland flow module detailed in Section 4.

TABLE 19

ECO NO./ LOCATION	Soil Class %				SURFACE COVER
	A	B	C	D	
1. Danville Vt.	0	45	18	36	64 % Hardwood forest, 16 % pasture - small grains 17 % Cultivated hay, 1 % row crops 3 % Dense brush and grass
2. Coshocton Ohio	0	14	86	0	23 % Hardwood forest, 58 % grassland, 11 % Cultivated, 8 % misc.
3. Blacksburg Va.	0	39	61	0	59 % pasture, 8 % corn, 28 % cultivated hay, 4 % forest, 2 % idle (grass), 1 % impermeable
4. Oxford Miss.	0	50	50	0	23 % Rowcrops, 35 % pasture & fallow, 40 % forest, 2 % base
5. Fennimore Wisc.	0	100	0	0	23 % Corn, 10 % grain, 21 % hay, 23 % pasture, 16 % fallow, 7 % roads
6. Chickasha, Okla.	0	100	0	0	48 % Graincrops, 44 % Rowcrops 8 % Alfalfa
7. Waco Texas	0	4	0	96	60 % Pasture, 6 % grain, 3 % corn, 7 % cotton, 9 % Rowcrops, 2 % roads, 13 % Weeds
8. Safford Ariz.	0	7	0	93	85 % Bare, 15 % grass
9. Reynolds Ohio	0	17	60	23	95 % Pasture, 2 % forest, 3 % Alfalfa

SUMMARY OF SURFACE COVER AND SOILS DATA FOR THE NINE TEST WATERSHEDS

TABLE 20 SUMMARY OF COMPUTED PLANNING MODEL DATA FOR THE NINE TEST WATERSHEDS

ECO NO.	LOCATION	TIME OF CONC. (1) hrs	SUBSURFACE ABSTRACTIONS				CN (4)	$\bar{Q}/\bar{P}$	Avg Surface Friction Coef
			$\dot{I}_o$ cm/hr.	$\dot{I}_f$ cm/hr	(2) $\overline{Sa}$ m/m	(3) $\bar{a}$ (Holtan)			
1	Danville, Vt.	1.6	8.3	0.33	.24	0.82	71	0.46	0.079
2	Coshocton, Ohio	0.39	5.3	0.30	.20	0.56	74	0.37	0.048
3	Blacksburg, Va.	0.50	7.2	0.38	.21	0.72	75	0.11	0.039
4	Oxford, Miss.	1.7	6.4	0.41	.23	0.56	71	0.18	0.060
5	Fennimore, Wisc.	0.53	5.0	0.58	.23	0.42	70	0.14	0.034
6	Chickasha, Okla.	1.9	2.44	0.48	.26	0.16	76	0.04	0.038
7	Waco, Tex.	0.72	6.10	0.08	.21	0.65	84	0.18	0.035
8	Safford, Ariz.	0.9	2.06	0.08	.20	0.23	94	0.05	0.020
9	Reynolds, Ohio	1.28	2.95	0.23	.20	0.31	74	0.19	0.036

(1) BY KERBY'S EQUATION (2) AVERAGE WATER STORAGE CAPACITY (3) EMPIRICAL CONSTANT IN HOLTANS INFILTRATION FORMULA

(4) SCS CURVE NO. CN

The peak flow thus predicted from the new model - - which for ease of recall we shall hereinafter refer to as the ECO model - - was then compared to each of the nine watershed's streamgage records.

Finally, the predictions of the other three planning models in widest current use - - the Rational formula method, Cook's method, and the SCS method - - were computed for the nine watersheds under the same conditions, and their results compared with the streamgage records and with the predictions from the ECO model.

5.3.1 50-Year Peak Flow from Actual Records

The mean peak flow and its variance were developed from the records for each test watershed. The Q_{50}, i.e. the peak flow corresponding to a 50-year return period, was calculated using Gumbel's extreme frequency distribution:

$$Q_{50} = \overline{Q}_p + K\,\sigma_{Q_p}$$

Where:

Q_{50} = peak flow with 50-year return period

$\overline{Q}_p$ = average yearly peak flow

σ_{Q_p} = variance of the average peak flow

K = Gumbel constant which is a function of recurrence period and length of record.

The values of K are presented in Table 21.

TABLE 21

VALUES OF K FOR DIFFERENT SAMPLE SIZE & RECURRENCE

Sample size	Recurrence Interval					
	10	20	25	50	75	100
15	1.703	2.410	2.632	3.321	3.721	4.005
20	1.625	2.302	2.517	3.179	3.563	3.836
25	1.575	2.235	2.444	3.088	3.463	3.729
30	1.541	2.188	2.393	3.026	3.393	3.653
40	1.495	2.126	2.326	2.943	3.301	3.554
50	1.466	2.086	2.283	2.889	3.241	3.491
60	1.446	2.059	2.253	2.852	3.200	3.446
70	1.430	2.038	2.230	2.824	3.169	3.413
75	1.423	2.029	2.220	2.812	3.155	3.400
100	1.401	1.998	2.187	2.770	3.109	3.349

For example, to compute the 50-year event from a data base of 30 years of peak flow data, the corresponding value of K from the table would be 3.026. Therefore, in this case:

$$Q_{50} = \bar{Q}_p + 3.026\ \sigma_{Q_p}$$

Table 22 summarizes the results of the statistical analysis of the records. It was used as a basis to compare the ECO model and the three planning models in current practice.

5.3.2 Remote Sensing Model (ECO Model) and Results

The ground rules and assumptions employed in applying the simplified analytic formulation were:

1. The expression for the time of concentration must be made to represent the maximum time required for precipitation to reach the outlet from its point of impact.
2. Infiltration abstraction can be accounted for, by modifying the rainfall accordingly.

Referring back to the procedure detailed in Section 4, the time of concentration can be described as the maximum of:

$$t_c = \frac{l_o}{v_o} + \frac{l_c}{v_c} \qquad (1)$$

TABLE 22 Q_{50} FROM STATISTICAL ANALYSIS OF RECORDS

ECO NO.	LOCATION	AVERAGE YRLY. PEAK FLOW $\bar{Q}_p$, $m^3/sec/km^2$	PEAK FLOW VARIANCE σ_{Qp}, $m^3/sec/km^2$	YEARS OF RECORD	K_{50}	Q_{50} $m^3/sec/km^2$
1	DANVILLE, VT.	.35	.169	10	3.54	.95
2	COSHOCTON, O	2.46	2.28	8	3.60	10.6
3	BLACKSBURG, VA.	.32	.30	11	3.40	1.3
4	OXFORD, MISS.	3.18	2.61	11	3.40	12.0
5	FENNIMORE, WISC.	2.68	2.96	25	3.09	11.8
6	CHICKASHA, OKLA.	.17	.20	5	3.65	.89
7	WACO, TEX.	3.60	3.25	25	3.09	13.8
8	SAFFORD, ARIZ.	1.69	1.48	29	3.04	6.2
9	REYNOLDS, IDAHO	.18	.19	5	3.65	.87

ORIGINAL PAGE IS OF POOR QUALITY

Where:

v_o, l_o = overland surface velocity and length

v_c, l_c = channel flow velocity and length

From Manning's equation:

$$t_c = \frac{l_o n_o}{d_o^{2/3} s_o^{1/2}} + \frac{l_c n_c}{d_c^{2/3} s_c^{1/2}} \qquad (2)$$

Where:

n_o, d_o, s_o = overland surface friction, depth of flow, and slope

n_c, d_c, s_c = channel friction, depth of flow, and slope

Expressing channel characteristics as a function of surface characteristics:

$$\begin{aligned} n_c &= k_1 n_o \\ l_c &= k_2 l_o \\ d_c &= k_3 d_o \\ s_c &= k_4 s_o \end{aligned} \qquad (3)$$

Where k_1, k_2, k_3, k_4 are constants.

Substitution of these terms into equation (2) yields:

$$t_{c_{total}} = \frac{l_o n_o}{d_o^{2/3} s_o^{1/2}} + \frac{k_2 l_o k_1 n_o}{(k_3 d_o)^{2/3} (k_4 s_o)^{1/2}}$$

$$= \frac{l_o n_o}{d_o^{2/3} s_o^{1/2}} \left[1 + \frac{k_1 k_2}{k_3^{2/3} k_4^{1/2}} \right] \qquad (4)$$

ORIGINAL PAGE IS
OF POOR QUALITY

$$t_{c_{total}} = t_c \left[1 + \frac{k_1 k_2}{k_3^{2/3} k_4^{1/2}} \right]$$

Or:

$$t_{c_{total}} = \phi \, t_c \qquad (5)$$

Where:

$$\phi = \left[1 + \frac{k_1 k_2}{k_3^{2/3} k_4^{1/2}} \right]$$

The values of k_1, k_2, k_3, k_4 can be computed from flow records and from knowledge of watershed characteristics.

The correction for subsurface abstraction is made by reducing the rainfall input by the amount of water which becomes infiltrated. This was accomplished by introducing a factor into the rainfall expression to degrade the rainfall rate, leading to the modified expression:

$$i = \frac{k_{\alpha_1} T^{\alpha_2}}{(t_c)^{\alpha_3}} \qquad (6)$$

Where:

k = % of rainfall which does not infiltrate

i = precipitation excess

It is worth emphasizing again that this expression is only approximate, since in reality the relationship between rainfall and subsurface abstraction is non-linear.

Thus, the results expected are necessarily approximate; more accurate results should be available from the complete model.

The k term above was calculated by comparing the rain rate occurring over the time of concentration with the average infiltration rate for the same period. For example, the rate ($\dot{P}$) for the 50-year recurrence, t_c duration rain within the Blacksburg watershed is 0.109 meters/hour. The infiltration equation, using the constants for this watershed, derived as explained in Section 5.1, is:

$$\dot{I}_{cm/hr} = .72(4.97 - I)^{1.4} + .38 \qquad (7)$$

For t_c = .52 hours (from the Kirpich formula), the infiltration rate will fall from 7.1 cm/hr to 3.4 cm/hr, with an average value equal to approximately 4.2 cm/hr.

The k factor, therefore, for this case equals:

$$1 - \frac{\dot{I}}{\dot{P}} = 1 - \frac{0.042 \text{ m/hr}}{0.109 \text{ m/hr}} = 0.62 \qquad (8)$$

In other words, for this particular rain event, and for the Blacksburg watershed, approximately 62% of the rainfall becomes runoff.

When both ground rules and assumptions are included, the ECO formula for the overland flow module becomes:

$$Q = 2L\bar{l}\xi \left[\frac{\phi\ (\overline{\ln})^{3/5}}{\xi^{2/5}\ s^{3/10}(3600)} \right]^{\frac{1}{0.4-1/\alpha_3}} \qquad (9)$$

Where:

$$\xi = k_{\alpha_1} T^{\alpha_2}$$

Table 23 supplies values for the constants developed above for the nine test watersheds. The 50-year recurrence flows, as calculated from the ECO formula, are presented in the final column.

5.3.3 Comparison of the Four Planning Models

The predictions of the ECO remote sensing model in its simplified form were compared to the predictions of the three principal planning models in present use for ungaged watersheds. The predictions were calculated using exactly the same base parameters for all models, namely the ARS and USGS data as described in Section 5.1. Computed values for the overall results are tabulated in Table 24, and depicted in Figure 37 for the nine test watersheds.

In Figure 37, the solid line of unit slope (45°) is the locus of the points for which the predictions equal the measurements. Points falling above this line are underestimates; i.e., the predictions fall short. Points

TABLE 23

ECO FORMULA PARAMETERS

ECO NO.	LOCATION	ξ_{50}	MAIN CHANNEL LENGTH L, m	OVERLAND FLOW LENGTH l, m.	Φ	$\bar{n}$	$\bar{s}$	Q_{50} m3/sec/km2
1	DANVILLE, VT.	4.9×10^{-6}	9314	605	2.0	.079	.12	.91
2	COSHOCTON, O.	1.4×10^{-5}	515	163	1.73	.049	.172	26.5
3	BLACKSBURG, VA.	1.4×10^{-5}	5000	167	12.1	.039	.123	1.01
4	OXFORD, MISS.	1.4×10^{-5}	12,000	856	2.61	.060	.114	10.8
5	FENNIMORE, WISC.	1.4×10^{-5}	1545	165	3.28	.034	.080	12.5
6	CHICKASHA, OKLA.	2.0×10^{-5}	34719	600	34.4	.038	.069	.08
7	WACO TEX.	2.2×10^{-6}	3285	263	3.1	.035	.021	11.5
8	SAFFORD, ARIZ.	1.2×10^{-6}	3549	133	6.5	.020	.020	5.3
9	REYNOLDS IDAHO	2.8×10^{-7}	21451	169	32.2	.036	.176	.001

ORIGINAL PAGE IS OF POOR QUALITY

TABLE 24 COMPARISON OF RESULTS FOR PEAK OF THE FIFTY YEAR EVENT

	Q_{50} - $m^3/sec/km^2$				
	Records	ECO	Rational	SCS	Cook
1. Danville Vt.	0.95	0.91	4.8	2.14	5.49
2. Coshocton, Ohio	10.6	25.5	17.6	4.4	12.6
3. Blacksburg Va	1.33	1.01	12.7	7.5	11.1
4. Oxford Miss.	11.9	10.8	7.3	3.1	8.4
5. Fennimore Wisc.	11.8	12.5	18.8	3.5	13.1
6. Chickasha, Okla	0.88	0.08	3.3	2.9	6.44
7. Waco, Texas	13.6	11.5	15.4	22.8	5.7
8. Safford, Ariz.	6.25	5.3	14.4	15.2	5.0
9. Reynolds, Ohio	0.87	0.001	1.7	13.7	3.9

FIGURE 37 COMPARISON OF PREDICTIONS OF Q_{50}

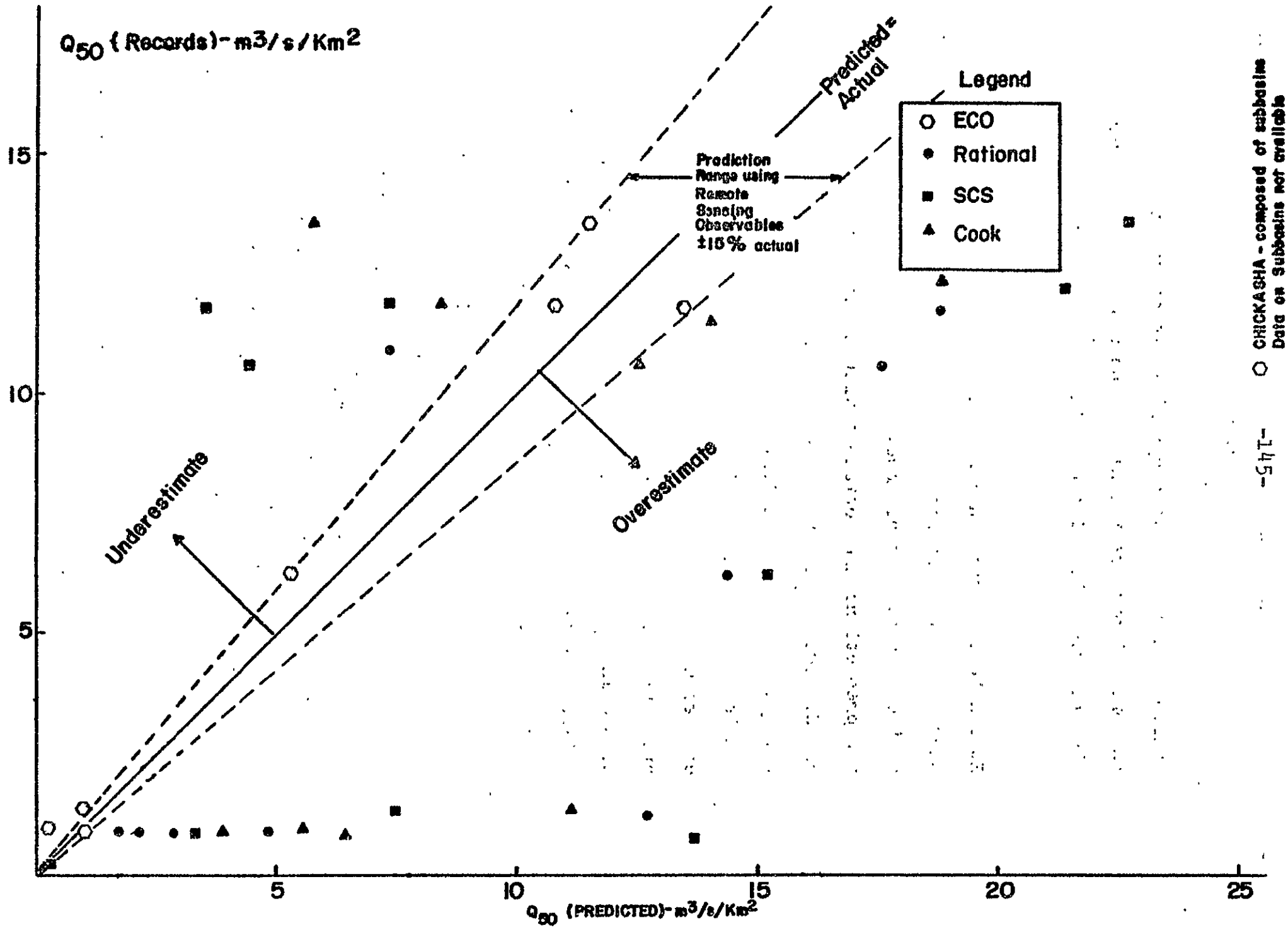

falling below the unit slope line are overestimates; the predictions are too high. The dashed lines around the unit slope line indicate the region bounded by ± 15% error around the measured, or "true," quantities.

It can be seen that in most cases the ECO model, even though only used in its simplified form, is an improvement over conventional models. 66% (6 out of 9) of its predictions are contained within the ± 15% error bound. Two of the three predictions which fall outside the ± 15% bound, specifically Chickasha, Oklahoma, and Reynolds, Idaho, pertain in reality to very large, complex watersheds which require a somewhat different procedure. Namely, that the model be applied to each of the individual subwatersheds of which they are comprised, and that the outputs be then coalesced by routing. This approach is reserved for future effort.

It would of course be premature to claim that the results from this limited sample provide proof that the ECO model concept is valid for all regions of the U.S. and for all flood regimes. Rather, the results tend to support the validity of, and encourage the approach of constructing a hydrologic planning model highly sensitive to remote sensing data inputs. Further effort is required to deter-

mine the sensitivity of this type of model to its key parameters: drainage density, variation of slope, basin area, multiple watersheds, etc. The approach does, however, appear to offer promise of yielding a practical model capable of using satellite data inputs, particularly in the future complete version.

The following section describes the relationship of conventional and future remote sensing techniques to the hydrologic planning model described.

INTENTIONALLY

LEFT

BLANK

6.0 THE RELATIONSHIP OF REMOTE SENSING TECHNIQUES TO HYDROLOGIC PLANNING MODELS

The preceding analysis indicates that the surface features of a watershed play a significant role in the prediction of the peak runoff. This section addresses the applicability and feasibility of measuring surface features, and inferring subsurface characteristics, by remote sensing techniques.

Virtually all the requirements for the measurement of the geometry of surface features have already been adequately matched by remote sensing from aircraft. It remains to assess whether spaceborne sensors of modest geometric resolution but with high radiometric content limit the accuracy of the data.

The requirements for the identification of the types of species on the surface hinge upon multispectral techniques of discrimination. Techniques to satisfy them are currently in the advanced development stages. What needs to be assessed is whether the identification accuracies currently being experienced are consonant to the accuracy of prediction required from hydrologic planning models.

Table 25 depicts the important information required for the development of hydrologic planning models employing remote sensing techniques.

PRECEDING PAGE BLANK NOT FILMED

TABLE 25

INFORMATION ELEMENTS OF SIGNIFICANCE FOR THE CONSTRUCTION OF HYDROLOGIC PLANNING MODELS BASED UPON REMOTE SENSING TECHNIQUES

PRINCIPAL REQUIREMENTS	ANCILLARY REQUIREMENTS
Directly Observable	
Watershed Area	
Surface Friction of Overland Flow Path	
Drainage Density	
Drainage Pattern	
Channel Width	
Slope	
Potentially Inferrable	
Channel Capacity	Areal Extent and Trajectory Statistics of Rainfall
Soil Permeability	
Soil Moisture Statistics	Statistics of Evapotranspiration Drivers (Insolation, Plant Species, etc.)
Currently Requiring Ground Measurement	
Soil Depth	Statistics of Evapotranspiration Drivers (Surface Air Temperature)

ORIGINAL PAGE IS
OF POOR QUALITY

6.1 Remote Sensing Observations

Several of the information requirements of Table 25, such as area and channel width, can be met by direct measurement from remote sensing imagery of digital tapes. Other information requirements result from combining two or more remote sensing measurements. For example, drainage density is measured by using directly observed drainage pattern plus area mensuration. Table 26 summarizes, for each element of information, the existing technique(s), the degree of feasiblity already demonstrated, the principal researchers in each technique, and the typical numerical values of accuracy attained at present from processing of ERTS data.

6.2 Relationship of Remote Sensing Observables to Hydrologic Planning Model Requirements

The modules developed in the previous sections fundamentally require six elements of data: watershed area, overland surface friction coefficient,drainage density, channel width, subsurface abstraction and slope. Significant information is currently available, in the U.S. and developed nations, on four of these elements: area, surface friction coefficient, drainage density, channel width. Additionally, a considerable body of direct and inferential evidence exists from which to deduce the subsurface abstraction component. The last element, slope, can be addressed in three ways:

ORIGINAL PAGE IS
OF POOR QUALITY

TABLE 26

REMOTE SENSING OBSERVATIONS REQUIRED IN HYDROLOGIC PLANNING MODELS

Information Element	Technique	Feasibility	Accuracy Achieved
Watershed Area	Boundary delineation by averaging between recognized drainage patterns or other indicators of adjacent watersheds.	Under development by: Rango/Salomonson, GSFC; M. Deutsch, USGS	± 1/4 pixel
	Mensuration. Use of contour algorithms for small watersheds.	Demonstrated in ERTS. Theory in Reference 8	5% for A≈1000 ha. Better with border algorithm.
Surface Friction Coefficient	Inference from land use by multispectral classification, photo-interpretation.	Landgrebe, Purdue Colwell, U. of Cal.	85-90% 85-95%
Drainage Density and Drainage Pattern	Measurement of total length of streams by contrast enhancement, density slicing, visual interpretation.	Polycn - ERIM Salomonson/Rango, GSFC	± 5%
Channel Width	Subpixel processing.	Castruccio/Loats Theoretical treatment	± 1/8 pixel or ≈ ± 10 m theoretically possible.

1. Where topographic maps exist, overlays can be made and adjusted to known benchmarks.

2. Use can be made of the existing Defense Mapping Agency topographic digital tapes (which cover the entire U.S. at 100 meter contours).

3. Where there is overlap in the ERTS pictures, stereo pairs can be developed from which to measure the slope. In the future, this stereo capability may become routinely available in advanced Earth Observation Satellites.

Table 27 synopsizes the techniques to extract the information required by hydrologic planning models from the remotely sensed observables corresponding to each information element.

6.3 Visual Interpretation of an ERTS Image of a Test Watershed

A test was made to determine the extent of the information requirements of Table 25 which can be satisfied by analysis of ERTS imagery. Figure 38 shows a 4x enlargement of a section of a 9" Band-5 ERTS transparency. Shown is the test watershed at Chickasha, Oklahoma, and its surroundings. Figure 39 gives a comparable USGS topographic map. The 4x magnification was chosen to match the scales of the two maps (1:250,000).

TABLE 27

RELATIONSHIP BETWEEN REMOTE SENSING OBSERVABLES AND INFORMATION ELEMENTS REQUIRED BY THE PLANNING MODEL

Information Element Required	Observable Parameter	Technique
Watershed Area	Ridge lines and other direct indicators. Drainage pattern of subject and adjacent basins.	Boundary can be delineated by direct tracing, or by weighted averaging the separation between drainage patterns of adjacent basins. Then mensuration can be performed by pixel count. Contour algorithm for very high precision, or for small watersheds.
Surface Friction Coefficient	Cover type distribution. Land use.	Use available empirical correlations between cover type, land use and the Chezy or Manning's coefficient to develop a seasonally adjusted surface friction coefficient.
Drainage Density	Watershed area. Length of streams.	Measure total length of streams. Divide by watershed.
Drainage Pattern	Convolution of streams.	Measure convolution of streams to derive meander coefficient.
Channel Width	Channel width.	Measure by using "pixel splitting" in high contrast situation between water and surrounding land surface.
Slope	Apparent relief.	Stereophotogrammetry techniques on overlapped imagery.
Channel Flow Capacity	Channel width. Drainage density. Drainage pattern.	Use existing empirical relationships between channel width, channel meander, drainage pattern to estimate bankfull capacity of channel as a function of channel length.
Soil Permeability and Moisture Statistics	Land use.	Use soil associations by classification.

FIGURE 38 4x ERTS IMAGE, CHICKASHA, OKLA.
FIGURE 10 WATERSHED

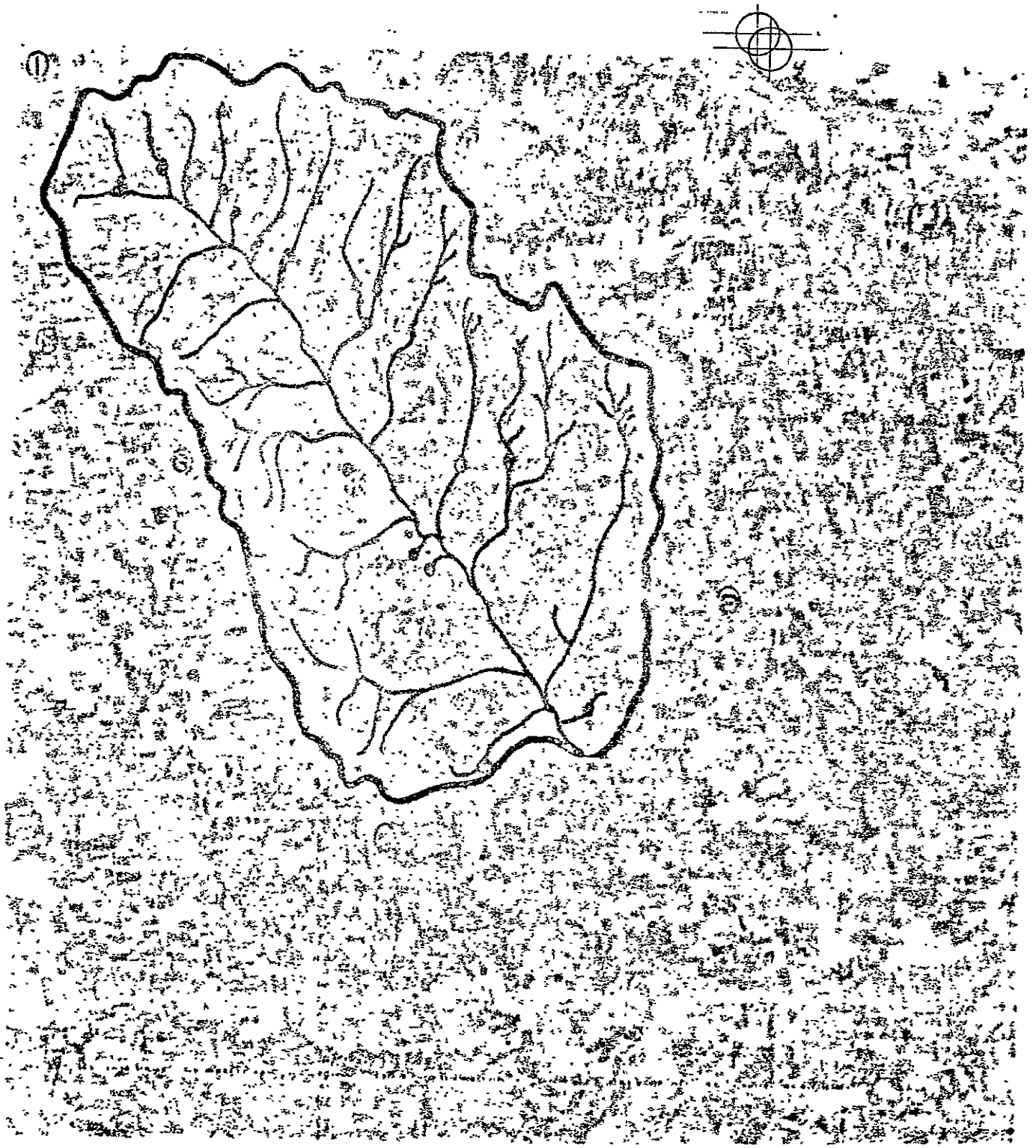

ORIGINAL PAGE IS
OF POOR QUALITY

FIGURE 39 USGS 1:250,000 TOPOGRAPHIC MAP, CHICKASHA, OKL. TEST WATERSHED

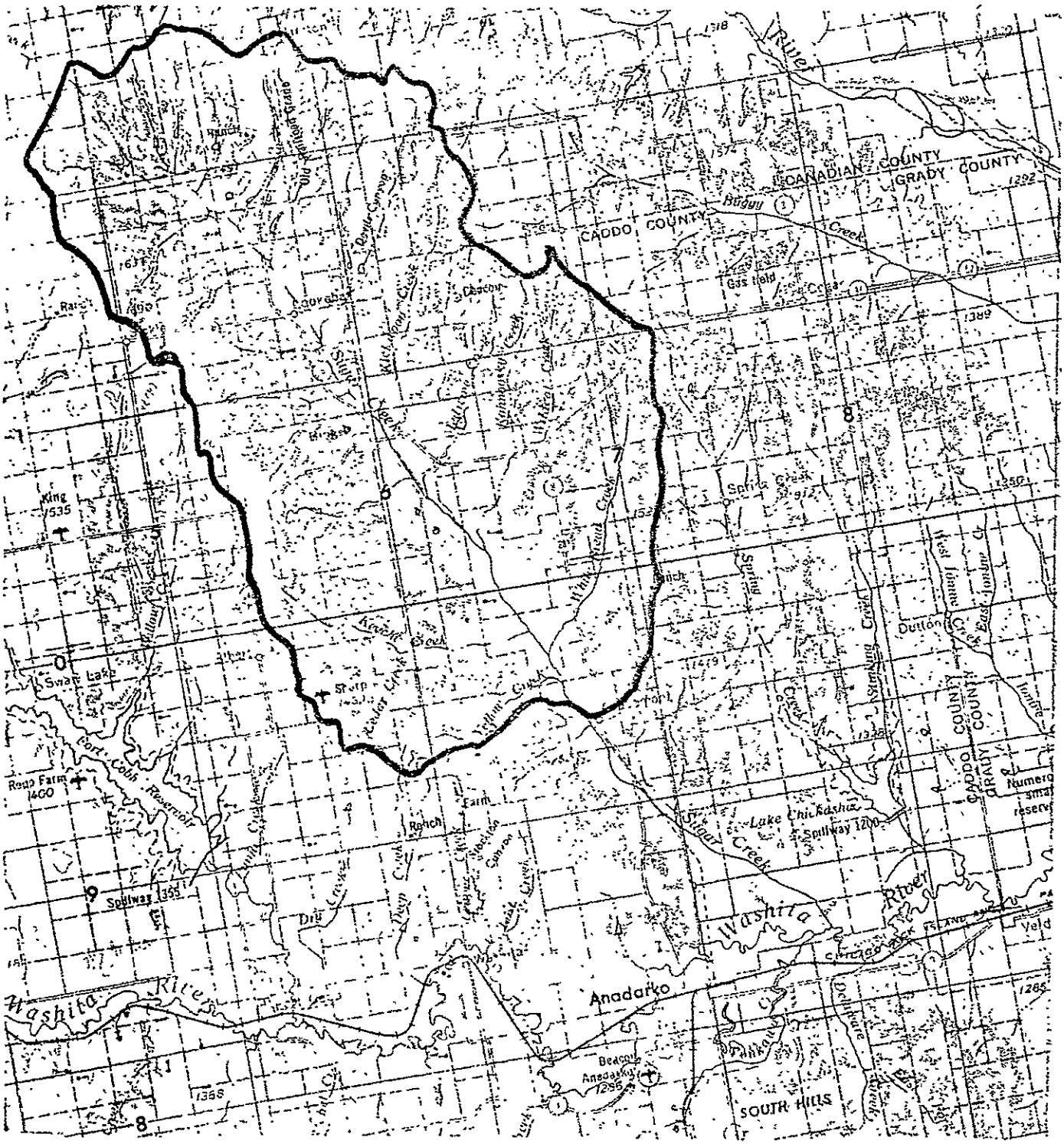

ORIGINAL PAGE IS
OF POOR QUALITY

The general outline of the watershed is apparent in the upper left and central areas of the ERTS image. The delineation of the exact boundaries of the basin was accomplished in this case by comparison with the topographic map, simply because the map was available. However, where maps are unavailable or of doubtful reliability, two methods exist for determining watershed boundaries directly from the ERTS image:

1. The segments lying between streams which drain into the watershed under study and those which drain away from it into other watersheds may be divided in some weighted fashion. If no other information is available, division can occur at their mid-point. Referring to the ERTS image, streams which drain into neighboring basins can be seen at points A through I, while the streams of the test watershed are shown in the overlay. By this means, several reference points are established and can be connected to form an approximation of the watershed area.

2. In regions where the land relief is pronounced, ridge lines are visible and can be followed to delimit the drainage area. The average slope in the Chickasha watershed is less than 6%, however, so this method is not reliable for this case.

The determination of drainage pattern and density builds upon the information derived above. Referring to the image and the overlay, the central channel is visible as a light gray strip running almost North to South. Secondary and tertiary channels are also visible.

An advantage of ERTS imagery is apparent here. This image was taken in October of the year when vegetation density is low. This makes obvious streams which might not have been apparent in the aerial photographs from which the topographic maps are made. This appears to be the case at this location. More streams can be seen from the ERTS image than are recorded on the map, yielding an improved measure of drainage density. Stream length may be measured directly from the ERTS image and divided by watershed area to yield drainage density.

Drainage pattern, in this case one central channel branching into several ancillary streams, is immediately apparent. A second advantage of ERTS image analysis is clear. The USGS has noted that a majority of the secondary streams of this watershed are ephemeral, that is, water does not always flow in them. Actual drainage density, therefore, may change seasonally. Consequently, unnecessary errors could be introduced into hydrologic models. The high frequency return period of ERTS provides the capability of measurement of drainage density at time intervals adequate to insure accuracy.

An important measurement is the determination of channel width, which, as noted earlier, is a determinant of flood potential. The channel boundaries are visible on the 4x enlargement and more apparent on the 8x magnification (Figure 40). A precise measurement would require sub-pixel processing or a quantitative examination of the contrast between land and water on the image.

A combination of drainage density and pattern and of channel width information will yield an indirect measure of channel carrying capacity, as described in Section 4.

To measure surface friction ERTS imagery can improve surface cover estimation. For example, ARS records for this watershed show cover to be 48% sowed crops, 44% row crops, and 8% alfalfa: This most recently published data is from 1967. It is clear from the image that changes have taken place since; for example, about 20% of the watershed is covered with forest, exemplified by the dark gray areas surrounding streams. This is confirmed by the location of shaded (forest) areas on the USGS map. Further, changes in cover can be expected to take place seasonally. These fluctuations can cause up to a tenfold change in overland flow velocity.

Other types of cover are equally visible. Surface water appears as very dark areas on the positive. Large bodies such as Fort Cobb Reservoir (lower left) and Lake Chickasha (lower right) are examples. Smaller bodies form black spots, as called out on the

FIGURE 40 8x ERTS IMAGE: SECTION OF CHICKASHA, OKLA. WATERSHE

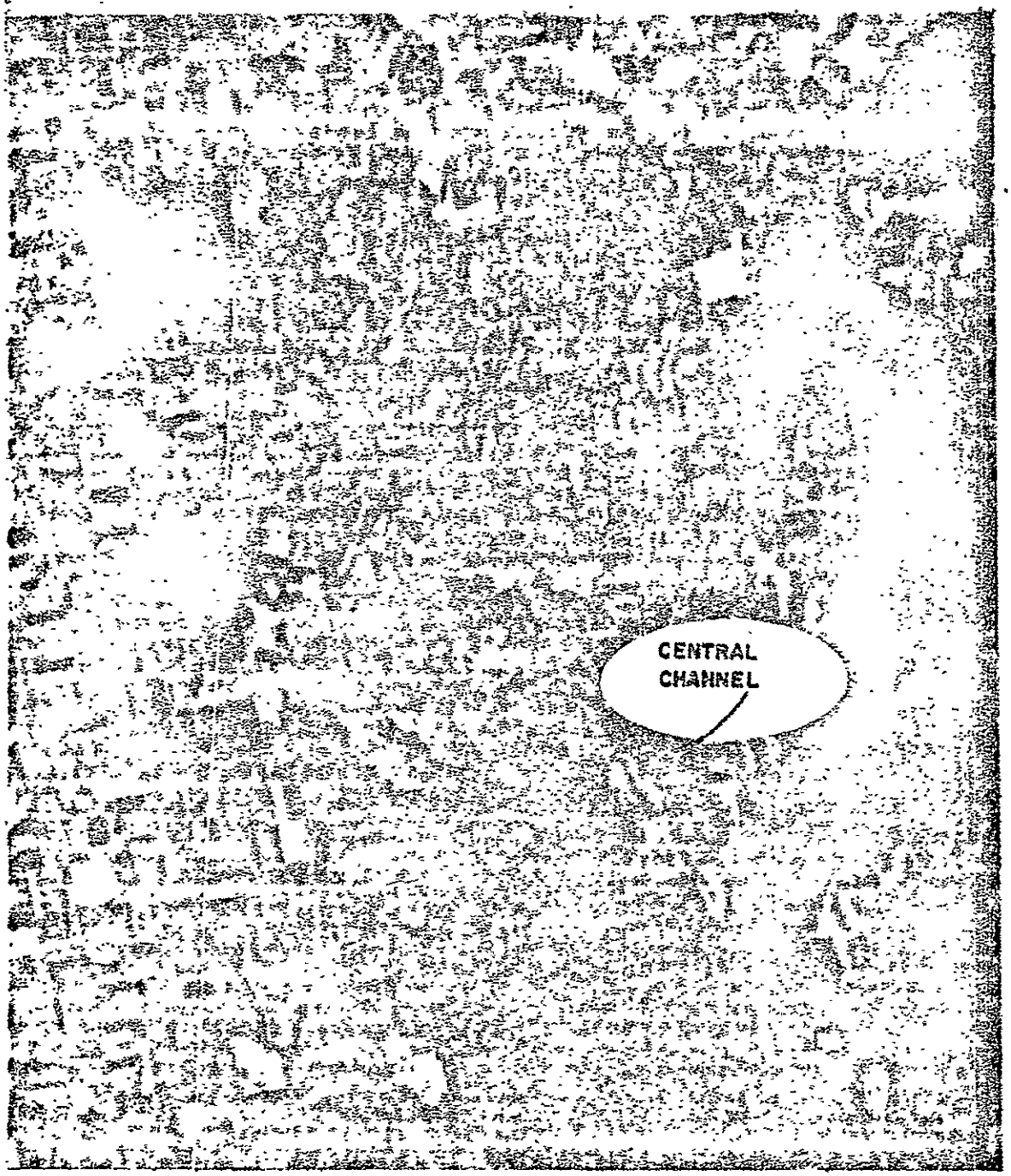

ORIGINAL PAGE IS
OF POOR QUALITY

overlay. Here again, it is clear that some changes have taken place since the topographic map was assembled. For example, a new impoundment exists on Wildcat Creek (point J).

Urban areas can also be noted. Binger, a town of population 603, lies within the watershed and can be distinguished as a rectangular area at point K. Even more geometric regularity is present in cultivated areas.

No effort was made at this juncture to infer subsurface parameters from the ERTS image. The subsurface parameters are in this case available from records. In combination with such information, it appears that techniques for extracting information from ERTS imagery, when fully operational, could play a significant role in supplying data required by hydrologic planning models.

INTENTIONALLY

LEFT

BLANK

7.0 CONCLUSIONS

1. An improved model for the prediction of peak flow events has been structured, which is specifically designed to take maximum advantage of the data and information stream available from remote sensing.

2. The development of the model has been carried to the point where the overall framework has been constructed and five modules simulating the behavior of significant hydrologic processes have been developed.

3. The improved model is considerably more sophisticated than conventional hydrologic planning models. In particular, its modules are not simply interconnected, but require feedback. In spite of this greater complexity, however, the model is readily adaptable to analog computation with modest amounts of hardware. Preliminary sizing shows that the technique can also be programmed onto one of the smaller types of digital minicomputers.

4. The model was exercised -- not in its fully interconnected form, but rather in a simplified version -- to predict the peak runoff from nine experimental Agricultural Research Service watersheds, selected

PRECEDING PAGE BLANK NOT FILMED

at random from among a set of 158 instrumented and well-described watersheds.

5. The predictions of the new model in its simplified version were tested against:
   a. The predictions from three of the most employed contemporary planning models -- i.e., the Rational formula method, Cook's method, and the Soil Conservation Service method.
   b. The streamgage records of the nine test watersheds.

6. The results indicate that, within the range of applicability of its simplified version, the new model appears to be considerably more accurate than conventional hydrologic planning models. Specifically, in six out of nine of the watersheds tested, the new model supplied predictions of peak flow for the 50-year event falling within error bounds of ± 15%. For these same six watersheds, conventional models yielded discrepancies with respect to the records ranging from a minimum of 1.2 to 1 to a maximum of 15 to 1. For the 3 remaining watersheds, the new model yielded predictions of lesser accuracy -- the worst being 2 to 1. Reasonable explanations for the discrepancy are:

a. The fact of having oversimplified the model by not operating it in its fully interconnected version.

b. The three watersheds are considerably more complex than the other six, and they need to be split into subwatersheds, predicting the output from these, then routing all outputs through the watershed channels. This technique, which appears to be well in hand, is proposed for future phases of the effort.

7. The appropriate techniques whereby to extract the inputs and parameters required by the new model from remotely sensed information -- whether imagery or digital tapes -- were explicitly defined. Their feasibility was identified from specific past and ongoing ERTS investigator efforts.

8.0 APPENDIX

The Appendix, which summarizes pertinent data for the 158 ARS test watersheds, includes the following information:

- Watershed number
- Location
- Area
- Slope
- Shape
- Shape correction factor
- Time of concentration in hours and minutes

PRECEDING PAGE BLANK NOT FILMED

TEST WATERSHED DATA

Location Code	Location	Area (ha)	Slope	Shape	C	Time of Concentration	
						Hrs.	Mins.
A1	N. DANVILLE, VT. W-1	4293.8	.120	T	1.32	.79	47.4
A2	W-2	59.1	.145	E:L=2W	1.59	.16	9.8
A3	W-3	836.5	.139	E:L=1.7W	1.47	.43	25.9
A4	W-4	4351.3	.158	W:L=1.5W	1.73	.88	52.7
A5	W-5	11116.6	.139	C	1.13	.95	57.3
B6	COSHOCTON, O. #5	141.2	.155	E:L=1.9W	1.55	.22	13.0
B7	#10	49.4	.162	E:L=1.7W	1.47	.14	8.2
B8	#92	372.3	.166	C	1.13	.25	14.8
B9	#94	615.1	.159	E:L=1.7W	1.47	.36	21.8
B10	#95	1040.1	.169	W:L=1.3W	1.61	.47	28.0
B11	#97	1853.5	.172	E:L=2.2W	1.67	.60	35.8
B12	#194	75.7	.172	SQ	1	.12	7.1
B13	#196	122.6	.162	C	1.13	.16	9.5
B14	#994	7082.2	.172	E:L=2.5W	1.78	1.05	62.9

CODE- R= RECTANGLE SQ= SQUARE C= CIRCLE

E= ELLIPSE T= TRIANGLE W=WEDGE

ECOSYSTEMS INTERNATIONAL INC

TEST WATERSHED DATA

Location Code	Location	Area (ha)	Slope	Shape	C	Time of Concentration	
						Hrs.	Mins.
C15	BLACKSBURG, VA. T.C.: W-1	1235.9	.123	E:L=2.6W	1.82	.62	37.2
C16	B.C.:W-1	361.4	.160	E:L=1.7W	1.47	.30	17.8
C17	C.C.:W-1	318.1	.119	SQ	1	.23	14.1
C18	P.C.:W-1	73.7	.085	W:L=2W	2	.26	15.6
C19	L.W.C:W-1	595.3	.055	C	1.13	.45	27.2
C20	C.R.:W-1	818.7	.200	T	1.32	.34	20.6
C21	R.R.B.:W-1	224.6	.056	W:L=2W	2	.48	28.8
C22	P.M.B.:W-1	77.7	.081	SQ	1	.16	9.7
C23	F.C:W-1	157.4	.062	E:L=1.8W	1.51	.32	19.0
C24	C.B.W.:W-1	428.2	.152	R:L=4.7W	2.17	.43	26.1
C25	STAUNTON,VA. W-1	157.8	.145	R:L=3.2W	1.79	.26	15.6
C26	W-II	983.4	.126	R:L=1.3W	1.14	.39	23.5
C27	W-III	2486.4	.142	R:L=2.5W	1.6	.69	41.7
D28	HIGH PT., N.C. W-1	8539.1	.072	E:L=2.3W	1.71	1.52	91.7

CODE- R= RECTANGLE SQ= SQUARE C= CIRCLE

E= ELLIPSE T = TRIANGLE W= WEDGE

ECOSYSTEMS INTERNATIONAL INC.

TEST WATERSHED DATA

Location Code	Location	Area (ha)	Slope	Shape	C	Time of Concentration	
						Hrs.	Mins.
D29	W-II	4168.4	.072	E:L=2.9W	1.93	1.27	76.4
D30	W-III	2925.9	.116	T	1.32	.71	42.4
D31	AHOSKIE, N.C. W-A1	14763.3	.011	E:L=E.1W	1.98	4.35	261.2
D32	W-A2	6216.1	.109	SQ	1	.76	45.8
D33	W-A3	958.3	.010	C	1.13	1.05	62.9
D34	W-A4	673.4	.013	C	1.13	.83	49.7
E35	OXFORD, MISS. W-4	809.4	.114	R:L=1.9W	1.4	.44	26.6
E36	W-5	457.3	.088	SQ	1	.30	18.2
E37	W-10	2238.0	.114	T	1.32	.63	37.6
E38	W-12	9227.0	.104	E:L=2W	1.59	1.29	77.5
E39	W-17	12990.7	.096	C	1.13	1.17	70.1
E40	W-19	98.3	.132	T	1.32	.18	10.7
E41	W-24	206.8	.139	T	1.32	.23	13.9
E42	W-28	437.1	.123	R:L=2.6W	1.61	.38	22.7

CODE- R= RECTANGLE SQ= SQUARE C= CIRCLE

E= ELLIPSE T = TRIANGLE W=WEDGE

ECOSYSTEMS INTERNATIONAL INC.

TEST WATERSHED DATA

Location Code	Location	Area (ha)	Slope	Shape	C	Time of Concentration Hrs.	Mins.
E43	W-30	45.7	.105	C	1.13	.13	7.7
E44	W-32	8093.9	.088	C	1.13	1.0	60
E45	W-34	30352.1	.087	T	1.32	1.90	113.8
E46	W-35	3055.4	.074	E:L-2.5W	1.78	1.05	63.0
F47	COLBY, WISC. W-1	139.6	.025	R:L=2W	1.41	.40	23.1
F48	IOWA CITY, IOWA	779.4	.103	E:L=3.4W	2.09	.62	37.0
F49	FENNIMORE, WISC. W-1	133.5	.08	E:L=2.1W	1.63	.29	17.1
F50	W-4	69.2	.05	C	1.13	.20	12.0
F51	COON VALLEY, WISC. W-1	19991.9	.193	C	1.13	1.05	63.3
F52	W-2	19969.2	.200	C	1.13	1.04	62.4
G53	NEWELL, S.D. W-2	46.5	.111	E:L=2.4W	1.75	.18	10.6
G54	W-4	42.5	.114	R:L=2.8W	1.67	.17	.10
G55	W-7	64.8	.075	R:L-2.7W	1.64	.23	13.6
G56	W-8	64.8	.122	E:L=1.5W	1.38	.16	9.7

CODE- R= RECTANGLE SQ= SQUARE C= CIRCLE

E= ELLIPSE T = TRIANGLE W=WEDGE

ECOSYSTEMS INTERNATIONAL INC.

TEST WATERSHED DATA

Location Code	Location	Area (ha)	Slope	Shape	C	Time of Concentration	
						Hrs.	Mins.
G57	W-9	329.8	.091	R:L=4.3W	2.07	.46	27.7
G58	W-10	113.3	.180	T	1.32	.17	10.0
G59	W-11	64.8	.102	W:L=1.6W	1.79	.21	12.7
G60	W-13	64.8	.059	W:L=3W	2.45	.33	19.9
G61	W-15	46.5	.051	W:L=4.5W	3	.36	21.7
G62	W-16	5261.0	.063	E:L=2W	1.59	1.29	77.6
H63	SHENANDOAH, IOWA W-1	51800.9	.072	R:L=10W	3.16	4.91	294.6
H64	W-11	27195.5	.061	R:L=13W	3.61	4.52	271.4
H65	HASTINGS, NEB. W-3	194.7	.059	E:L=1.5W	1.38	.33	19.6
H66	W-5	166.3	.061	W:L=2W	2	.41	24.8
H67	W-8	844.2	.057	E:L=2.7W	1.85	.73	43.7
H68	W-11	1412.7	.053	E:L=3.8W	2.20	1.04	62.7
H69	TREYNOR, IOWA W-3	43.3	.076	T	1.32	.16	9.8
H70	W-4	60.7	.073	T	1.32	.19	11.4

CODE- R= RECTANGLE SQ= SQUARE C= CIRCLE

E= ELLIPSE T = TRIANGLE W=WEDGE

ECOSYSTEMS INTERNATIONAL INC.

TEST WATERSHED DATA

Location Code	Location	Area (ha)	Slope	Shape	C	Time of Concentration	
						Hrs.	Mins.
H71	W-5	157.4	.076	E:L=2W	1.59	.31	18.7
I72	CHICKASHA, OKLA. 110	10178.1	.053	T	1.32	1.55	92.7
I73	111	6734.1	.056	C	1.13	1.15	68.7
I74	121	53298.3	.058	E:L=2W	1.59	3.15	189.2
I75	131	10384.5	.054	E:L=2W	1.59	1.78	107.0
I76	311	6153.8	.043	W:L=3W	2.45	2.17	130.0
I77	411	13832.5	.049	SQ	1	1.45	86.8
I78	511	15746.7	.043	W:L=2.8W	2.37	3.03	182.0
I79	512	9206.8	.060	R:L=2.5W	1.58	1.63	97.7
I80	513	4983.4	.047	W:L=4W	2	1.69	101.5
I81	514	2924.3	.061	W:L=3W	1.73	1.12	66.9
I82	522	53796.0	.025	E:L=1.5W	1.38	3.95	237.3
I83	611	1960.7	.047	R:L=75W	1.87	1.12	67.3
I84	612	227.8	.063	C	1.13	.30	17.8

CODE- R= RECTANGLE SQ= SQUARE C= CIRCLE

E= ELLIPSE T = TRIANGLE W=WEDGE

ECOSYSTEMS INTERNATIONAL INC.

TEST WATERSHED DATA

Location Code	Location	Area (ha)	Slope	Shape	C	Time of Concentration	
						Hrs.	Mins.
I85	621	8624.0	.041	SQ	1	1.26	75.6
I86	5141	1644.7	.051	W:L=2.8W	2.37	1.19	71.4
I87	5142	145.7	.048	C	1.13	.28	16.6
I88	5143	196.7	.049	W:L=2W	2.0	.48	28.8
I89	5144	589.2	.048	E:L=2W	1.6	.62	37.1
I90	5145	102.4	.095	E:L=2W	1.55	.24	14.2
I91	5146	308.4	.074	E:L=2W	1.59	.41	24.5
I92	STILLWATER, OKLA. W-4	83.4	.073	E:L=2.2W	1.78	.26	15.8
J93	VEGA, TEX. W-1	52.2	.026	T	1.32	.27	16
J94	WACO, TEX. C	234.3	.020	W:L=1.2W	1.55	.58	34.9
J95	D	449.2	.021	W:L=2W	2.0	.91	54.8
J96	G	1772.6	.021	W:L=2W	2.0	1.55	93
J97	J	2371.5	.022	R:L=4W	2	1.67	99.7
J98	W-1	71.2	.022	E:L=2W	1.59	.37	22.2

CODE- R= RECTANGLE SQ= SQUARE C= CIRCLE

E= ELLIPSE T = TRIANGLE W=WEDGE

ECOSYSTEMS INTERNATIONAL INC.

TEST WATERSHED DATA

Location Code	Location	Area (ha)	Slope	Shape	C	Time of Concentration Hrs.	Time of Concentration Mins.
J99	W-2	52.6	.025	E:L=2W	1.59	.31	18.4
J100	Y	125.1	.024	T	1.32	.39	23.1
J101	Y-2	53.4	.026	SQ	1	.22	13.0
J102	Z	125.5	.018	T	1.32	.43	25.8
K103	SONORA, TEX. W-14	12432.2	.036	W:L=2W	2.0	2.67	159.9
K104	S-9	717.9	.017	C	1.13	.77	45.9
K105	S-10	2182.1	.028	W:L=2.5W	2.24	1.60	96.0
K106	S-11	4365.4	.031	W:L=1.7	1.84	1.73	103.6
K107	S-12	1133.5	.043	C	1.13	.64	38.3
K108	S-13	277.6	.054	E:L=1.41	1.34	.23	13.9
L109	ALBUQUERQUE, N.M. W-1	40.5	.183	W:L-2.5W	2.24	.17	10.0
L110	47.0001	99.6	.183	-	1.32	.16	9.6
L111	W-111	68.0	.085	W:L=2W	2	.25	15.1
L112	MEXICAN SP., N.M. W-1	75.7	.054	E:L=1.41W	1.34	.23	13.9

CODE- R= RECTANGLE SQ= SQUARE C= CIRCLE

E= ELLIPSE T = TRIANGLE W=WEDGE

ECOSYSTEMS INTERNATIONAL INC.

TEST WATERSHED DATA

Location Code	Location	Area (ha)	Slope	Shape	C	Time of Concentration	
						Hrs.	Mins.
L113	W-2	246.9	.350	R:L=1.5W	1.22	.16	9.8
L114	W-111	536.2	.290	T	1.32	.26	15.5
L115	W-6	2246.4	.275	T	1.32	.46	27.5
L116	W-7	3437.9	.214	W:L=1.6W	1.79	.82	49.2
L117	W-8	8462.2	.229	T	1.32	.76	45.9
L118	W-10	6968.8	.255	T	1.32	1.13	67.7
L119	W-11	18648.3	.220	T	1.32	.49	29.2
L120	W-12	1032.0	.150	R:L=2.6W	1.61	.58	34.5
L121	W-13	1359.8	.198	R:L=4W	2.0	.58	345
L122	W-14	1440.7	.345	E:L=2.4W	1.74	.43	25.6
L123	W-15	1918.3	.238	R:L=4W	2	.61	36.7
L124	SANTA FE, N.M. W-1	57.1	.086	W:L=2W	1.41	.18	10.6
L125	W-11	319.7	.084	R:L-4.1W	2.02	.46	27.7
M126	SAFFORD, ARIZ. W-1	210.0	.020	R:L=5.3	2.3	.76	45.3

CODE- R= RECTANGLE SQ= SQUARE C= CIRCLE

E= ELLIPSE T = TRIANGLE W= WEDGE

ECOSYSTEMS INTERNATIONAL INC.

TEST WATERSHED DATA

Location Code	Location	Area (ha)	Slope	Shape	C	Time of Concentration	
						Hrs.	Mins.
M127	W-11	276.0	.170	R:L=7W	2.65	.41	24.6
M128	W-IV	309.2	.120	E:L=9W	3.38	.59	35.5
M129	W-5	292.6	.110	E:L=8W	3.19	.57	34.3
M130	TOMBSTONE, ARIZ. W-6	9510.3	.107	E:L=2.5	1.78	1.41	84.6
M131	63.007	1351.7	.119	T	1.32	.52	31.2
M132	63.008	1550.0	.112	W:L=5W	3.16	1.07	64.3
M133	63.001	823.6	.120	E:L=2W	1.59	.48	28.9
M134	63.111	57.9	.129	R:L=2W	1.41	.16	9.4
N135	EMMETT, IDAHO	88.6	.203	R:L=5.9	2.43	.15	8.8
N136	MOSCOW, IDAHO	59.5	.161	R:L=2W	1.41	.14	8.3
N137		72.0	.164	R:L=1.7W	1.30	.15	8.8
N138	PULLMAN, WASH. S.F.R. River	21003.6	.194	R:L=5W	2.23	1.81	108.6
N139	M.F.C.	7122.6	.163	R:L=4.4W	2.10	.87	52.4
N140	F.M.C.	18615.9	.178	R:L=3W	1.73	1.3	89.0

CODE- R= RECTANGLE SQ= SQUARE C= CIRCLE

E= ELLIPSE T = TRIANGLE W=WEDGE

ECOSYSTEMS INTERNATIONAL INC.

TEST WATERSHED DATA

Location Code	Location	Area (ha)	Slope	Shape	C	Time of Concentration	
						Hrs.	Mins.
N141	G.S 7	6758.4	.163	P:L=4.2W	2.05	.86	51.4
N142	G.S 8	308.4	.174	R:L=3W	1.73	.31	18.6
N143	G.S 9	355.7	.167	E:L=2.7W	1.85	.27	16.3
N144	G.S 10	1792.8	.171	R:L=1.8	1.34	.50	30.2
O145	REYNOLDS, IDAHO W-1	23350.9	.176	W:L=1.9W	1.95	1.77	105.9
O146	W-2	3638.2	.342	SO	1	.41	24.6
O147	W-3	3175.2	.297	W:L=2W	2	.70	42.0
O148	W-4	54444.4	.147	C	1.13	.73	43.6
O149	W-11	123.8	.286	R:L=4W	2	.20	12.2
O150	W-12	83.0	.244	R:L=1.7W	1.3	.13	7.8
O151	W-13	40.5	.217	W:L=1.6W	1.79	.13	7.9
P152	SANTA PAULA, CAL. W-1	167.1	.476	R:L=1.7	1.30	.14	8.1
P153	W-111	42.9	.503	P:L=2.4W	1.55	.08	4.6
P154	W-6	66.0	.062	R:L=2.2W	1.48	.21	12.5

CODE- R= RECTANGLE SQ= SQUARE C= CIRCLE

E= ELLIPSE T = TRIANGLE W=WEDGE

ECOSYSTEMS INTERNATIONAL INC.

TEST WATERSHED DATA

Location Code	Location	Area (ha)	Slope	Shape	C	Time of Concentration	
						Hrs.	Mins.
P155	Honda	297.5	.341	R:L=5W	2.25	.19	11.6
P156	Milligan	650.3	.263	R:L=6W	2.45	.29	17.3
P157	Perkins	741.4	.220	R:L=6W	2.45	.33	19.5
P158	Honda, Colo.	2403.5	.188	R:L=2.4W	1.55	.54	32.7

CODE- R= RECTANGLE SQ= SQUARE C= CIRCLE

E= ELLIPSE T = TRIANGLE W=WEDGE

ECOSYSTEMS INTERNATIONAL INC.

9.0 BIBLIOGRAPHY

Precipitation; Meteorology

1) Rainfall Frequency Atlas of the U.S., Dept. of Commerce, Weather Bureau, 1963.

2) Rainfall Intensity - Frequency Regime Report #29, Vol. 1-5, Eastern U.S., Dept. of Commerce, Weather Bureau, 1958.

3) Climatic Atlas of the U.S., Dept. of Commerce, E.S.S.A., Environmental Data Service, 1968.

4) Probable Maximum Precipitation, Susquehanna River Drainage Above Harrisburg, Pa., Hydrometeorological Report No. 40, Dept. of Commerce, Weather Bureau, May, 1965.

5) Probable Maximum and TVA Precipitation Over the Tennessee River Basin Above Chattanooga, Hydrometeorological Report No. 41, Dept. of Commerce, Weather Bureau, June, 1965.

6) Probable Maximum Precipitation, Northwest States, Hydrometeorological Report No. 43, Dept. of Commerce, Weather Bureau, November, 1966.

7) Probable Maximum Precipitation Over South Platte River, Colorado, and Minnesota River, Minnesota, Hydrometeorological Report No. 44, Dept. of Commerce, Weather Bureau, January, 1969.

8) Probable Maximum Precipitation, Mekong River Basin, Hydrometeorological Report No. 46, Dept. of Commerce, Weather Bureau, May, 1970.

9) Meteorology of Flood-Producing Storms in the Mississippi River Basin, Hydrometeorological Report No. 34, Dept. of Commerce, Weather Bureau, July, 1956.

10) Meteorology of Hydrologically Critical Storms in California, Hydrometeorological Report No. 37, Dept. of Commerce, Weather Bureau, December, 1962.

11) Meteorology of Flood-Producing Storms in the Ohio River Basin, Hydrometeorological Report No. 38, Dept. of Commerce, Weather Bureau, May, 1961.

12) "Accuracy of Precipitation Measurements for Hydrologic Modeling", L. W. Larson & E.L. Peak, presented at A.G.U. Spring Meeting, 1974.

13) "Methods of Estimating Areal Average Precipitation", A.F. Rainbird, Report No. 5, World Meteorological Organization, Reprinted in 1970.

14) "Measurement and Estimation of Evaporation and Evapotranspiration", Technical Note No. 83, World Meteorological Organization, Reprinted in 1971.

15) Storm Rainfall in the U.S.; Depth - Area - Duration Data, U.S. Army Corps of Engineers, July 1973.

16) Climatological Data, and Local Climatological Data for Washington, D.C.; Maryland; & Delaware, Aug. 1972 to present, U.S. Dept. of Commerce, N.O.A.A.

17) Meteorological Drought, Research Paper No. 45, U.S. Dept. of Commerce, Weather Bureau, 1965.

Soils

1) Soil Survey Manual, Soil Conservation Manual, 1951.

2) Soil Survey, Dorchester County, Md., U.S.D.A. and Maryland Agricultural Experiment Station, 1963.

3) Soil Survey, Carroll County, Md., U.S.D.A. and Maryland Agricultural Experiment Station, 1969.

4) Soil Survey, Prince George's County, Md., U.S.D.A. (S.C.S.) and Maryland Agricultural Experiment Station, 1967.

5) Soil Survey, Marshall County, Miss. U.S.D.A. (S.C.S.) and Mississippi Agricultural Experiment Station, 1972.

6) Soil Survey, Caddo County, Okla., U.S.D.A. (S.C.S.) and Oklahoma Agricultural Experiment Station, 1973.

7) Soil Survey, Webster County, Neb. U.S.D.A. (S.C.S.) and University of Nebraska, Conservation and Survey Division, 1974.

8) Soil Survey, Grant County, Wisc. U.S.D.A. (S.C.S.); Wisconsin Geological and Natural History Survey; Wisconsin Agricultural Experiment Station, [illegible].

9) Soil Survey, McLannan County, Texas U.S.D.A. (S.C.S.) and Texas Agricultural Experiment Station, 1942.

10) Aerial-Photo Interpretation in Classifying and Mapping Soils, Agriculture Handbook 294, Soil Conservation Service, U.S.D.A., 1966.

11) World Soils, E.M. Bridges (University Press: Cambridge, 1970).

12) S.C.S. Soil Group Classes, S.C.S. Hydrology Handbook.

Models & Modeling

1) Digital Simulation in Hydrology: Stanford Watershed Model IV, N.H. Crawford & R.K. Linsley, Dept. of Civil Engineering, Stanford University, July 1966.

2) Numerical Simulation of Watershed Hydrology (Texas Watershed Model), OWRR Technical Report HYD 14-7001.

3) Network Analysis of Runoff Computation (Chicago Hydrograph Model), C. J. Keifer, J.P. Harrison, T.O. Hixson, 1970.

4) "A Uniform Technique for Determining Flood Flow Frequencies Water Resources Council", 1967.

5) "Development of a Mathematical Model for the Simulation of Flat-Land Watershed Hydraulics", D.W. Deboer & H.P. Johnson, Iowa State University , November 1, 1969.

6) "Evaluation of a Deterministic Model for Predicting Water Yields from Small Agricultural Watersheds in Virginia", V.O. Shanholtz, J.B. Burford, & J.H. Lillard, Dept. of Agric. Engineering Research Division, Virginia Polytechnic Institute and State University, August, 1972.

7) "Investigation of a Linear Model to Describe Hydrologic Phenomenon of Drainage Basins", F.A. Schmer, Technical Report 19, Water Resources Institute, Texas A&M University, December, 1969.

8) National Weather Service River Forecast System Forecast Procedures, (HYDRO-14), Staff, Hydrologic Research Laboratory, December, 1972.

9) Computer Program for Project Formulation - Hydrology, Technical Release No. 20, U.S.D.A., Soil Conservation Service, May 1965.

10) A Generalized Streamflow Simulation System, U.S.D.C. (National Weather Service) and California Dept. of Water Resources, March, 1973.

11) A Distributed Linear Representation of Surface Runoff, W.O. Maddaus and P.S. Eagleson, MIT, Dept. of Civil Engineering, June 1969.

12) Water Balance Program, U.S. Forest Service, July, 1968.

ORIGINAL PAGE IS
OF POOR QUALITY

13) "Continuous Hydrograph Synthesis With An API-Type Hydrologic Model", W.T. Sittner, C.F. Schauss, J.C. Monro, Water Resources Research, Oct. 1969 P 1007-1021.

14) Analog Computer Simulation of the Runoff Characteristics of an Urban Watershed, V.V. Dhruva Narayana, J.P. Riley, E.K. Israelson; Utah State University, Jan. 1969.

15) Mathmatical Simulation of Hydrologic Events on Ungaged Watersheds, L.F. Huggins & E.J. Monke, Purdue Univ. Water Resources Research Center, March 1970.

16) Calibration of U.S. Geological Survey Rainfall/Runoff Model for Peak Flow Synthesis - Natural Basins, U.S.G.S., October 1973.

17) USDAHL-74 Revised Model of Watershed Hydrology, H.N. Holtan, G.J. Stiltner, W.H. Henson, N.C. Copey. U.S.D.A., July, 1974.

18) COSSARR Model - Streamflow Synthesis and Reservoir Regulation, U.S. Army Engineer Division, North Pacific, Portland, Oregon, January, 1972.

19) Runoff Evaluation and Streamflow Simulation by Computer, U.S. Army Engineer Division, North Pacific, Portland, Oregon, May, 1971.

20) Generalization of Streamflow Characteristics from Drainage Basin Characteristics, D.M. Thomas & M.A. Benson, U.S.G.S., 1969.

21) "Soil Surface Characteristics and Rainfall-Runoff-Moisture Relationships on Coastal Plain Soils", Ronald E. Hermanson, Water Resources Research Institute, Auburn University, 1970.

22) "Stochastic Analysis of Hydrologic Systems", Ven Te Chow, Dept. of Civil Engineering, University of Illinois at Urbana-Champaign, Research Report No. 26, December, 1969.

23) "The Use of Analog and Digital Computers in Hydrology", Proceedings of the Tucson Symposium, International Hydrological Decade, UNESCO, 1969.

Floods & Flooding

1) Magnitude and Frequency of Floods in the U.S., U.S.G.S., 1964.

Part 2-A - South Atlantic Slope Basins, James River to Savannah River;

Part 2-B - South Atlantic Slope and Eastern Gulf of Mexico Basins, Ogeechee River to Pearl River;

ORIGINAL PAGE IS
OF POOR QUALITY

Part 3-A - Ohio River Basin Except Cumberland and Tennessee River Basins;

Part 3-B - Cumberland and Tennessee River Basins;

Part 5 - Hudson Bay and Upper Mississippi River Basins;

Part 6-A - Missouri River Basin above Sioux City, Iowa;

Part 6-B - Missouri River Basin below Sioux City, Iowa;

Part 7 - Lower Mississippi River Basin;

Part 8 - Western Gulf of Mexico Basins;

Part 9 - Colorado River Basin;

Part 10 - The Great Basin;

Part 11 - Pacific Slope Basins in California - (Vol. 1 - Coastal Basins South of the Klamath River Basin & Central Valley Drainage from the West);

Part 11 - Pacific Slope Basins in California - (Vol. 2 - Klamath and Smith River Basins and Central Valley Drainage from the East);

Part 13 - Snake River Basin

2) "Estimation of 100 Year Flood Magnitudes at Ungaged Sites," C. H. Hardison, U.S.G.S., Water Resources Div., 1973.

3) Meteorology of Hypothetical Flood Sequences in the Mississippi River Basin, Hudrometeorological Report No. 35, Dept. of Commerce, weather Bureau, December 1959.

4) Meteorological Criteria For Extreme Floods For Four Basins in the Tennessee and Cumberland River Watersheds, Hydrometeorological Report No. 47, Dept. of Commerce, National Oceanic and Atmospheric Administration, May 1973.

5) Arizona Floods of September 5 and 6, 1970, Natural Disaster Survey Report 70-2, Dept. of Commerce, National Oceanic and Atmospheric Administration, July 1971.

6) Black Hills Flood of June 9, 1972, Natural Disaster Survey Report 72-1, Dept. of Commerce, National Oceanic and Atmospheric Administration, August 1972.

7) The National River and Flood Forecast and Warning Service - (A Plan for Improving), Dept. of Commerce, Weather Bureau, December, 1969.

8) "Flood-Hydrograph Analyses and Computations," Engineering & Design, Corps of Engineers, U.S. Army, 31 Aug. 59.

9) "Generalized Skew Coefficients of Annual Floods in the U.S. and Their Application," C. H. Hardison, U.S.G.S., 1974.

10) "Implicit Dynamic Routing of Floods and Surges in the Lower Mississippi," D. L. Fread, for presentation at A.G.U. Spring Meeting, 1974.

11) "Estimation of Maximum Floods," World Meteorological Organization, Reprinted in 1972.

12) "Forecasting of Heavy Rains and Floods," World Meteorological Organization, 1970.

13) "Floods and Their Computation," Proceedings of the Leningrad Symposium, Volume 1, August, 1967 - UNESCO-WMO.

Hydrology & Hydrologic Processes

1) Water Atlas of the United States, Water Information Center, 1973.

2) The Water Encyclopedia, D. K. Todd, Water Information Center, 1970.

3) The Nation's Water Resources, U.S. Water Resources Council, 1968.

4) Water Publications of State Agencies, Water Information Center, 1972.

5) Representative and Experimental Research Basins in the United States, International Hydrological Decade, 1969.

6) Water Resource Development in Maryland, U.S. Army Corps of Engineers, North Atlantic Division, 1973.

7) Baltimore County Hydraulic Design Manual, Baltimore Co., Md., 1968.

8) Anne Arundel County Hydraulic Design Manual, Anne Arundel Co., Maryland.

9) The Missouri River Basin Comprehensive Framework Study, Missouri Basin Inter-Agency Committee, Vol. 1-7, December 1971.

ORIGINAL PAGE IS
OF POOR QUALITY

10) "River Runoff Theory and Analysis," D. L. Sokolovskii, Environmental Science Services Administration, Dept. of Commerce, 1971.

11) "Suggested Criteria for Hydrologic Design of Storm-Drainage Facilities in the San Francisco Bay Region California," Dept. of the Interior, Geological Survey, Water Resources Division, November 24, 1971.

12) National Atlas of the United States of America, Dept. of the Interior, Geological Survey, 1970.

13) "A Concept for Infiltration Estimates in Watershed Engineering," H. Holtan, Agricultural Research Service, U.S.D.A., 1961.

14) "Derivation of an Equation of Infiltration," H. J. Morel-Seytoux and J. Khanji, Water Resources Research, August 1974.

15) "Systematic Treatment of Infiltration With Applications," H. J. Morel-Seytoux, Environmental Resources Center, Colorado State University Report No. 50, June 1973.

16) Annotated Bibliography on Hydrology And Sedimentation 1966-1968, U.S. and Canada, Joint Bulletin No. 10, Water Resources Council for Soil Conservation Service U.S.D.A.

17) Handbook of Applied Hydrology, Ven Te Chow McGraw-Hill Book Co., 1964.

18) Open Channel Hydrology, Ven Te Chow, McGraw-Hill Book Co., 1959.

19) Introduction to Hydrology, Viesmann, Harbauh & Knapp, Intext Educational Publishers, 1972.

20) "Time of Concentration for Overland Flow," W. S. Kerby, Civil Engineering, March 1959, p. 60

Watershed Sample

1) "Representative and Experimental Basins," C. Toebes and V. Ouryvaev, eds., International Hydrological Decade, UNESCO, 1970.

2) "Hydrologic Data for Experimental Agricultural Watersheds in the U.S., 1956 - 1967, Misc. Publications No. 1262, 1226, 1216, 1194, 1164, 1070, 994, & 945, Agricultural Research Service, U.S.D.A.

3) Monthly Precipitation and Runoff for Small Agricultural Watersheds in the U.S., U.S., U.S.D.A., Agricultural Research Service, June 1957.

4) Selected Runoff Events for Small Agricultural Watersheds in the United States, U.S.D.A., Agricultural Research Service, January 1960.

5) Annual Maximum Flows from Small Agricultural Watersheds in the United States, U.S.D.A., Agricultural Research Service, June 1958.

TABLE OF CONTENTS

	Page
1.0 INTRODUCTION AND BACKGROUND	1
1.1 State of the Art of Planning Models	4
1.1.1 Method 1: The Empirical Approach	4
1.1.2 Method 2: The Statistical Approach	11
1.1.3 Method 3: Semi-Empirical Macro Models - The Rational Approach	13
2.0 GENERAL APPROACH	17
3.0 INVESTIGATION OF DRIVER PHENOMENA	23
3.1 Precipitation	25
3.2 Subsurface Processes	36
3.2.1 Subsurface Abstraction	36
3.2.2 Percolation and Interflow	50
3.3 Evapotranspiration	51
3.4 Interception	58
3.5 Depression Storage	59
3.6 Overland Flow	59
3.7 Important Processes and Drivers for Hydrologic Planning Models	70
4.0 GENERALIZED HYDROLOGIC PLANNING MODEL	79
5.0 DATA ANALYSIS AND MODEL VERIFICATION	97
5.1 Analytical Procedure	98
5.2 Results of the Analysis	109

Figure 36a	Danville, Vt. Watershed
Figure 36b	Coshocton, O. Watershed
Figure 36c	Blacksburg, Va. Watershed
Figure 36d	Oxford, Miss. Watershed
Figure 36e	Fennimore, Wisc. Watershed
Figure 36f	Chickasha, Okla. Watershed
Figure 36g	Waco, Tex. Watershed
Figure 36h	Safford, Ariz. Watershed
Figure 36i	Reynolds, Idaho Watershed
Figure 37	Comparison of Predictions of Q_{50}
Figure 38	4x ERTS Image: Chickasha, Okla. Watershed
Figure 39	USGS 1:250,000 Topographic Map, Chickasha, Okla. Test Watershed
Figure 40	8x ERTS Image: Section of Chickasha, Okla. Watershed

Table 16e	Rainfall Duration Recurrence Data - Fennimore, Wisc.
Table 16f	Rainfall Duration Recurrence Data - Chickasha, Okla.
Table 16g	Rainfall Duration Recurrence Data - Waco, Tex.
Table 16h	Rainfall Duration Recurrence Data - Safford, Ariz.
Table 16i	Rainfall Duration Recurrence Data - Reynolds, Ida.
Table 17	Summary of the Results of Empirical Fit of Rainfall Recurrence Data for the Test Watersheds
Table 18	Physiographic Data Summary for the Nine Test Watersheds
Table 19	Summary of Surface Cover and Soils Data for the Nine Test Watersheds
Table 20	Summary of Computed Planning Model Data for the Nine Test Watersheds
Table 21	Values of K for Different Sample Size and Recurrence
Table 22	Q_{50} from Statistical Analysis of Records
Table 23	ECO Formula Parameters
Table 24	Comparison of Results for Peak of the Fifty-Year Event
Table 25	Information Elements of Significance for the Construction of Hydrologic Planning Models Based Upon Remote Sensing Techniques
Table 26	Remote Sensing Observations Required in Hydrologic Planning Models
Table 27	Relationship Between Remote Sensing Observables and Information Elements Required by the Planning Model

TABLES

Table 1	Principal Planning Models in Current Use
Table 2	Summary Descriptions of Hydrologic Processes
Table 3	Potentially Important Drivers as Related to Hydrologic Processes
Table 4	Principal Infiltration Formulations
Table 5	Average Interflow Rates
Table 6	Average Evapotranspiration Rate for the Test Watershed Areas
Table 7	Hydrologic Parameters for Different Channel Cross Sections
Table 8	Values for the Computation of the Roughness Coefficient
Table 9	Manning's Roughness Coefficient for Overland Flow for Various Surface Types
Table 10	Sensitivity of Runoff to the Principal Drivers
Table 11	Infiltration Rates by Soil Class
Table 12	Available Storage Capacity by Soil Type
Table 13	Vegetative Cover Factors (a) for Holtan's Equation
Table 14	SCS Curve Numbers
Table 15	Retardance Coefficients - Kerby's Equation
Table 16a	Rainfall Duration Recurrence Data - Danville, Vt.
Table 16b	Rainfall Duration Recurrence Data - Coshocton, O.
Table 16c	Rainfall Duration Recurrence Data - Blacksburg. Va.
Table 16d	Rainfall Duration Recurrence Data - Oxford, Miss.

FIGURE 5
ERROR IN ESTIMATING LONG TIME MEAN RUNOFF FROM SHORT TIME RECORDS

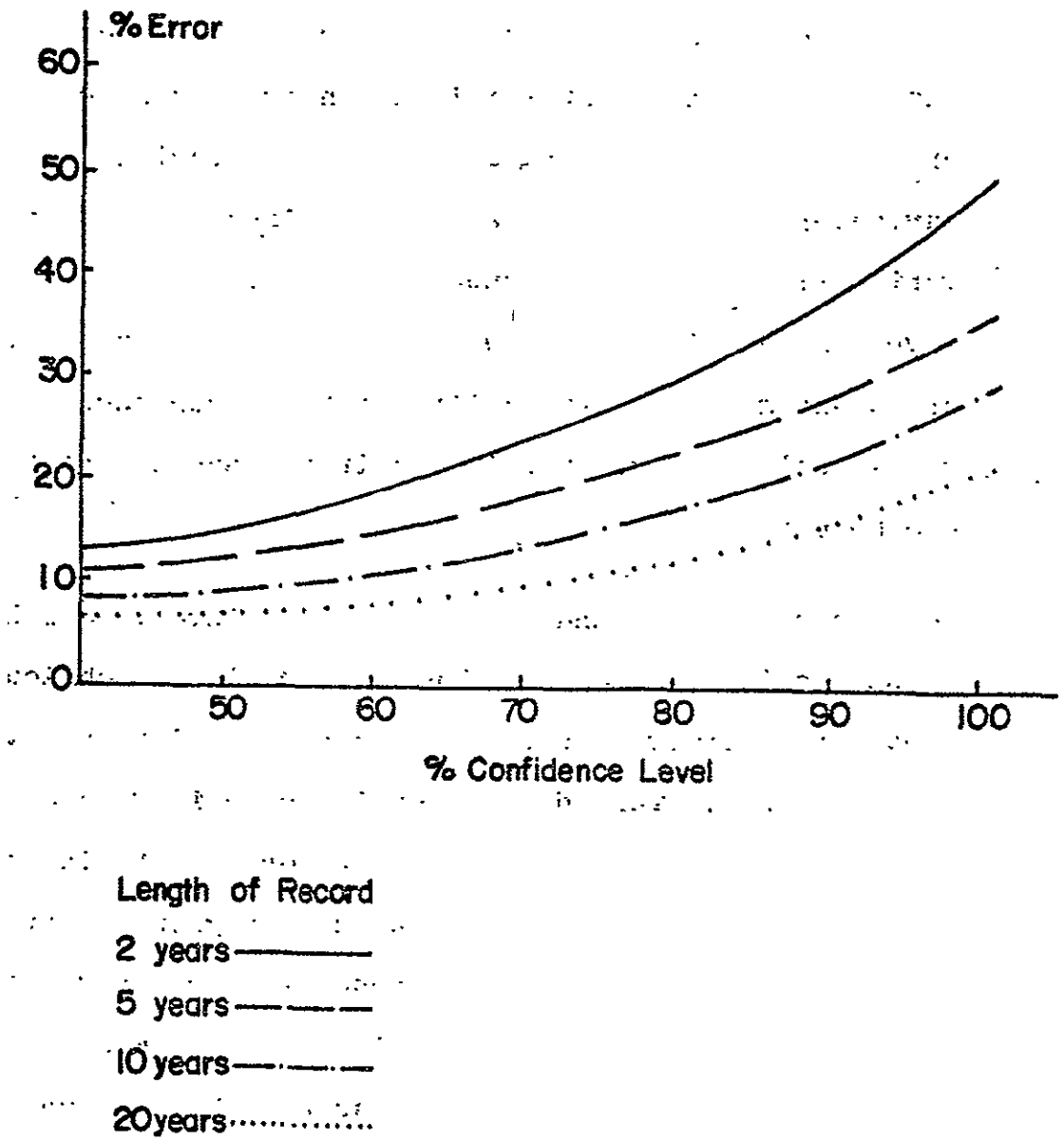

FIGURES

Figure 1	Comparison of Principal U.S. Planning Model Predictions
Figure 2	Comparison of Selected Foreign Planning Model Predictions
Figure 3	Divergence of Prediction Between Planning Models
Figure 4	Typical Uncertainties in Predictions of Conventional Planning Models for Gaged Watersheds
Figure 5	Error in Estimating Long Time Mean Runoff from Short Time Records
Figure 6	Deviation of Predictions of the Principal Methods - Statistical Models
Figure 7	Program Flow Chart, NAS8-30539
Figure 8	Agricultural Research Basins
Figure 9	Watershed Response to Constant and Uniform Rain
Figure 10	Water Balance for Overland Flow
Figure 11	Typical Peak Event Rainfall Recurrence
Figure 12	Rainfall Rate/Mass Relationship
Figure 13	Typical Dependency of Peak Rain Event upon Duration and Recurrence
Figure 14	The Effect of Watershed Area on the Peak Rain Rate
Figure 15	Time of Concentration Vs. Area for Basins of Different Geometries
Figure 16	Representative Physical Properties of Soils
Figure 17	Effect of Infiltration upon Runoff

Figure 18	Influence of Soil Depth Upon Runoff
Figure 19	Effect of Antecedent Soil Moisture Content on Infiltration and Runoff
Figure 20	Infiltration Rate vs. Time for Danville, Vt. Watershed
Figure 21	Infiltration Formulations
Figure 22	Overland Flow and Interflow Rates for Different Soils and Covers
Figure 23	Principal Overland Flow Parameters
Figure 24	Comparison of Flow of Channels of Different Cross Sections, Assuming Same Area and Top Width
Figure 25	Rates of Hydrological Processes
Figure 26	ARS Basins: Average Annual Runoff/ Average Annual Precipitation
Figure 27	Initial Partition
Figure 28	Analog Circuit for Constant Rain With Expotentially Decaying Infiltration; Constant ET
Figure 29	Analog Circuit for Sinusoidal Precipitation and Evapotranspiration With Constant Infiltration Rate
Figure 30	Curve for Computing the Spatial Correction Factor
Figure 31	Peak Flow for Surface Dominated Watersheds Overland Flow Contribution
Figure 32	Additional Detention Time Caused by Channel
Figure 33	Sensitivity of the Model to Surface Observables
Figure 34	Effect of Overland Flow on Flood Conditions
Figure 35	Nine Watershed Sample

Page

5.2.1 Recurrence Rainfall 111

5.2.2 Watershed Physiography, Vegetative Cover, and Soils 111

5.3 Results of the Model and Comparison with Actual Records and Existing Planning Models 132

5.3.1 50-Year Peak Flow from Actual Records 135

5.3.2 Remote Sensing Model (ECO Model) and Results 137

5.3.3 Comparison of the Four Planning Models 142

6.0 THE RELATIONSHIP OF REMOTE SENSING TECHNIQUES TO HYDROLOGIC PLANNING MODELS 149

6.1 Remote Sensing Observations 151

6.2 Relationship of Remote Sensing Observables to Hydrologic Planning Model Requirements 151

6.3 Visual Interpretation of an ERTS Image of a Test Watershed 153

7.0 CONCLUSIONS 163

8.0 APPENDIX 167

9.0 BIBLIOGRAPHY

10.0 REFERENCES

10.0 REFERENCES

1) USDAHL-74, Revised Model of Watershed Hydrology; H. N. Holtan, G. J. Stiltner, W. H. Henson, N. C. Lopez, U.S.D.A., July, 1974

2) Soil Conservation Service, National Engineering Handbook, Section 4

3) Handbook of Applied Hydrology Ven Te Chow, McGraw-Hill Book Co., 1964, p. 21.37

4) Ibid. p. 21.39

5) Introduction To Hydrology, Viesmann, Harbaugh & Knapp, Intext Educational Publishers, 1972.

6) Rainfall Frequency Atlas of the U.S., Technical Report No. 40, Dept. of Commerce, 1963.

7) "Time of Concentration for Overland Flow," W. S. Kerby, Civil Engineering, March 1959, p. 60.

8) Crop Forecasting by Remote Sensing from ERTS, contract NASW-2488, P. A. Castruccio & H. L. Loats, July 1974.

C. 3

FIGURE 8 AGRICULTURAL RESEARCH BASINS

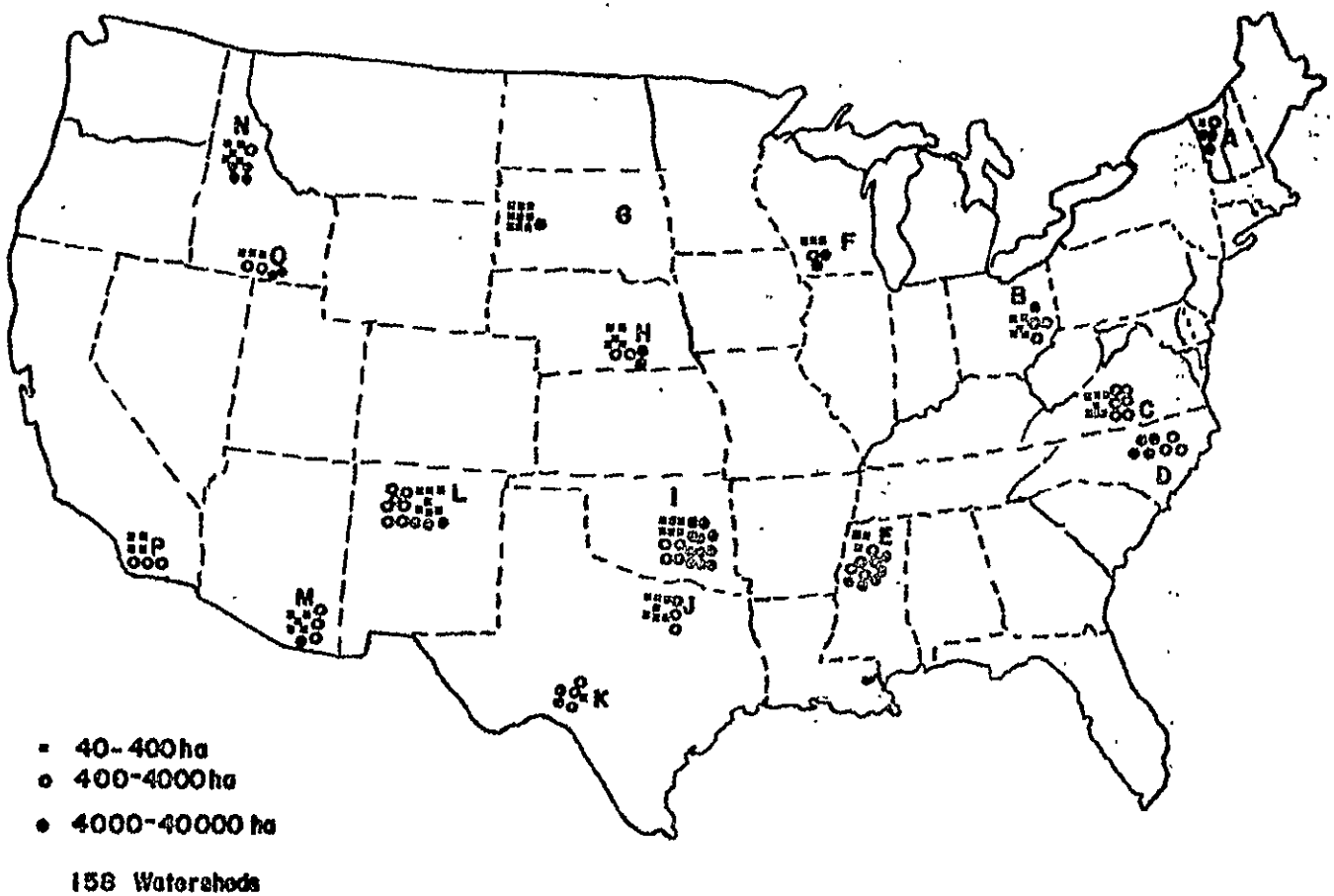

ORIGINAL PAGE IS
OF POOR QUALITY